

Università degli Studi di Padova
Dipartimento di Biologia
Corso di Laurea Magistrale in Biotecnologie Industriali



**Gram variability and prodigiosin production in isolate
of *Serratia marcescens* obtained from blackberries**

Relatore: Prof. Tomas Morosinotto
Dipartimento di Biologia

Correlatore: Dr. Dariusz Latowski
Dipartimento di Fisiologia vegetale e Biochimica

Controrelatore: Prof. Paola Venier
Dipartimento di Biologia

Laureando: Mariasole Gobbo

Anno Accademico 2021/2022

Index

ABSTRACT

1.	INTRODUCTION.....	7
1.1.	Prodigiosin production and its properties.....	7
1.1.1.	Production conditions and parameters.....	8
1.1.2.	Biosynthesis and gene regulation.....	11
1.1.3.	Spectrophotometric characterization of prodigiosin.....	12
1.1.4.	Inhibition prodigiosin production mediated by glucose.....	13
1.1.5.	Biofilm influence on prodigiosin production.....	14
1.1.6.	Prodigiosin localization.....	15
1.2.	Observed Gram variability in <i>S. marcescens</i> isolates.....	16
2.	METHODS.....	17
2.1.	Gram variability.....	17
2.1.1.	Media preparation for liquid and solid cultures.....	17
2.1.2.	Dilution in Petri plates and ERIC-PCR (Enterobacterial Repetitive Intergenic Consensus Polymerase Chain Reaction) control Procedure	17
2.1.3.	Growth curve measurements in 300 mL flasks	17
2.1.4.	Growth curve measurements in 96-wells-microplates	18
2.1.5.	Gram staining	18
2.1.6.	LPS isolation, hydrolysis of polysaccharides, monosaccharides labelling and Bradford assay control.....	18
2.2.	Prodigiosin quantification and assessment.....	20
2.2.1.	Antioxidant capacity quantification.....	20
2.2.2.	Prodigiosin quantification	21
2.3.	Prodigiosin spectrophotometric characterization.....	21
2.3.1.	Pigment isolation and lyophilisation.....	21
2.3.2.	Spectra analysis and sample preparation.....	21
2.3.3.	Lifetime measurements	22
2.3.4.	Prodigiosin extraction and purification by TLC.....	22
3.	RESULTS.....	25
3.1.	Gram variability.....	25
3.1.1.	Cultivation conditions	25
3.1.2.	First growth curve attempts in flasks.....	26
3.1.3.	Growth curve measurements in 96-wells-microplates.....	29
3.1.3.1.	<i>Growth and size analysis</i>	29
3.1.3.2.	<i>Gram staining and microscope analysis</i>	34
3.1.4.	LPS isolation and HPLC analysis.....	44
3.1.4.1.	<i>Sugars analysis</i>	44
3.1.4.2.	<i>Bradford assay</i>	52
3.1.5.	Glucose inhibition in D6 isolate.....	52
3.2.	Prodigiosin quantification and assessment.....	53
3.2.1.	Antioxidant capacity	53

3.2.2.	Prodigiosin quantification.....	56
3.3.	Spectrophotometric characterization.....	61
3.3.1.	Absorption and fluorescence spectra.....	61
3.3.2.	Lifetime measurements	65
3.3.3.	Prodigiosin extraction and purification by TLC.....	66
4.	DISCUSSION.....	69
4.1.	Gram variability.....	69
4.2.	Prodigiosin quantification and assessment.....	70
4.3.	Prodigiosin spectrophotometric characterization.....	71
5.	CONCLUSIONS	73
	APPENDICES	75
	BIBLIOGRAPHY.....	109

ABSTRACT

Prodigiosin is a secondary metabolite produced by Gram negative *Serratia marcescens* (*S. marcescens*) bacteria and it is characterized by a pyrrolyl pyrromethene skeleton and different alkyl substituents. In its production are involved different enzymes and it is a pigment capable of inducing the apoptosis of several cancer cell lines, so its antioxidant, antifungal, antitumoral and antibiotic potential is very important. Prodigiosin production needs dissolved oxygen, an incubation time of ≈ 60 hours, a solution pH of ≈ 8 , a growth temperature of 28°C , and presence of dissolved phosphates. Its production is controlled by a complex regulatory network of both N-acyl-L-homoserine lactone-quorum-sensing-dependent and independent pathways. Prodigiosin can exist in two forms, depending on the hydrogen ion concentration of the solution: in an acid medium, the red pigment exhibits a sharp spectral peak at 535 nm, while in the alkaline medium the pigment is coloured orange-yellow and has a broader spectral curve at 470 nm. In my work, three isolates of *Serratia marcescens* from blackberry fruit (*Rubus fruticosus*, cultivar "Polar"), later named D2, D4 and D6, were used, while the isolate *Serratia marcescens* var *kiliensis* PCM 550 (designated as PJ), from the *Polish Collection of Microorganisms* of the *Institute of Immunology and Experimental Therapy of the Polish Academy of Sciences* in Wrocław was used as reference microorganism. The aims of the work were, firstly, to characterize the pigment prodigiosin and, secondly, to verify if the Gram variability of *S. marcescens*, noticed in previous works, was correlated to prodigiosin production. To understand the spectrophotometric characteristics of the pigment, extraction and purification methods were performed. On the other hand, the Gram variability was studied through growth curve analysis in LB and LB + 1% glucose, which inhibits the prodigiosin production: in this way, slide samples at different timepoints were collected for Gram staining. Further understanding of the phenomenon was proved by HPLC analysis for lipopolysaccharides' (LPS) carbohydrates, isolated from bacteria grown in shaking conditions, where no prodigiosin production was seen, and stable conditions, where prodigiosin was observed. All these analyses are supported by previous information found in the literature to understand the growing conditions of *S. marcescens* (e.g., oxygen, glucose, and nutrients influence) and the localization of prodigiosin.

1. INTRODUCTION

Serratia marcescens (*S. marcescens*) is a saprophytic Gram-negative bacillus that belongs to the *Enterobacteriaceae* order, composed of species that are known for being pathogens as *Salmonella* and *Escherichia coli* (Hejazi et al. 1997), and to the *Yersiniaceae* family. *S. marcescens*, whose name was assigned in 1819 by Bartolomeo Bizio, a chemist and microbiology pioneer from Padua (Hejazi et al. 1997), is also an opportunistic human pathogen that has been recognized as one of the main causes of hospital-acquired diseases as septicemia, meningitis, infections of the urinary tract, eyes, bloodstream, and respiratory apparatus, (Abreo et al. 2019), as well as endocarditis (Hejazi et al. 1997). Environmental isolates of this species were found also in water, soil, plants, insects, and food (Abreo et al. 2019), above all the starchy ones, for instance, bread; it is favored by damp conditions, where phosphorus-containing materials or fatty substances are its main feeding sources (Williamson 2006). *S. marcescens* is famous for producing prodigiosin, a red pigment that in medieval times was mistaken for fresh blood, as presumably in the *Eucharistic miracle of Bolsena* in 1263 (Hejazi et al. 1997); it was also first discovered by Bizio as a result of red discoloration of polenta (Sehdev et al. 1999).

Prodigiosin is a secondary metabolite produced by both Gram-positive and negative bacteria, for instance, *S. marcescens*, *Vibrio psychoerythrus*, *Streptovorticillium rubrreticuli* and some other eubacteria (Darshan et al. 2015). It is characterized by a pyrrolyl pyrromethene skeleton and different alkyl substituents, that confer different properties (Godvin Sharmila et al. 2020). This pigment and its derivatives are proapoptotic agents towards different cancer cell lines and cellular targets, as well as drug resistant cells, without causing any or little toxicity (Darshan et al. 2015); furthermore, its antioxidant, antitumoral, and antibacterial potential is very important (Khanafari et al. 2006). For its unique pink color, prodigiosin has also been used in carbonated drinks, textiles, cosmetic, and dairy products (Godvin Sharmila et al. 2020). In fact, microorganisms' pigments could serve as an alternative source to replace synthetic pigments used in the food industry, with few limitations including sensitivity, solubility, and short stability upon exposure to pH, light and high temperatures (Namazkar et al. 2013). In Suryawanshi and collaborators' work, it was demonstrated how prodigiosin could help in the increasing of sunscreen protection factors (SPF) of commercial sunscreens products if combined with *Aloe vera* leaf and *Cucumis sativus* fruit, that owns photo-protective activity (Suryawanshi et al. 2014).

In this work, three isolates of *S. marcescens*, obtained by PhD student Martyna Rogala from blackberry fruit (*Rubus fruticosus*, cultivar "Polar") and named D2, D4 and D6, were used in the following experiments; particularly I focused on the isolate D6. In addition, the isolate *S. marcescens* var *kiliensis* PCM 550, from the Polish Collection of Microorganisms of the Institute of Immunology and Experimental Therapy of the Polish Academy of Sciences in Wrocław, was used as the reference microorganism; it will be designated as PJ. The aims of the following experiments were, firstly, to characterize spectrophotometrically the pigment and, secondly, to understand the possible Gram variability of the bacteria, considering

hypothetical role of prodigiosin in this process. In fact, previous works of PhD student Martyna Rogala and B.S. student Aleksandra Odrobina (Odrobina 2021) have shown that not only the isolates of this bacteria produce the wanted pigment, but also changed from Gram negative to Gram positive at the late development stage. Experiments have already demonstrated that prodigiosin production should not be correlated to Gram variability, but further attempts to assess the role of prodigiosin in the phenomenon were needed to better understand this behaviour, that was also seen in different other species (Beveridge 1990). In addition, the characterization focused on spectrophotometric techniques: extraction and purification experiments pointed to obtain clear absorbance, fluorescence, and excitation spectra, while quantification during different growth phases underlined differences between the isolates. All these analyses were supported by previous information found in the literature to understand the growing conditions of *S. marcescens* (e.g., oxygen, glucose, and nutrients influence) and the localization of prodigiosin.

1.1. Prodigiosin production and its properties

1.1.1. Production conditions and parameters

The ecological and physiological role of the pigment as a secondary metabolite for its antibacterial, antifungal, or antiprotozoal activity is evident, but there are still some points to clarify. Evidence suggests that prodigiosin takes part in competition against other organisms, regulation of proton gradients, energy, pH homeostasis, and determination of surface hydrophobicity (Slater et al. 2003). Prodigiosin production needs an incubation time of ≈ 60 h, a solution pH of ≈ 8 , growth temperature of 28°C , and presence of dissolved phosphates (Williamson et al. 2005). Its production is controlled by a complex regulatory network of both N-acyl-L-homoserine lactone-quorum-sensing-dependent and -independent pathways (Williamson et al. 2005). Differently from what happens at lower pH values, where the pigment condensation can occur spontaneously, the reaction is sensitive to temperatures (Williamson et al. 2005).

Knowing that *Serratia* is a facultative aerobe, dissolved oxygen can also influence the pigment production: in fact, it requires a supply of dissolved oxygen that could be obtained only with high rate of oxygen transfer in baffled flasks or in fermenters supplied with both aeration and agitation (Heinemann et al. 1970). In fact, it has been seen that, the fermentation proceeded faster with a higher oxygen transfer rate, while the pH increases (Heinemann et al. 1970). Prodigiosin can exist in two forms, depending on the hydrogen ion concentration of the solution: in an acid medium, the red pigment exhibits a sharp spectral peak at 535 nm, while in the alkaline medium the pigment is coloured orange-yellow and has a broader spectral curve at 470 nm (Darshan et al. 2015).

1.1.2. Biosynthesis and gene regulation

Prodigiosin appears only at the late stages of bacterial growth (*Figure 1*), and in previous works, they have found over 30 genes involved in its production. Its biosynthesis develops along a bifurcated pathway that leans on an enzyme condensing the 4-methoxy-2-2'-bipyrrole-5-carbaldehyde (MBC) with a monopyrrole; later, the MBC is also condensed with a 2-methyl-3-pentylpyrrole (MPP) molecule to form prodigiosin (Darshan et al. 2015). Several clusters encoding the enzymes involved in prodigiosin production from several species have been sequenced: these include the *pig* clusters from two *Serratia sp.*¹ (Harris et al. 2004). All clusters own a set of homologous and conserved genes for the biosynthesis of MBC, which seems highlighting a common route requiring proline, acetate or malonate, serine and, methionine (Williamson et al. 2006).

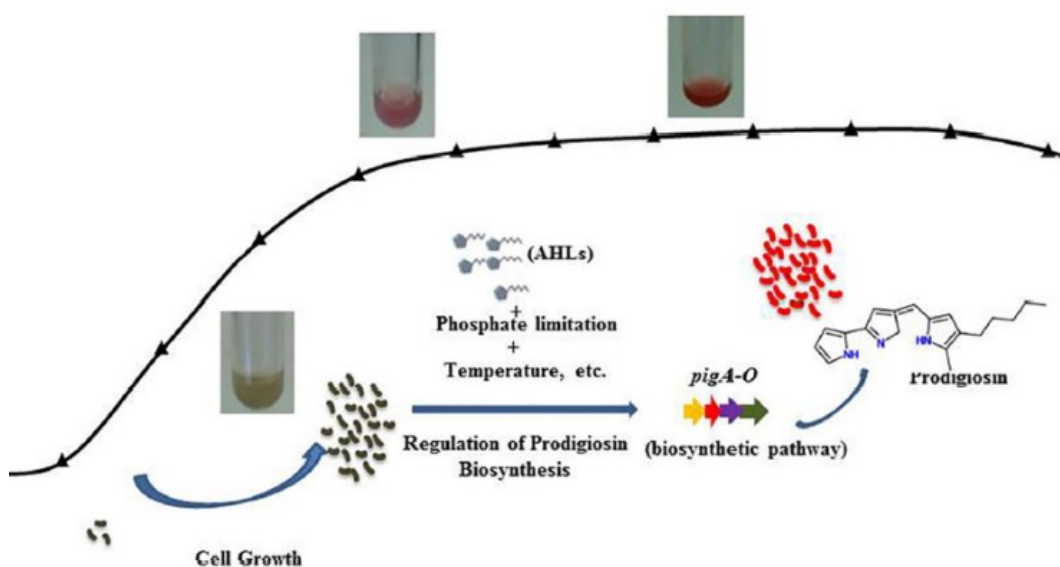


Figure 1. Regulation of prodigiosin in S. marcescens: prodigiosin is produced during the stationary phase and its peak arrives after 60 h (Khanafari et al. 2006).

Commonly, the process starts with the pyrrolic ring formation by incorporating the proline in the ring A, which is the first one out of 3 (A, B, C): the reaction is catalyzed generally by PigA, PigG, and PigI or their homologues. Later, a C₂ unit from malonyl-CoA and a C₂N unit from serine are decarboxylated and incorporated by PigI and PigH (or homologues) to form 4-hydroxy-2,2'-bipyrrole-5-methanol (HBM) molecule (Williamson et al. 2005). As final step, PigM catalyzes the oxidation of an alcohol group present in HBM to form the 4-hydroxy-2,2'-bipyrrole-5-carbaldehyde (HBC); the hydroxyl group is then methylated in order to form MBC (Williamson et al. 2005). This final methylation step is performed by PigF (or homologous) and facilitated by homologues of PigN.

¹ It must be noted that many of the reported articles on the regulation of the prodigiosin gene cluster were a result of studies on *Serratia sp.* ATCC 39006.

Serratia sp. starts the condensation with MBC with a different monopyrrole molecule, the methyl amyl pyrrole (MAP), and the synthesis is catalyzed by different enzymes and substrates (Ravindran et al. 2019): those have been predicted through homology, gene knock-out, mass spectrometry, liquid chromatography, and complementation experiments (Williamson et al. 2005). The responsible genes are organized in an operon characterized by a total of 14 genes, from *pigA* to *pigN*, that are under the control of a promoter element upstream *pigA*. The operon is then transcribed as a polycistronic mRNA, and the multistage process starts from L-proline and trans-octenal (Ravindran et al. 2019). MAP is synthesized by PigD, PigE and PigB (Figure 2); the last one should be involved in the final oxidation of H₂MPP. The condensation of MBC to MAP should be catalyzed by a family of pyrrole-condensing enzymes, characterized by PigC (Williamson et al. 2005), that was found in all sequenced species (Figure 2).

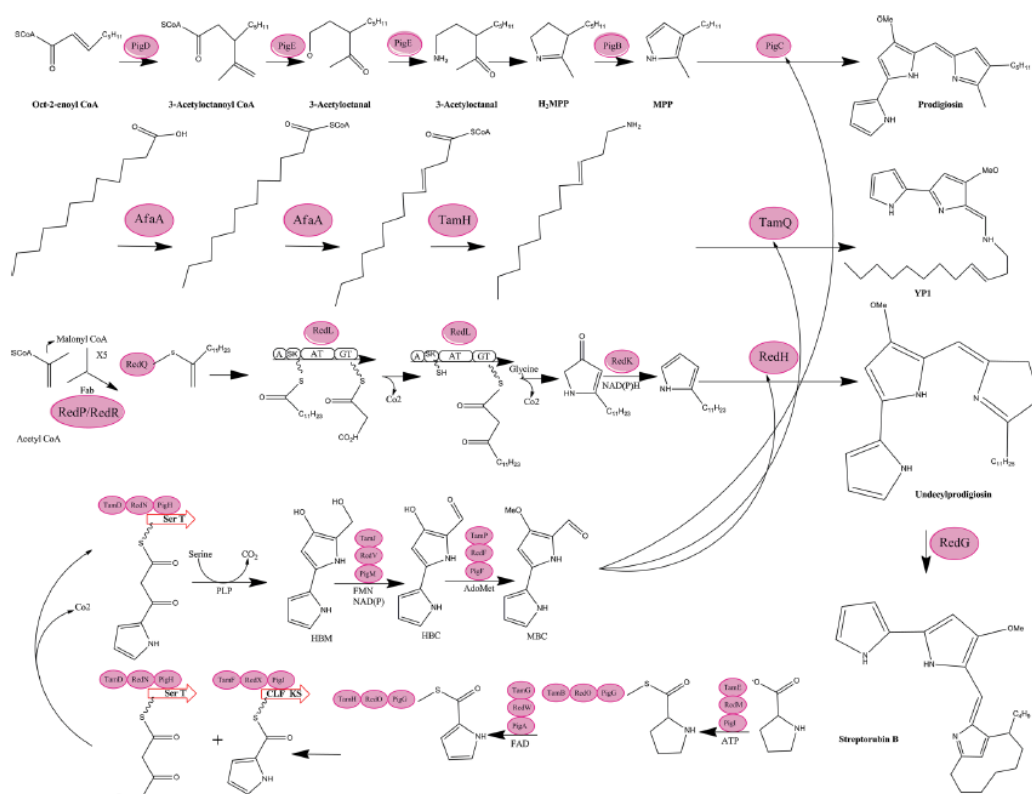


Figure 2. Proposed biosynthetic pathway of the prodigiosin molecules (Darshan et al. 2015).

S. marcescens prodigiosin is chemically similar to the secreted undecylprodigiosin, by *Streptomyces coelicolor* A3, and to prodigiosin R1, produced by *Streptomyces griseoviridis* (Kawasaki et al 2009). Undecylprodigiosin is the result of undecyl pyrrole and MBC condensation from malonyl-CoA and L-proline precursors and the catalysing proteins are encoded by the so-called red gene cluster. The enzymes required for this last reaction are arranged in three different reading frames (Ravindran et al. 2019): two of the 23 genes in the cluster encode pathway-specific regulator, while 6 are involved in 4-methoxy-2,2'-P-bipyrrole-5-carboxaldehyde biosynthesis, eight in 2-undecylpyrrole biosynthesis and two are housekeeping genes (Darshan et al. 2015).

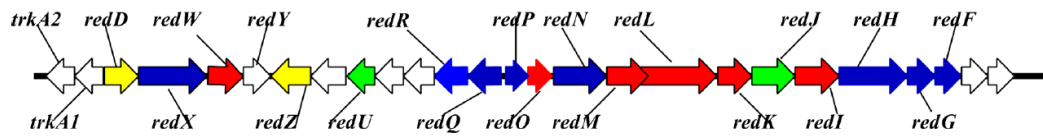


Figure 3. Organization of the prodigiosin biosynthetic gene cluster in *S. coelicolor* A3. Genes deduced to be involved in 2-undecylpyrrole biosynthesis are blue, genes deduced to be involved in 4-methoxy-2,2'-Pbipyrrole-5-carboxaldehyde biosynthesis are red, putative housekeeping genes are green, regulatory genes are in orange and genes of unknown function are white (Darshan et al. 2015).

Concerning its genetic regulation, prodigiosin production is controlled by some global regulators, like the one from the carbon (*crp*) and energy metabolism (*fnr*), nucleoid proteins (*fis*, IHF) and purine utilization regulator (*pucR*), while some of them are local (Ravindran et al. 2019). The role of nutrition sources like glucose, nitrites, phosphate, and maltose have an impact on the pigment production, as well as cell density and copper ions. The presence of elements for specific nutritional requirements like iron, cysteine, leucine, glycerol, and fatty acids could shed light on the role and need for prodigiosin in *Serratia*. It is thought that glycine cleavage system (GcvA) element could have a role in the operon regulation as glycine is involved in the pigment production; on the other hand, the *AlgU* element, important in the detection of oxidation and envelope stress, provides interesting information for future research, as well as various factors monitoring the growth phase of the cell and biofilm production (Figure 4) (Ravindran et al. 2019).

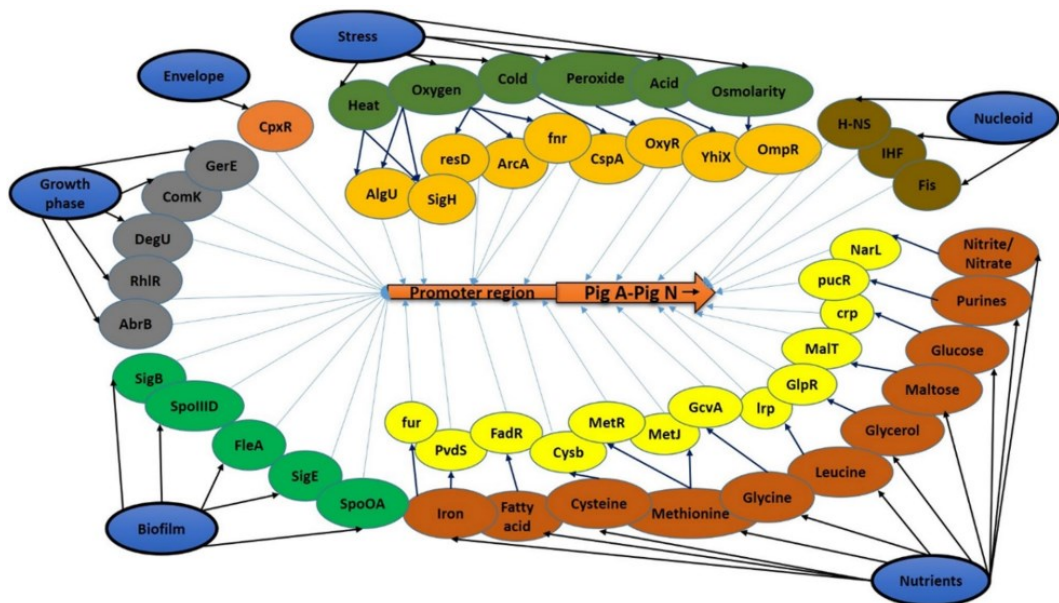


Figure 4. Global and local regulators of the prodigiosin operon; the six main categories of regulators are indicated in blue (Ravindran et al. 2019).

1.1.3. Spectrophotometric characterization of prodigiosin

From the literature, it is known that the archetypal prodigiosin has a pyrrolyl dipyrromethene core skeleton (Darshan et al. 2015) with a tripyrrole structure containing a common 4-methoxy-2-2'-bipyrrole ring (*Figure 5*); differently from this last one, the mono and bipyrrole precursors are synthesized separately and then condensed together (Khanafari et al. 2006). These three rings are conventionally reported as ring A, ring B and ring C (Darshan et al. 2015), but prodigiosin have been classified into linear, as undecylprodigiosin, and cyclic derivatives, for example streptorubin B (Williamson et al. 2006). In addition, prodigiosin exists in two rotamers, the *cis* or β and the *trans* or α , whose balance depends on the solution pH, because the *trans* structure can be easily protonated (*Figure 6*).

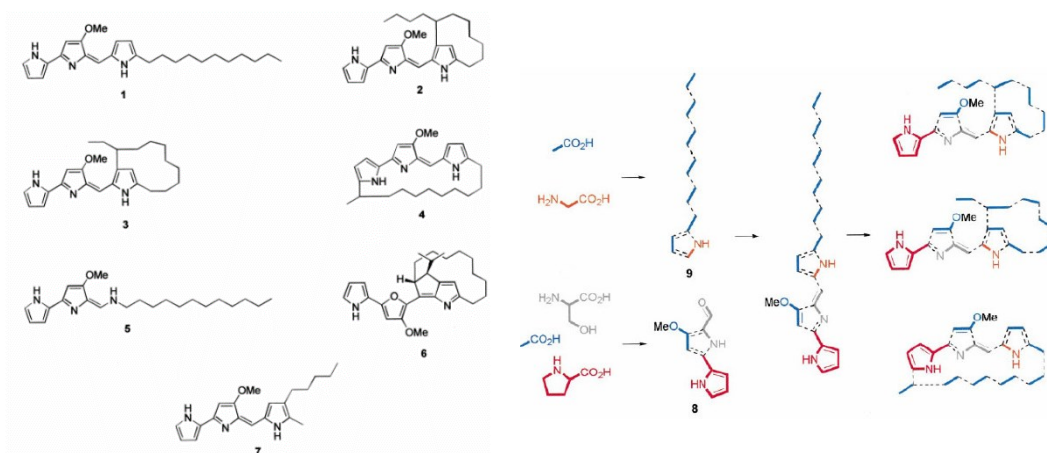


Figure 5. On the left, from number 1 to 6, prodigiosin structures from different actinomycetes species, while the number seven is the one produced by *Serratia marcescens*; on the right, biosynthetic origin of undecylprodigiosin examined by the incorporation of labelled precursors (Khanafari et al. 2006).

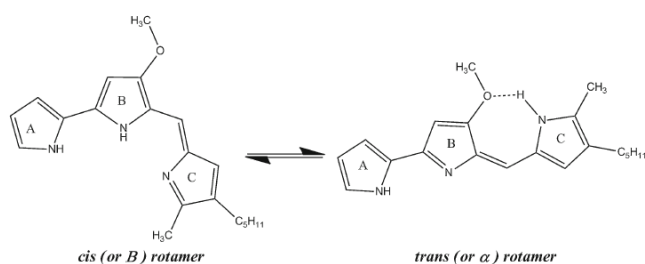


Figure 6. Structure of archetypal prodigiosin with the reported A, B and C rings; the form exists in *cis* or *trans* rotamer depending on the pH.

Regarding the absorption spectra from previous works, it is known that prodigiosin shows different spectral curves at acid, neutral and alkaline pH (Hubbard et al. 1956). In fact, the pigment exhibits a sharp peak at 535 nm and a red colour when in acid medium (*Figure 7*); on the contrary, in basic solution, the prodigiosin presents an orange-yellow shade and has a wider curve shifted (*Figure 7*) to 470 nm (Hubbard et al. 1956).

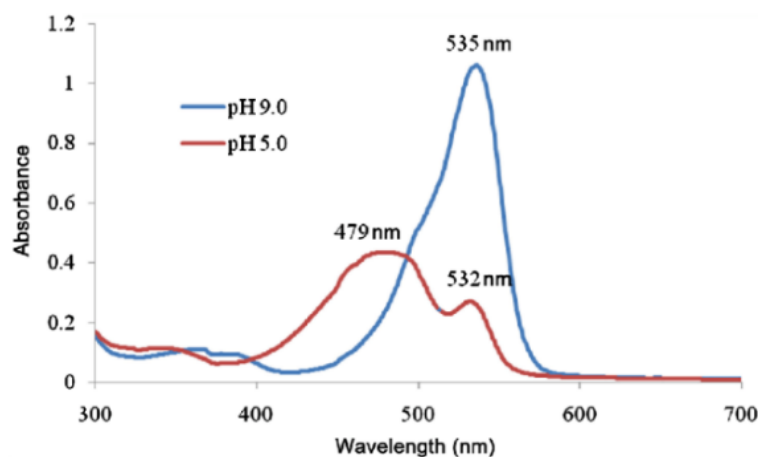


Figure 7. The UV-Vis spectrum of the prodigiosin in acid and alkaline medium (Qui Fu et al 2019).

1.1.4. Inhibition prodigiosin production mediated by glucose

D-glucose is a good carbon source to promote growth of *S. marcescens*, but since the 50s, it is known to be a potent inhibitor of prodigiosin production (Bunting et al. 1949). In James E. Fender and collaborators' work, it is explained why the production of prodigiosin is inhibited in glucose-rich media: if previous studies indicated that this inhibitory effect was pH-dependent and did not require cyclic AMP (cAMP), genetic engineering techniques such as transposon mutagenesis and DNA manipulation focused on the identification of involved genes in the inhibition mediated by glucose (Fender et al. 2012). If the genes required for the response to the pH change are unknown, it is evident that the inhibition involves *crp* mutants and does not require cyclic AMP (cAMP) receptor protein (CRP) (Solé et al. 2000).

Quinoprotein glucose dehydrogenase's (GDH) multi loci are involved both in the inhibition of prodigiosin production and pyrroloquinoline quinone (PQQ) and ubiquinone (UBI) biosynthetic genes regulation. They observed that D-glucono-1,5-lactone and D-gluconic acid, but not D-gluconate, were able to inhibit the pigment production in the *wt* and in the *gdhS* mutant (glucose dehydrogenase gene): these data support a model in which the oxidation of D-glucose by quinoprotein GDH starts a reduction of pH that inhibits prodigiosin production through transcriptional control of the prodigiosin biosynthetic gene cluster (Fender et al. 2012). The fact that also the mutant presents the inhibition suggests that the product of its activity, which is the D-glucono-1,5-lactone, the cyclic ester of D-gluconic acid, is involved in GIP (glucose inhibition of the prodigiosin phenotype). This molecule spontaneously converts to D-gluconic acid in aqueous medium, and its hydrolysis causes the acidification of its environment, which causes the inhibition. The reason why PQQ and UBI mutants are able to produce the pigment in glucose-rich medium is that they are defective in *gdhS* activity. The inhibition acts particularly on the transcriptional control of *pigA-N*, for example, the mutation of the transcription factor hexS, that directly binds *pigA* promoter, inhibits its expression. In addition, the *gdhS* mutant produced higher amounts of prodigiosin in LBG (Luria Bertani supplemented with D-glucose 110 mM) than in LB: this may be expected, as glucose inhibits cAMP production in LBG, and, in return, cAMP inhibits prodigiosin production.

Consistently with the cAMP model, the increased prodigiosin in the *gdhS* mutant and LBG was absent compared to that in LB and in the cAMP receptor protein (CRP) and *gdhS* double mutant with and without glucose, because CRP is required to respond to glucose-initiated changes in cAMP levels.

The energetic reasons of this inhibition in glucose-rich media are to be searched in the independent and antagonistic regulatory pathways that mediate the prodigiosin production. This is due to the establishment of a proton gradient mediated by quinoprotein GDH, which is used for the uptake of amino acids and other molecules, while prodigiosin promotes H^+/Cl^- symport across membranes uncoupling the proton gradient established through glucose oxidation. In Haddix and collaborators' work, they suggest that *S. marcescens* uses prodigiosin to reduce ATP production to limit the generation of damaging reactive oxygen species during stationary phase (Haddix PL et al. 2008).

1.1.5. Biofilm influence on prodigiosin production

It is known that at low cell densities and during the early phases of growth, the transcription of the *car* (carbapenem) and *pig* (prodigiosin) gene clusters is low (Slater et al. 2003). These genes are controlled by SmaR, which represses the transcription of the genes themselves both directly, as in the case of *carR*, and indirectly, by blocking the growth-phase dependent activator genes. As cell numbers increase, BHL/HHL molecules, that are part of the N-AHLs family, accumulate linearly; once the cellular population is quorate, BHL and HHL might bind to the SmaR protein and free the *pig* and *car* gene clusters from transcriptional repression. The transcriptional activation of those gene clusters is mediated by Rap protein and other growth phase-dependent or environmentally regulated transcription factors (Ravindran et al. 2019). Expression of *smal* and the *pig* gene cluster is also under the Pho regulon (PhoR) control, whose activity is regulated by Pst (phosphate transport); in fact, when phosphorous is exhausted, PhoB, which is under the control of PhoR, is activated by phosphorylation, and this activates the elements (Figure 8) (Slater et al. 2003).

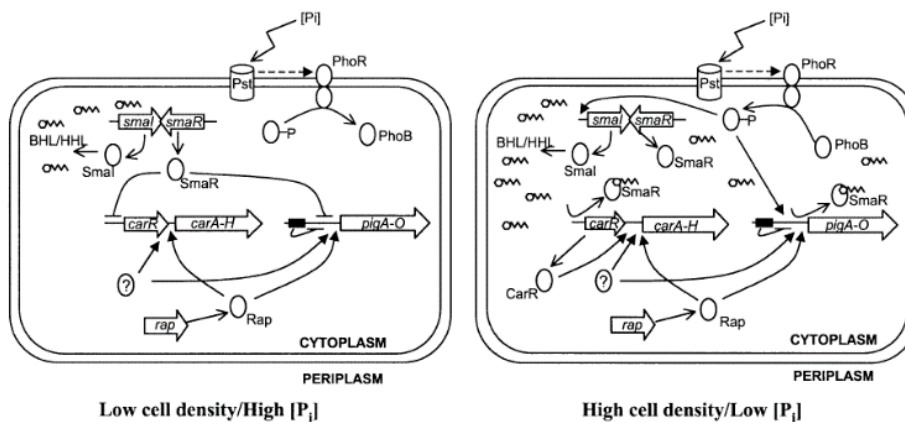


Figure 8. Model of the regulatory mechanisms controlling prodigiosin and carbapenem production in response to cell density and phosphate (Pi) concentration (Slater et al. 2003).

In *E. coli* and *Salmonella*, all Pho regulon genes are preceded by a promoter containing an upstream activation site with a consensus Pho box sequence for transcriptional activation by the phosphorylated PhoB. So, it is suggested that the prodigiosin and carbapenem genes clusters are part of a *Serratia* Pho regulon: searches for Pho box elements revealed two potential candidates within the *pigA* and *smalI* promoters (Slater et al. 2003). When phosphorous is limiting, the transcription of *smalI* and the *pig* gene cluster is increased, leading to increased prodigiosin and carbapenem production. Consistent with the model that SmaR exerts a negative regulatory effect in the absence of BHL/HHL, disruption of this gene further increased both prodigiosin and carbapenem. The results in Slater and collaborators' work shown that prodigiosin production by *S. marcescens* is elevated by Pi concentrations lower than 0.3 mM (Slater et al. 2003).

1.1.6. Prodigiosin localization

Prodigiosin is localized in vesicles (extracellular and cell associated) or intracellular granules, secreted extracellularly (Matsuyama et al. 1986): this could be very interesting to improve the extraction methods. Particularly, in Matsuyama and collaborators' work, a small amount of bacterial mass from colonies of *S. marcescens* was mixed with a drop of water on a clean glass surface (Figure 9): the suspension presented a wetting activity by spreading spontaneously on the glass surface and showed red granular material surrounding the cluster of colourless bacterial cells. Thanks to some observations with a phase contrast microscope, it was evident the presence of many extracellular vesicles, with the diameter of about 0.1-3.0 μm , and vesicles associated to bacterial cells.

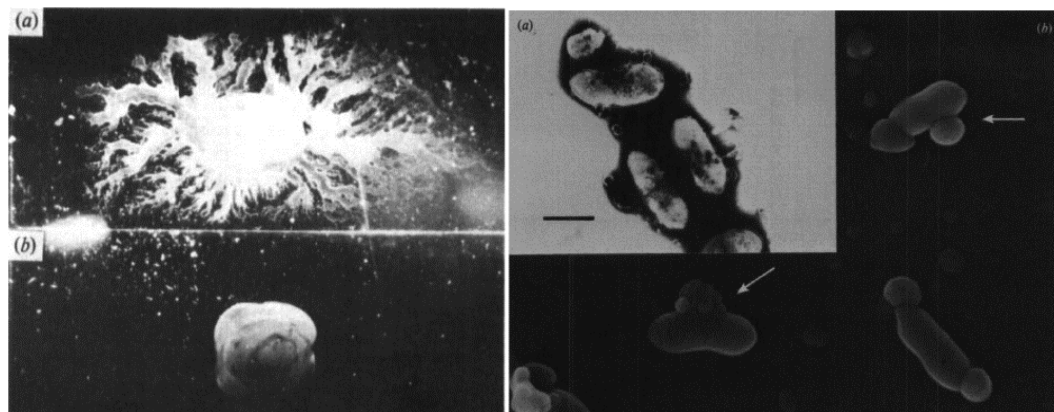


Figure 9. On the left, wetting activity of *S. marcescens* on a glass surface at 30°C (a) and 37°C (b). On the right, electron micrographs of *S. marcescens* at 30°C; (a) negative-stained micrograph; scanning electron micrograph (Matsuyama et al. 1986).

For development of wetting activity and extracellular vesicles, the growth temperature was important: in fact, if grown at 30°C, the strain shown both wetting activity and extracellular vesicles; on the contrary, if grown at 37°, the strains didn't have any wetting activity and vesicles were smaller and hardly seen (Figure 9) (Matsuyama et al. 1986). In addition, scanning electron microscopy and negative staining showed that vesicles seemed to be secreted from the surface (Figure 9 aside a) and contained amorphous material or part of cytoplasm (Figure 9 aside b): the

membrane extending from the outer membrane of the bacterial cell seemed to participate in vesicle formation. The wetting property could come from some amphiphilic amino lipids composing the vesicles (Matsuyama et al. 1986).

1.2. Observed Gram variability in *S. marcescens* isolates

Gram variability regards few bacteria that can't be classified as both Gram-positive and Gram-negative due to some changes happening on the membrane composition, so they present changed Gram stain. Particularly, some species, for example some from *Actinomyces* or *Mycobacterium* groups, become Gram-negative starting by the initial growth phase and, within the stationary phase, from 15 up to 50% of the cells have changed Gram nature, without changing shape (Beveridge TJ, 1990). On the other hand, some other groups, such as the *Bacillus* and *Clostridium* ones, became Gram-negative as culture ages, but, because they own a more complex cell wall, covered by an S layer, they stained as Gram-positive during lag and the initial exponential phases, but, when the time doubles, the S layer becomes thinner, so, within stationary phase, cultures are Gram-negative (Beveridge TJ, 1990).

S. marcescens has never been considered a Gram-variable bacteria, but in Fatimah and collaborators' work, they describe how, while studying lipase and protease-producing species, isolated from slaughterhouses waste in North Surabaya (Indonesia), a *S. marcescens* isolate, changed from Gram positive to negative (Figure 10) (Fatimah et al. 2019). This variability can be caused by growth stresses, for instance nutrients deprivation, temperatures, pH, or electrolytes, but certain bacterial species show Gram variability even under optimal growth conditions (Beveridge TJ, 1990). In this case, LII61 bacteria were isolated from an environment rich in proteins and lipids, given by animals' hulks, organs, bowels, bones, and metabolism products. Despite the original localization, the isolate was able to change Gram nature in Luria-Bertani (LB) medium, without undergoing any nutrient deprivation or stress. In addition, this isolate could produce lipase, about 29.39 U/mL at 24 hours, and protease enzymes, with index around 1.2 after 48 hours (Fatimah et al. 2019).

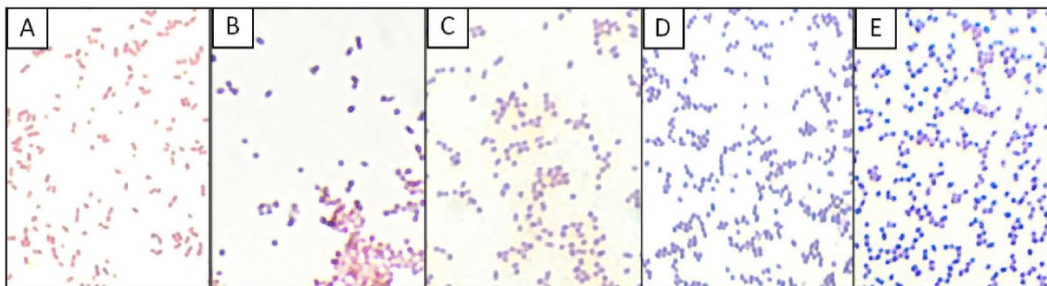


Figure 10. Gram staining of *S. marcescens* isolate after 16 h (A), 18 h (B), 24 h (C), 48 h (D) and 72 h (E) (Fatimah et al. 2019).

2. METHODS

2.1. Gram variability

2.1.1. Media preparation for liquid and solid cultures

For all experiments, Luria-Bertani (LB) broth (per 1 L: 25 g) was used in both liquid cultures and solid cultures (with 15 g of agar per 1 L). Bottles with liquid broth were sterilized in the Microjet Personal Microwave Autoclave®.

2.1.2. Dilution in Petri plates and ERIC-PCR (Enterobacterial Repetitive Intergenic Consensus Polymerase Chain Reaction) control procedure

Dilution experiment was performed by distributing 10 µL of the sample (D2, D4, D6, PJ) from serial dilutions (10^{-3} , 10^{-6} , 10^{-9}) of starting culture on Petri dish with solid LB medium. The OD₆₀₀ of each stock dilution was measured with Metertek SP-830® spectrophotometer to check the starting concentration. After 2 days of growth, the colonies with different shapes were collected by pipette touching in 6 mL Falcon® tube each and made growing for 24 hours. Then DNA isolation was performed for each tube with the kit Genomic Micro AX Plant Gravity® by A&A Biotechnology. Purity of DNA was measured with Nanodrop Lite Spectrophotometer® by Thermo scientific. Sequentially ERIC-PCR test was performed with following procedure: 30 times 1st cycle at 95°C for 3.5 min, 2nd cycle at 93°C for 0.5 min, 3rd cycle at 50°C for 1 min, 4th cycle at 65°C for 8 min; then 5th cycle at 65°C for 6 min and 6th cycle at 4°C forever using S100 Thermal cycler®. Each PCR mixture (in total 25 µL) contained: 12.5 µL of PCR mix plus® (A&A Biotechnology), different volumes of each DNA sample (depending on DNA concentration), 1 µL of ERIC1 primer, 1 µL ERIC2 primer, free-nuclease water (A&A Biotechnology) up to 25 µL per sample. Electrophoresis was performed with 1 % agarose with ethidium bromide for 1 hour (90 V). 10 µL of each sample was loaded on an electrophoresis gel, while on both sides 4 µL of DNA ladder mix® (0.1 µg/µL) (Fermentas) was added.

2.1.3. Growth curve measurements in 300 mL flasks

Cultures for obtaining growth curves of each isolate were acquired by adding 500 µL of bacteria inoculum to 300 mL of liquid LB medium. For every timepoint (at 0 h and after 2 h, 24 h, 28 h, 31 h, 41 h, 45 h, 48 h, 65 h, 72 h), 1 mL of each culture was taken to 1.5 mL Eppendorf® tubes in two repeats: one was centrifuged in Eppendorf Centrifuge 5818R® (5 min., 11 000g., RT) to obtain prodigiosin containing bacterial pellet and the other one was used for OD₆₀₀ measurements with Metertek SP-830® and pH evaluation with pH tape. Additionally, 10 µL for each sample were distributed in a glass slide for Gram staining procedure (2.1.5.) and later microscope analysis. Photos were taken with the NIB-620FL Nexcope® microscope using 100x lenses and Topview® software (version released in 16.02.2020).

2.1.4. Growth curve measurements in 96-wells-microplates

Cultures for this experiment were made by adding 200 μL of bacterial inoculum from the new banking flask (from 27th May culture) to 6 mL of liquid LB media in a 15 mL volume Falcon® tubes and left for the night to growth in shaking conditions (120 rpm). The day after, the cultures were centrifuged at maximum speed at 25°C for 5 minutes in Sigma Laboratory centrifuge®, then 4 mL of supernatant was taken off the tube and the pellet was resuspended, to create a high concentrated inoculum for the 96-wells-plate's cultivation. Each well of 96-wells-microplate was filled with 200 μL of LB or LB + 1% glucose (48 wells per each medium) and 5 μL of the previously prepared concentrated inoculum. The experiment was set for 10 timepoints (after 2 h, 4 h, 6 h, 10 or 12 h, 24 h, 30 h, 34 or 36 h, 48 h, 54 h and 58 or 60 h). Each time point included actions like: (1) collection of all volume from one well in 3 replicates for later prodigiosin quantification, (2) pH measurement in 3 replicates by placing 10 μL each on pH universal strip, (3) loading 10 μL on glass slide for later Gram staining procedure (9 replicates), (4) OD₆₀₀ measurement in 9 replicates using TECAN Infinite® M Nano microplate reader, (5) taking picture of the whole plate using CAMAG TLC Visualizer® and vision CATS 3.1® (version 3.1.21109.3) software. To measure the OD₆₀₀ with TECAN Infinite M Nano®, the following settings were used: 20°C, agitation 5 sec and orbital agitation 2 mm. To see the disposition of the wells', look at *Appendix*.

2.1.5. Gram staining

The first attempts were using some dilutes Lugol, whose dilution is unknown; then Lugol was prepared with 1% crystalized iodine and 2% potassium iodide. The first protocol used for the Gram staining procedure it is the following one: 2.5 minutes of crystal violet, 1.5 min of Lugol, 30 sec 80% ethanol and 30 sec of safranine. Later changes were made: 2-3 minutes of crystal violet, 1.5-2 min of Lugol, 30 sec 95% ethanol and 20 sec of safranine (Kostka 2014). Photos were later taken with the NIB-620FL Nexcope® microscope using 100x lenses and Topview® software (version released in 16.02.2020).

2.1.6. LPS isolation, hydrolysis of polysaccharides, monosaccharides labelling and Bradford assay control

The flasks with a volume of 300 mL and 500 μL of PJ or D6 inoculum were prepared in triplicates: in total there were 6 flasks, 3 for each of the two studied growth conditions, that means shaking, using the Sky Line® shaker at 120 rpm and stable conditions. On the 35th day, dialysis tubing cellulose membrane (avg. flat width 25 mm, 1.0 in.) by Sigma-Aldrich was cut into 40 cm pieces and put it into pre-warmed boiling water for 2 hours; a magnet was used to mix the water together with a magnetic steer while the holder was covered while boiling (Bonhomme et al. 2020). The membrane is ready when both sides are easily openable; in the meanwhile, samples were centrifuged in Sigma 6-16K centrifuge® at 6500 g and 20°C for 1 hour; supernatant was removed, and pellet was ready to be used. If the centrifugation occurs the following days, samples with the remaining pellet can be put directly to the -80°C freezer. The pellet was put in a 15 mL Falcon® tube, that was then filled with

20 mL of pre-warmed distilled water and, later, with 20 mL of pre-warmed 90% phenol (temperature should be higher than 68°C); the Falcon® was left on the bath for 12 minutes and mixed by inverting every 1-2 minutes. The Falcon® tube was centrifuged for 15 minutes, at room temperature and 3345 g with Sigma Laboratory centrifuge®; so, 2 phases were obtained: one aqueous in the upper part and a phenolic one in the below part. The two phases were divided into 2 different Falcon® tubes. After having taken 6 L big flasks (6 L) and added around 4 L of hot water, the membranes were filled with the different phases (for one sample 2 phases are obtained, so 2 membranes will be used), closed with knots at each side and bond to a floating structure (ex.: polystyrene), which helps in the fishing of the membrane the day after. So, each flask was blocked overnight in the New Brunswick's Innova 42 Incubator Shaker Series® machine at 40 rpm and 55°C.

The next day the membranes were taken off the flasks and syringes were used to take off the liquid; leftovers from the dialysis remained in membrane. After having filled the tubes, an ultracentrifugation was performed with Optima LE-BOK Ultracentrifuge® by Beckman for 3 hours, 28000 rcf and 4°C (Bonhomme et al. 2020). The supernatant was discarded the supernatant and the pellet dissolved in the littlest volume possible (around 200-300 µl) in some 1.5 mL Eppendorf® tubes, that should be weighted before. Finally, the samples were stored at -80°C (without liquid nitrogen) for lyophilization. For the lyophilisation, samples were taken from the -80° C freezer and put directly in the machine Alpha 1-2 LD Plus® for 3 days at around -50°C.

After lyophilization the samples (Eppendorfs® tubes + LPS powder) were weighted to measure the LPS weight; the volume of MilliQ ultrapure water (MQ), in which the total LPS mass should be dissolved, was calculated in order to have 1 mg of LPS in 200 µl. A volume of 200 µl of the LPS solution was put in Eppendorf® tubes with screw cap, which were dried in miVac®, then stored at -80°C. The following day, the thermoblock was set at 120°C and 1 mg of LPS (dissolved in 200 µl of MQ) was added to 200 µl of 1.75 mL MQ + 0.75 mL TFA solution. The samples were shortly vortexed and incubated in the thermoblock for 2 hrs. The samples are then transferred to ice and left to cool down (Bonhomme et al. 2020).

The following phase extraction, where there is the separation of lipids and monosaccharides, was started by adding 400 µl of chloroform to the hydrolyzed LPS solution. The samples were vortexed for 30 sec each and centrifuged for 2 minutes at 1000 rpm in Eppendorf Centrifuge 5818R®. The upper phase, containing the monosaccharides, was taken to new Eppendorf® tube; the samples were dried under gaseous nitrogen for few hours, then stored at -80°C. The bottom layer contained fatty acids but wasn't taken into consideration (Bonhomme et al. 2020).

Calculated amount (in mg) of 0.5 M MPP (3-methyl-1-phenyl-2-pyrazolin-5-one) was dissolved in adequate amount of MeOH. Later, the following solutions were added to the pellets: 25 µl of a freshly prepared 0.5 M methanolic MPP solution in MeOH, 15 µl of 0.5 M NaOH and 10 µl MQ. Samples were incubated for 2 hours at 70°C and then neutralized with 20 µl of 0.5 M HCl. The samples were vortexed

and shortly spinned at 20°C and 1000 rpm for 1 minute; 600 µl of chloroform were added. The Eppendorf® tubes were thoroughly vortexed and centrifuged at 20°C and 3000 rpm for 1 minute Eppendorf Centrifuge 5818R® the remaining drop of the water phase was taken to a new Eppendorf® tube (the steps must be repeated twice from the addition of chloroform). The samples were dried in miVac® with the following settings: method H₂O, 35°C, till dry. Everything was stored at -80°C (Bonhomme et al. 2020).

Bradford assay was performed in order to quantify the proteins present in the aqueous phase and phenolic phase obtained in the first steps of the LPS isolation: 1 mL from each phase was taken right after the centrifugation. For the assay procedure itself, standard protein solution was prepared with a concentration of 1 mg/ml albumin in 0.9% NaCl; the solution was put in 1.5 mL Eppendorf® tubes for the preparation of the standard curve, in the following concentrations:

	NaCl[µl]	Protein standard[µl]	Protein conc.[mg/ml]
1	1000	0	0
2	250	750	250
3	500	500	500
4	750	250	750
5	0	1000	1000

Table 1. Concentrations used for standard curve preparation.

Later Bradford reagent was mixed with each standard curve solution and samples at the ration 20:1, incubated for 5-15 min; absorption was measured in Tecan Infinite M Nano® at 595 nm.

2.2. Prodigiosin quantification and assessment

2.2.1. Antioxidant capacity quantification

For the quantification of antioxidant capacity, DPPH (α , α -diphenyl- β -picrylhydrazyl) solution was prepared by adding little of DPPH powder, dissolving it in 95% EtOH until it gets $Abs_{517} \sim 0.9$. In the meanwhile, 1.5 mL Eppendorf® tubes containing 200 µL of samples from each timepoint from the growth curve experiments were centrifuged in the Eppendorf Centrifuge 5818R® at least 5 minutes at maximum speed. After the centrifugation, only the supernatant was used, in particularly, 4 µL per well were placed in microplate, then 300 µL of the DPPH solution were added per well. After 30 minutes, 60 minutes, 24 hours, and 48 hours in the dark, absorbance was measured at 517 nm using Tecan Infinite M Nano®. Calculations of the antioxidant capacity were performed following the equation reported down below (A_0 is the absorbance of 4 µL of EtOH + DPPH solution, while A is the absorbance at 517 nm of the sample):

$$TAC \text{ (Total Antioxidant Capacity)} = \left(1 - \frac{A}{A_0}\right) \cdot 100\%$$

Equation 1. Total antioxidant capacity (TAC) of DPPH assay.

2.2.2. Prodigiosin quantification

For each timepoint of the growth curve experiments, 200 μL from the microplates were taken and centrifuged for at least 5 minutes at maximum speed: for this experiment only, the obtained pellet was used. The pellet of each 1.5 mL Eppendorf® tube was later dissolved in 200 μL of methanol, which is the solvent where prodigiosin is more stable, and a small amount of 100 μm diameter glass microbeads by Sigma-Aldrich was added (around 100 μg per well). The homogenizator Tissue-lyserLT® by Qiagen was used to break the solution containing the glass microbeads for 10 minutes and 50x1 oscillations per second. The samples were then centrifuged at maximum speed in the Eppendorf Centrifuge 5818R® for 5 minutes; 100 μL from each sample were placed in a microplate well. Using the Tecan Infinite M Nano® absorption spectra in the range from 350 nm to 700 nm were taken with the following settings: 25 measurements every 5 nm.

2.3. Prodigiosin spectrophotometrical characterization

2.3.1. Pigment isolation and lyophilisation

One week old cultures of PJ, D2, D4 and D6 strains were centrifuged in Sigma 6-16K centrifuge (series number 11080502500 UJ60104 UJKR) for 20 minutes at RFC set at 8000. Supernatant was then discarded while the containing pigment pellet was put into 25 mL Falcon® tubes and put into liquid nitrogen to be frozen for the -80°C freezer. For the lyophilisation, pigment samples were taken from the -80°C freezer and put in the machine Alpha 1-2 LD Plus (series number 110808613600 UJ60104 UJKR) for 3 days at around -50°C . After that, pigment was ready to be suspended and analysed.

Lyophilization products were diluted in 20 mL of ethanol and disintegrated with the disintegrator machine Sonics Vibra-Cells® (series number 110806205600 UJ60104 UJKR); the used parameters were the following: sonication for 3 cycles at pulse 9 (t1) and 15 (t2) and Amp1 35%. The sonication was repeated for other 5 cycles with the same parameters; after that, Falcon® tubes were centrifuged for 5 minutes at 1000 RCF in the Eppendorf Centrifuge 5818R® (series number 110805830800 UJ60104 UJKR), so supernatant was taken and distributed in 12 2 mL Eppendorf® tubes. These were centrifuged again at max speed (about 16,9 RFC) for 10 minutes: supernatant was collected in a glass bottle to avoid plastic contamination.

2.3.2. Spectra analysis and sample preparation

For spectra analysis quartz cuvettes were used to avoid plastic contamination and absorption noise. For comparisons among the different solvents, samples with different composition were prepared, as followed: first preparation with 2 mL of ethanol/100% methanol and 50 μL of two years old prodigiosin; second and third preparation with 3 mL of ethanol and 100 μL of fresh prodigiosin (diluted in ethanol); fourth preparation with 3 mL of ethanol and 100 μL of prodigiosin (evaporated with gaseous nitrogen); fifth preparation with 3 mL of methanol/ethanol and 100 μL of prodigiosin in 100% methanol (evaporated with gaseous nitrogen) and 250 μL of

prodigiosin in ethanol (evaporated with gaseous nitrogen); sixth preparation 250 μ L of prodigiosin in 100% ethanol (evaporated with gaseous nitrogen). Absorption spectra analysis were performed thanks to Jasco V-650 Spectrophotometer® (series number 110600536200 UJ60104 UJKR) and software Spectra Manager®, version 2.07.02 (scan speed at 400 nm/min, start from 750 nm, end at 250 nm, data pitch 1.0 nm, vertical scale 1-0, cycle times 1, photometric mode Abs, UV/Vis band width of 1.0 nm, response set in medium and scan mode in continuous), while fluorescence spectra were performed with UV detector Fluoro Max-P by Horiba Jobin Yvon® (series number 110600301700) and the software Fluorescence V3.5® (slit at 5 nm and variable excitation wavelength, while beginning of emission range was calculated adding 5 nm to the excitation wavelength and its end set at 800 nm); the excitation spectra were performed using the same spectrophotometer for the fluorescence (emission set at 554 nm, emission range from 250 to 520 nm, while increment at 1 nm).

2.3.3. Lifetime measurements

Lifetime measurements were done using a K2 phase-modulation fluorimeter (Dziwulska-Hunek et al. 2022). The sample was excited with 265, 270, and 280 nm waves and the fluorescence was observed through a KV550 cut-of filter ($\lambda > 550$ nm), following the observations made for absorbance and fluorescence spectra. Measurements were done in a 1 \times 1 cm cuvette, at room temperature, for 10 modulation frequencies in the range of 2–200 MHz, relative to the diffusing suspension Ludox® by Sigma Aldrich. Vinci2 software® was used in the analysis (Dziwulska-Hunek et al. 2022) and, if needed, some noisy points (not more than 3) were removed before analysis.

2.3.4. Prodigiosin extraction and purification by TLC

One week old cultures of PJ, D2, D4 and D6 strains were centrifuged in Sigma 6-16K® centrifuge for 20 minutes at RFC set at 8000. Supernatant was then discarded while containing pigment pellet was put into 25 mL Falcon® tubes and put into liquid nitrogen to be frozen for the -80°C freezer. For the lyophilisation, pigment samples were taken from the -80° C freezer and put in the machine Alpha 1-2 LD Plus® for 3 days at around -50°C. After that, pigment was ready to be suspended and analysed.

Lyophilization products were diluted in 20 mL of ethanol and disintegrated with the disintegrator machine Sonics Vibra-Cells®; the used parameters were the following: sonication for 3 cycles at pulse 9 (t1) and 15 (t2) and Amp1 35%. The sonication was repeated for other 5 cycles with the same parameters; after that, Falcon® tubes were centrifuged for 5 minutes at 1000 RCF in the Eppendorf Centrifuge 5818R®, so supernatant was taken and distributed in 12 of 2 mL Eppendorf® tubes. These were centrifuged again at max speed (about 16,9 RCF) for 10 minutes: supernatant was evaporated in Rotovapor R-200® by Büchi, dissolved in 2 mL of chloroform and collected in a glass bottle to avoid plastic contamination. The remaining pellet in the Falcon® was dissolved again in ethanol (a total volume of 20 mL) and left for about 2 months, to help the pigment to move to the supernatant.

For extraction, acidified methanol was used (pH 2.47): for each 2 mL of pigment dissolved in chloroform, 12 mL of the acidified solution were added in a 14 mL Falcon® tube (Xu et al. 2011). The tubes were made shaken at 150 rpm for 30 minutes at 30°C in Innova 42 Incubator Shaker Series® by New Brunswick. Later the tubes were centrifuged at maximum speed for 30 minutes in Sigma Laboratory® centrifuge; white pellet is obtained and the samples that previously presented different shades of pink and purple have all the same colour (Xu et al. 2011). The supernatant was taken off and evaporated in Rotovapor R-200® by Büchi, then suspended again in 2 mL of chloroform.

For TLC analysis two different plates were used: TLC-Plastic sheets silica gel 60® (without fluorescence indicator) pre-coated 25 sheets 20x20 cm and layer thickness 0.2 mm by Merk and TLC silica gel 60, 2 mm (12 Glass plates 20x20 cm) lot HX246150 (1.05745.0001). The plates were previously immersed in the TLC solution used and then made drying in the dark. The chloroform solution with the dissolved pigment was distributed in different amounts (depending on the type of plate used) on the plates with the machine Linomat 5®. The plates were put in glass holders, closed with aluminium foil, and made running about an hour in a 6 methanol:3 ethyl acetate:1 chloroform solution (Vu Trong Luong et al. 2018). Pigment was then scratched, put in 2 mL Eppendorf® tubes, diluted in 1.5 mL of methanol and centrifuged at maximum speed for 5 minutes in Eppendorf Centrifuge 5818R®; the supernatant was taken and put in other Eppendorf® tubes for further analysis.

3. RESULTS

3.1. Gram variability

3.1.1. Cultivation conditions

A first cultivation of the D2, D4, D6 and PJ isolates shown that prodigiosin production is inhibited when flasks are in shaking conditions and is influenced by the freshness of inoculum. In fact, during the first attempts, it was evident how isolates, let grown for several weeks and later used as inoculum in fresh LB, didn't produce any pigment anymore; on the contrary, using fresh cultures (maximum 15 days old) as inoculum in new flasks permitted to obtain high amounts of prodigiosin.

Generally, it was seen that after 3 days, cultures started to become pink, while after 15 days, they reached an highly violet colour (*Figure 11*); different isolates (D2, D4, D6 and PJ) presented differences in violet/pink shade, as well as different amounts of produced biofilm (*Figure 12*). Prodigiosin produced by those first attempts was lyophilized to perform the following spectrophotometric measurements.

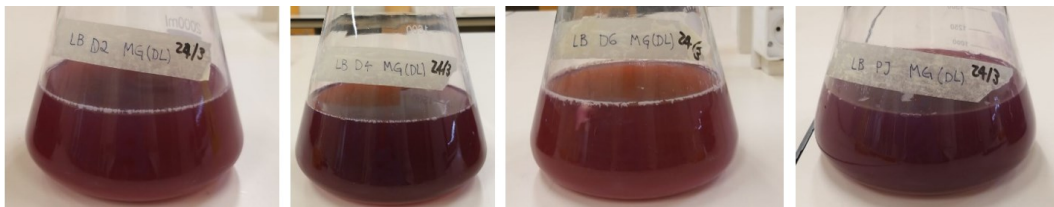


Figure 11. D2, D4, D6 and PJ in 1L volume after a month: cultures are highly violet with differences in shade.

Before starting the growth curve experiments, the 4 isolates were grown in Petri plates to see if there was some contamination and to analyse the isolates' growth on solid medium. For these reasons, 3 different dilutions (10^{-3} , 10^{-6} , 10^{-9}) were used to isolate the colonies of D2, D4, D6 and PJ, for a total of 12 Petri plates. Because of differences in morphology and colour between the colonies on the plates (*Figure 13*), ERIC-PCR test was performed to verify a possible contamination (*Figure 14*); so 7 samples were taken (named D2, D4A, D4B, D6A, D6B, PJA, PJB). After electrophoresis, all samples in gel had the same pattern (*Figure 14*) and differences in colony morphology could be explained by isolates' different sensitiveness to the environmental conditions on solid media and diversified prodigiosin production; so, the test also confirmed the absence of external contamination.



Figure 12. Second cultivation of the isolates D2, D4, D5 and PJ after 7 days; the flasks presented different shades because of differences in the prodigiosin and biofilm amount isolate-dependent.

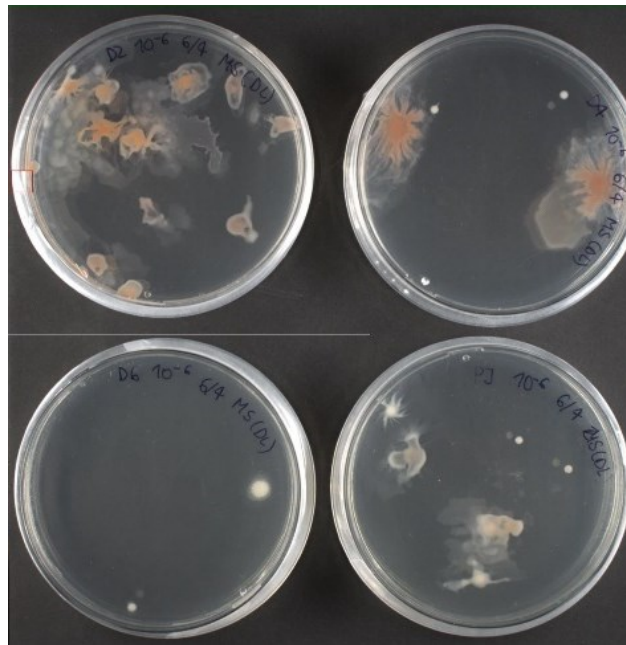


Figure 13. Petri plates for 10^{-6} dilutions.

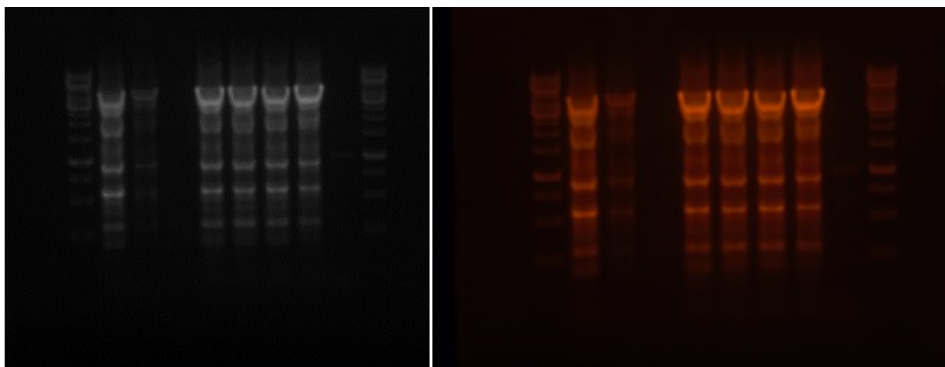


Figure 14. ERIC results, in two different colours, for the D2, D4, D6 and PJ cultures taken by Petri plates; contamination possibility was verified because of differences in shape and colour among the colonies. In the electrophoresis gel, starting from the right, there is the marker lane, D2, D4A, D4B, D6A, D6B, PJA, PJB and second lane of marker: the sample of D4A gave no results, but, because all the other samples presented the same pattern, it is evident that there was no contamination.

3.1.2. First growth curve attempts in flasks

Measurement of PJ growth curve was performed in bigger volume cultures to understand when changes in bacterial shape and Gram nature should have been expected. For this first experiment, from a starting volume of 300 mL of LB media with 500 μ L of PJ inoculum, 2 samples of 1 mL for each time point were collected: one it was used for the OD₆₀₀ measurements, while the other one, after centrifugation, was put in the freezer for later prodigiosin quantification. Slides for Gram staining were also taken to see at which exact point Gram variability happened, while pH was measured with pH tape to check the increase of its value. Samples were collected at the following timepoints: (t₀) 0 h, (t₁) 2 h, (t₂) 4 h, (t₃) 6 h, (t₄) 24 h, (t₅) 26 h, (t₆) 28 h, (t₇) 30 h, (t₈) 48 h, (t₉) 50 h, (t₁₀) 54 h, (t₁₁) 74 h.

This experiment needed to be repeated because some important growth values were missing (ex.: 10th-24th hour, 30th-48th hour), so the results wouldn't be reported. Nevertheless, it was noticeable the influence of oxygen in the pigment production: never opened cultures, used for other experiments, produced higher amount of prodigiosin, while aerated cultures, used for the growth curve measurements, didn't produce the same quantity of the wanted pigment. To verify this growth condition and to complete the missed information, another attempt was made, but, in this second case, one flask was used for the measurement, while a second one was kept closed to promote prodigiosin production.

After a week, prodigiosin production started also in the flask that was used for the growth curve measurements, after that the bottle was taken closed and never moved because of the end of the experiments (*Figure 15*): this confirmed the possible role of the opening and closing of the bottle in the prodigiosin production.

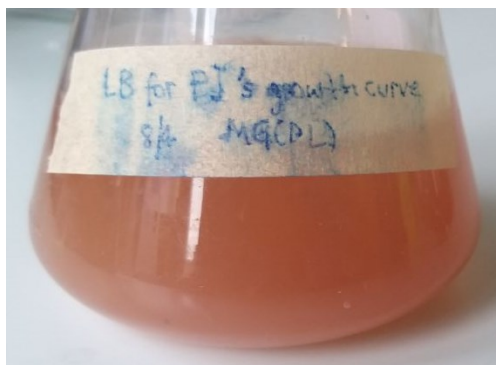


Figure 15. Flask used for the first growth curve measurement. During the experiment it presented no pigment production, while after the ending of the experiment, prodigiosin started to be produced, because, probably of changes in aerated and static conditions.

So, a second growth curve attempt was made, using the previous experiment parameters, but two flasks were prepared, as said before, to evaluate the pigment production. The second flask, prepared to check prodigiosin production in closed conditions, presented the pink colour (*Figure 16*) and the maximum OD₆₀₀ value, of about 1,2, was reached in 5 days' time.



Figure 16. Comparison between the never-opened bottle, that presents the prodigiosin's pink colour, and the one used for the measurements after 11 days' time (264 h).

The prodigiosin production followed the growth curve found in literature (Figure 1); in fact, the cultures started to become pink when entering the stationary phase (Figure 17) (Khanafari et al. 2006). If the pigment was produced only in non-aerated conditions, and its amount was necessary to make correlations between pigment production and bacterial growth, techniques for measuring the OD₆₀₀ without opening the flask should be used, like Erlenmeyer flasks.

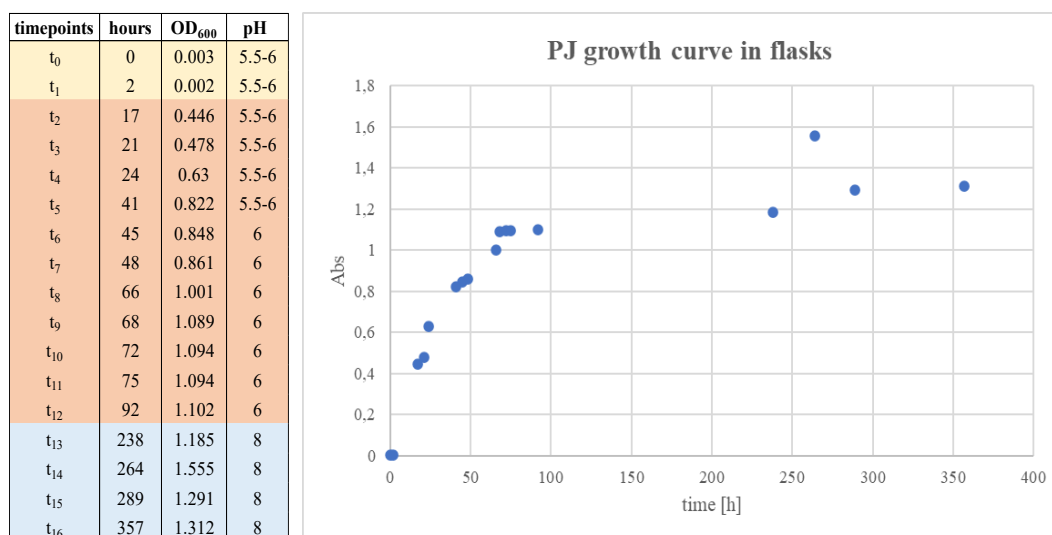


Figure 17. On the right, there is the table with the pH and OD₆₀₀ values for each timepoint, while on the left the values are put in a graph; different colours represents different growth phases (lag phase - yellow, exponential growth - red, stationary phase - blue).

Photos at the microscope from the first growth curve experiment were taken, as said before, to see when bacteria changed their Gram nature, but repetition of the experiment were needed. In fact, timepoints pictures were missing due to bacterial low concentration; secondly, the taken photos had different coloured background, so it was not possible to be sure about the Gram nature of those samples (Figure 18).

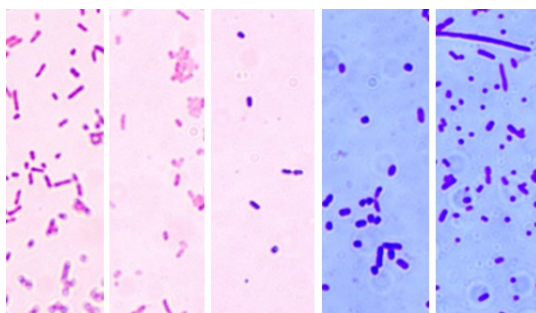


Figure 18. Some shortcuts from the microscope pictures from first growth curve attempts in flasks.

3.1.3. Growth curve measurements in 96-wells-microplates

The aims of these experiments, that represented the replication of B.S. student Aleksandra Odobrina's work (Odobrina 2021), were (1) to follow the growth of *S. marcescens* isolates in both LB and LB + 1% glucose medium, where prodigiosin production is inhibited, (2) to collect slides for Gram nature analysis and (3) to assess differences in pigment production, that was later quantified. The OD₆₀₀, pH value, Gram nature and prodigiosin amount were checked after (t₁) 2 h, (t₂) 4 h, (t₃) 6 h, (t₄) 12 h, (t₅) 24 h, (t₆) 30 h, (t₇) 36 h, (t₈) 48 h, (t₉) 54 h and (t₁₀) 60 h (see *paragraph 7.1.1* in the *Appendix* for microplate configuration, OD₆₀₀ and pH values details).

3.1.3.1. Growth and size analysis

In the first attempt using only PJ, the controls were contaminated, firstly, because of the use of parafilm to close tightly the cover, reason why this attempt will be referred as "not aerated conditions", and, secondly, due to some condensation phenomena happening inside the plate. Besides the cross-contamination, it was already visible the difference in prodigiosin production and the increasing of pH values, related to prodigiosin production (all values are reported in *paragraph 7.1.1.1* in *Appendix*).

A second attempt with only PJ was made taking measurements at the same timepoints but not using the tape to close tightly the cover, reason why the attempt will be referred as "aerated conditions"; in addition, some precautions were taken to avoid the cross-contamination: at every measurement the covers were disinfected using sterilized papers with ethanol 70%; to avoid condensation, a different plate disposition was used to let each filled well being surrounded by empty wells (*Table A11* and *A12* in the *Appendix*), so at the end 4 plates were used, instead of 1 (2 for LB medium and 2 for LB + 1% glucose medium); while taking the measurements under the laminar, the plates have never been placed on the colder metal desk to avoid the differences in temperatures that could have contributed to the previous condensation phenomena. Using these care tips, the cross-contamination did not happen.

A third attempt with only PJ was performed with the same plate configuration of the previous attempt, but the experiment was done with fresh inoculum, coming from the -80°C freezer, for this reason the experiment will be referred as "fresh inoculum". In fact, it was seen that after the ending of the second attempt, the LB

wells had not only continued to produce more prodigiosin, but the samples colour was more orange than pink (*Figure 19*). The culture tends to become orange and loose the capacity of producing the pigment as time goes by (*Figure 19*), so starting with a fresh inoculum helped in the prodigiosin quantification; last time, an inoculum from almost two months old flask was used, but the wells produced less pigment than expected even if the initial flask was very purple because of the prodigiosin. In this third attempt, the wells were pinker just by sight (*Figure 20*) and the pH increased more rapidly than before, probably because of higher growth rate and prodigiosin amount.



Figure 19. On the left, picture of the first attempt plate after 36 days (the samples are particularly orange); in the middle, flasks produced the 16th of May (PJ culture was used for the inoculum of first and second attempt); on the right, flasks from 22nd of April. It is evident how the pink and purple shade changed from time to time; in addition, by the time the culture aged and produced less pigment, the colour got more orange.

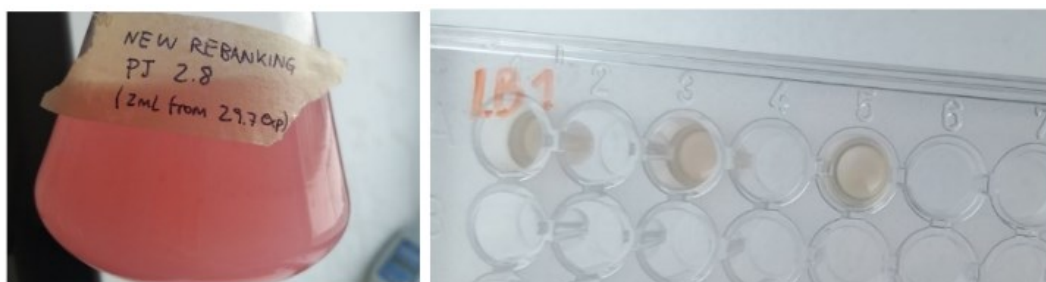


Figure 20. On the right, the flask from the 29th of July produced by using the fresh inoculum; on the left, detail of the third experiment plate at the end of the 3 days measurements: the wells were particularly pink.

For the fourth attempt, a Gram-positive and a Gram-negative species, whose Gram nature was sure, were used to better assess the later Gram staining results of PJ isolate; the experiment was performed using the same microplate configuration and timing. In addition, from this attempt on, even tape pieces, used to guarantee the plates closing and to avoid external contamination, were definitely removed: in this way, every variable that could have influenced the aeration was deleted.

After having used PJ to improve the experimental conditions and to collect the first data regarding pigment quantification, Gram variability, and growth speed, a fourth, fifth and sixth attempt were performed using a second isolate, D6, chosen because in Aleksandra Odrobina's work (Odrobina 2021) it was the one producing more prodigiosin. From these last attempts, it was evident that, even in this case, bacteria changed shape from bacillus to round because of glucose. In addition, D6 grew faster than PJ and growth was faster in glucose than LB. After having left the microplates in the wardrobe after the end of the experiments, it was seen that prodigiosin production has started even in glucose-rich medium: this topic will be analysed in *paragraph 3.1.5.*, where cultures in glucose were grown in bigger volumes.

In conclusion, from growth curve experiments in microplates, it was evident that PJ grew slower than the D6 and produced less prodigiosin as well. In addition, glucose presence influenced not only the growth rate in both PJ and D6, that grow faster than in just LB, but also the bacterial shape. In fact, it was noticed that after around 12 hours, in both isolates, the initial bacillus shape started to get rounder in LB + 1% glucose, while in normal LB, bacteria maintained their elongated shape. This last phenomenon could be explained by changes in division speed: because glucose accelerates the growth, bacteria don't have enough time to reach the elongated shape. Besides changes in shape and medium, it was seen that bacteria decreased their size with the time going by, as it is normally expected with cultural aging. In addition, changing the operative conditions, it was possible to improve the experiment development, for example, filling alternatively the wells, using a new microplate configuration and disinfecting at each measurement with ethanol the microplates' covers helped in avoiding the cross-contamination and condensation inside the plates. Furthermore, prodigiosin production is highly correlated to inoculum freshness, which should be taken into consideration. Down below, results from 5th and 6th attempt are reported because representative of the final consideration; pH values related to prodigiosin amount are reported in *Figure 27* and *Figure 28*.

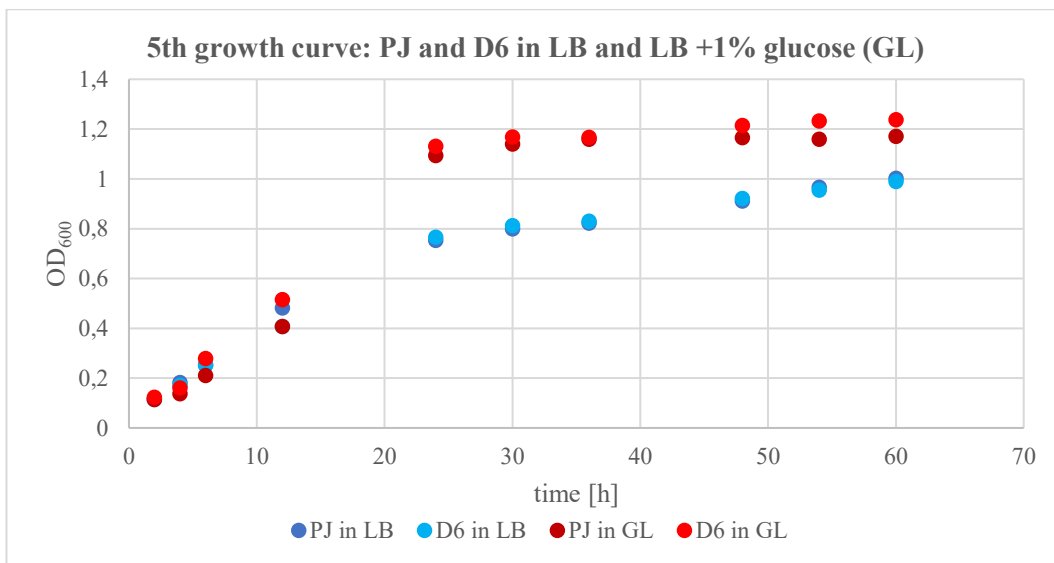


Figure 21. Growth curve of PJ and D6 in both LB and LB +1% glucose (GL) from the 5th growth curve attempt. Standard deviation values will be reported in the Appendix.

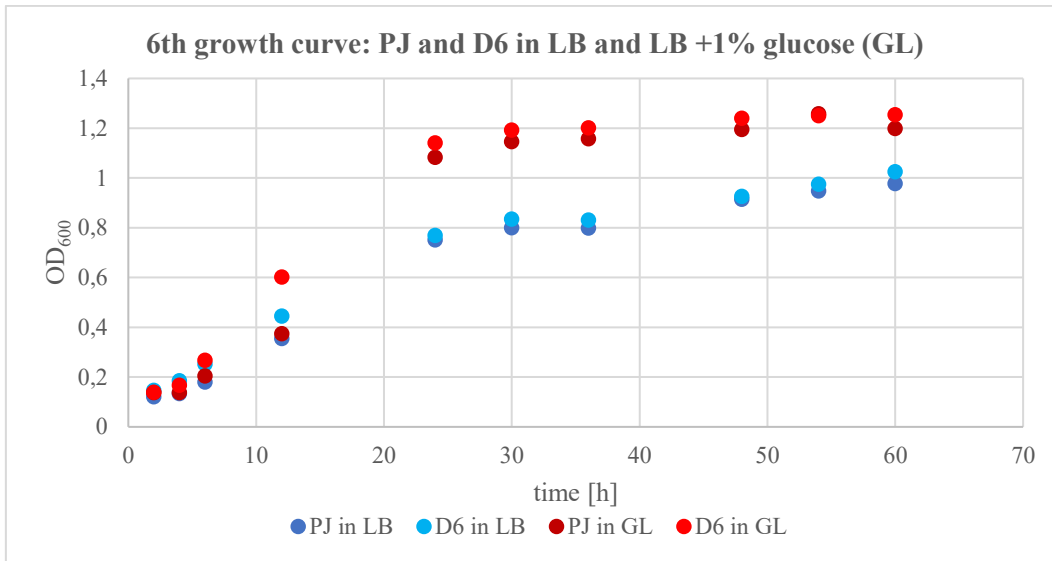


Figure 22. Growth curve of PJ and D6 in both LB and LB +1% glucose (GL) from the 5th growth curve attempt. Standard deviation values will be reported in the Appendix.

From the growth curve graphs it is visible that D6 presents higher OD₆₀₀ values than PJ, both in LB and LB + 1% glucose (GL); also, differences between values in LB or glucose are evident (Figure 21 and Figure 22). Concerning the rounding phenomenon in glucose, in LB, the length and width values of both PJ and D6 (Figure 23 and Figure 24) don't get closer with the time going by, while in LB + 1% glucose, the distance between length and width values gets closer measurement after measurement (Figure 23). In the Appendix, standard deviation values are reported with all respectively OD₆₀₀, length and width values.

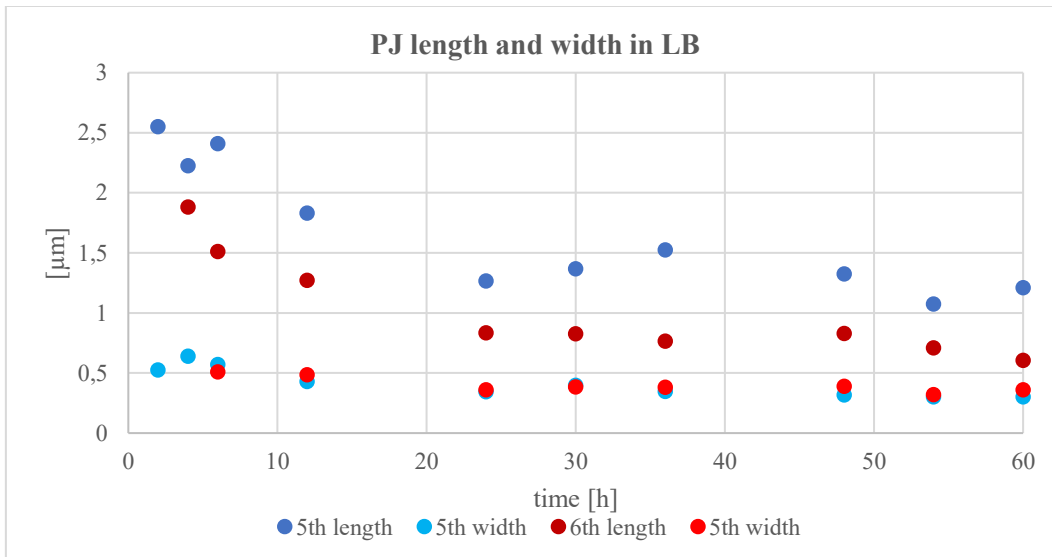


Figure 23. Graphs reporting the length and width average values of PJ in LB, measured for each timepoint during the 5th and 6th attempt. Deviation standard values will be reported in the Appendix.

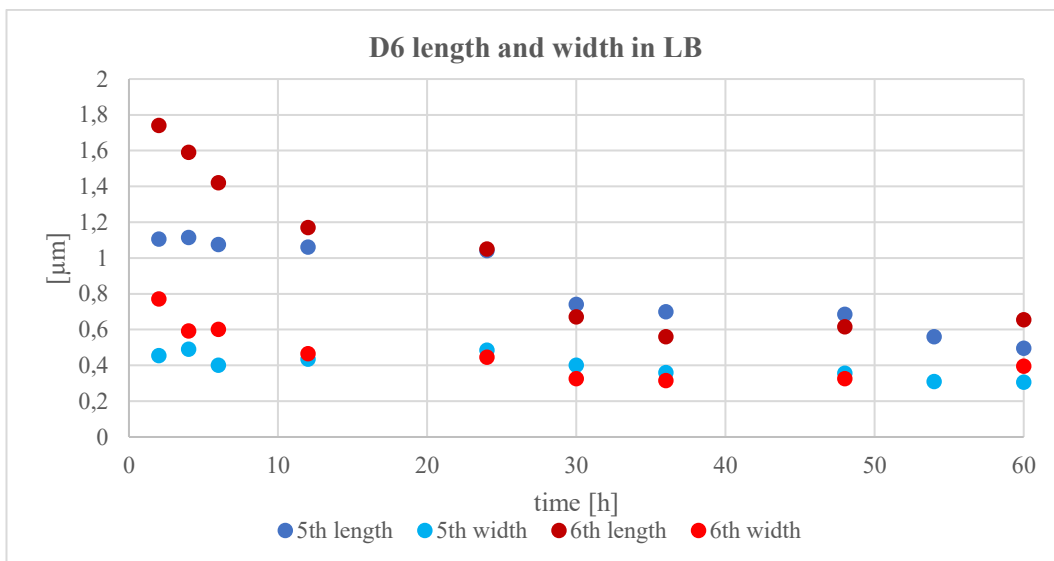


Figure 24. Graphs reporting the length and width average values of D6 in LB, measured for each timepoint during the 5th and 6th attempt. Deviation standard values will be reported in the Appendix.

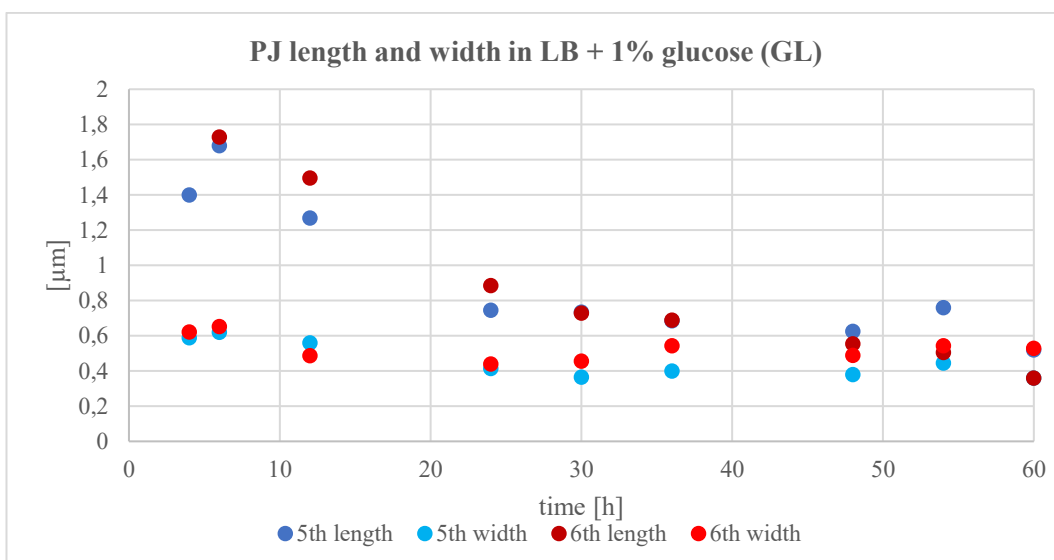


Figure 25. Graphs reporting the length and width average values of PJ in LB + 1% glucose (GL), measured for each timepoint during the 5th and 6th attempt. Deviation standard values will be reported in the Appendix.

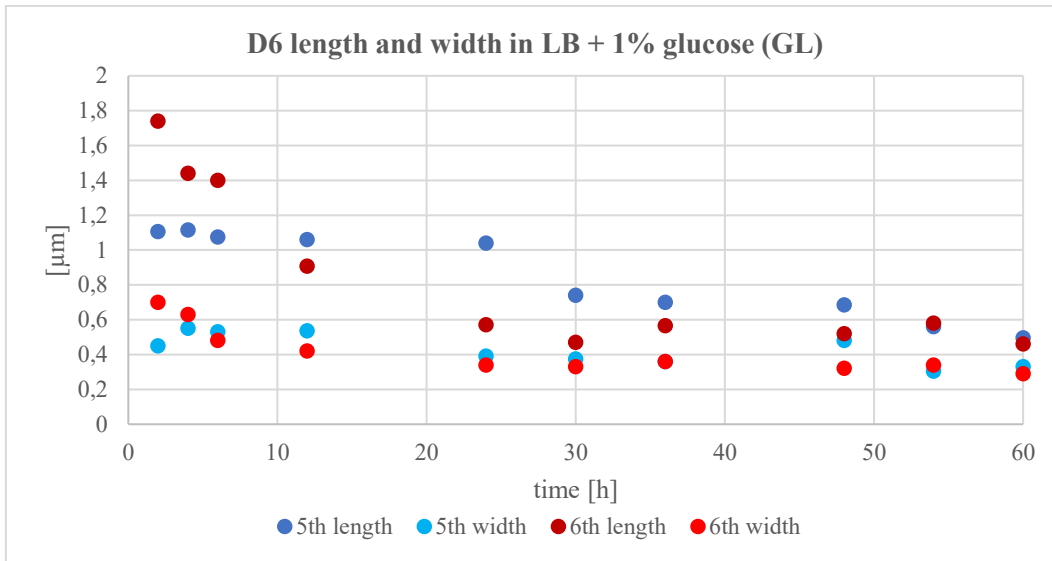


Figure 26. Graphs reporting the length and width average values of D6 in LB + 1% glucose (GL), measured for each timepoint during the 5th and 6th attempt. Deviation standard values will be reported in the Appendix.

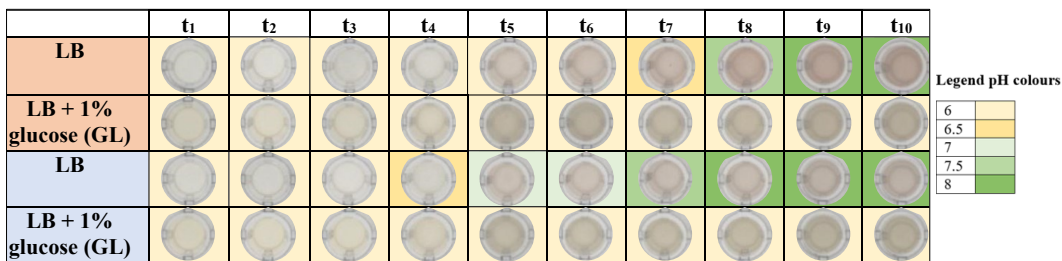


Figure 27. Prodigiosin production differences between LB and LB + 1% glucose from fifth attempt (PJ in red and D6 in blue); D6 isolate's pH becomes alkaline faster and less gradually than PJ, as its growth rate is faster (on the right the legend of pH colours is reported).

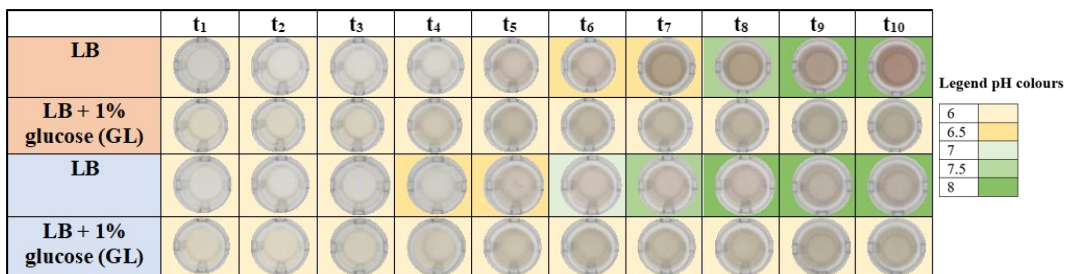


Figure 28. Prodigiosin production differences between LB and LB + 1% glucose from sixth attempt (PJ in red and D6 in blue); D6 isolate's pH becomes alkaline faster and less gradually than PJ, as its growth rate is faster (on the right the legend of pH colours is reported).

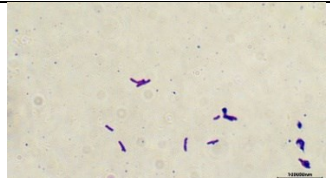
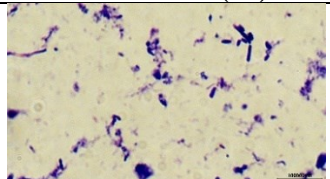
3.1.3.2. Gram staining and microscope analysis

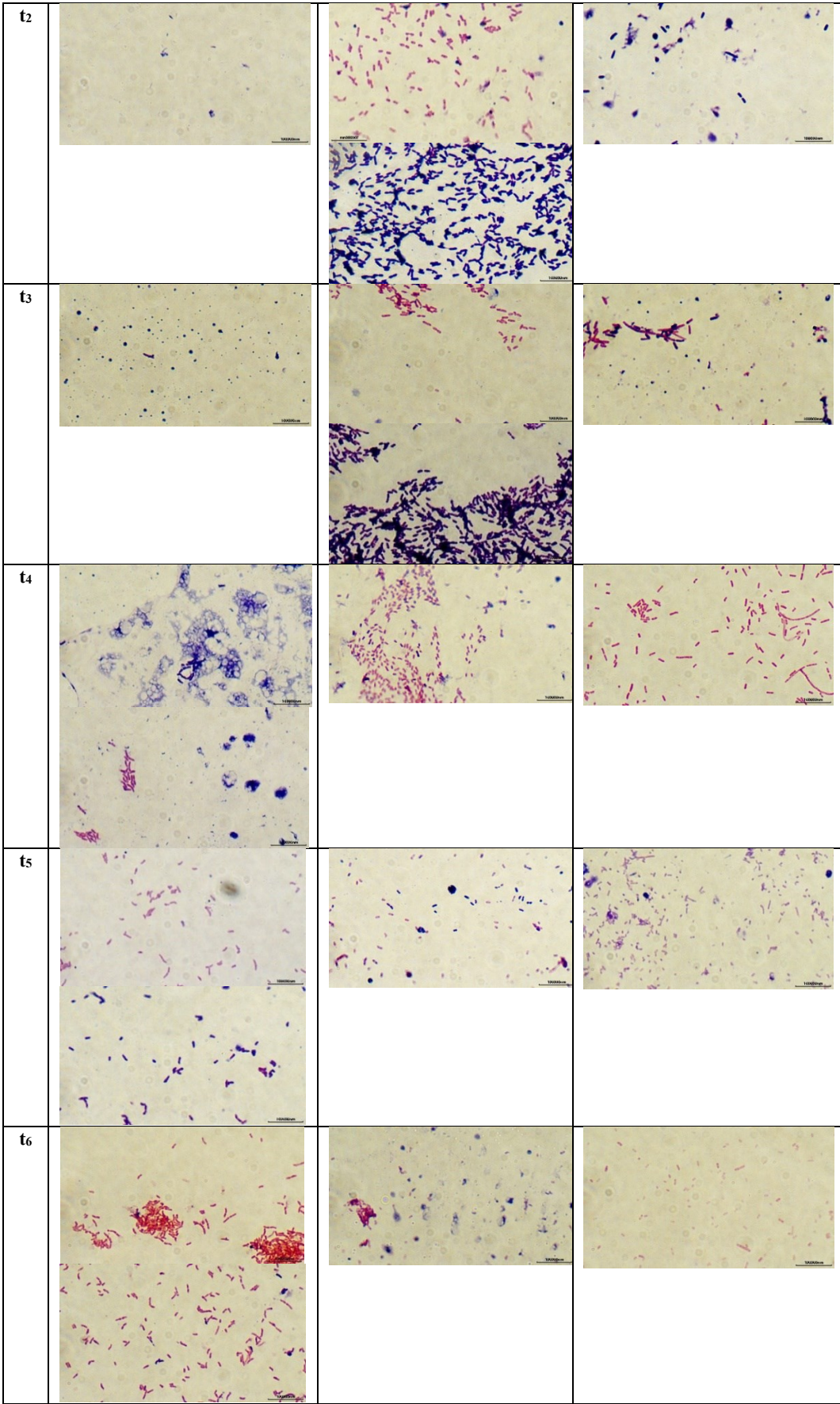
Improvements in the microscope analysis were made after several attempts, in particular, it was evident that the low quality of the pictures and the differences in the color background were caused by the overuse of tape to label the slides and dirtiness of them. So, the results from “not aerated” (first attempt) and “aerated conditions” (second attempt) shown that the isolate PJ didn't change Gram nature, because the bacteria had the typical Gram-negative red color.

After the first and second attempt were performed, few adjustments have been done: firstly, the Gram staining method was slightly changed using the one by “*Mikrobiologia środowiska*” (Kostka 2014), secondly the Lugol solution was freshly produced (see details in *Methods* section). In addition, control samples were made with two different Gram-positive and Gram-negative species: in this way, it was possible to understand the shade that is expected from Gram-negative or positive bacteria independently of the microscope settings, light intensity, and background contrast. The staining results from the third attempt, referred as “fresh inoculum”, confirmed the Gram-negativity of PJ isolate, differently from B.S. student Aleksandra Odrobina's results (Odrobina 2021), where bacteria started to become Gram positive from t_6 . As said before, the bacteria grown in LB +1% glucose medium had rounder shape, that could be better studied using the electronic microscope.

The results of the fourth attempt, where both PJ and D6 were used, were not clear: even Gram-positive and negative bacteria, whose nature was certain, presented changed Gram nature, which should have not (*Table 2*). Because the only thing that was different was the used crystal violet solution, which came from a new bottle, that wasn't shaken before usage, the cause of the unreliable results was considered being stain wise. So, during PJ and D6 growth curves measurements, four samples for each timepoint were taken (8 in total considering both PJ and D6): two of the four were stained with “crystalized” violet, which means that the solution wasn't shaken or put into a centrifuge to dissolve the crystals, and “not crystalized”, where a volume of about 30 mL of crystal violet was put into centrifuge for 10 minutes at maximum speed. This last solution presented a pellet made of all the precipitated crystals (≈ 5 mL), accumulated at the bottom of the Falcon® tube, meaning that the crystals amount was high considering the used volumes. It is evident the difference between the “crystalized” and “not crystalized” samples: in the first ones Gram nature changes, while the in the second ones it doesn't. In this last case the picture are also clearer and the *S. marcescens* isolates stain always as Gram-positive. For these reasons, it is reasonable to think that, from the obtained results, the isolates don't change nature and the Gram variability, that was seen in previous works, was probably caused because of human mistakes. In fact, this phenomenon was impossible to check by Gram staining, so this hypothesis will be confirmed by HPLC analysis, reported in the next chapter (3.1.4). Results from the sixth attempt (*Table 3*) are reported as representative of the whole experiment; all microscope pictures from other attempts are reported in the *paragraph 7.1.1.2* in the *Appendix*.

Table 2. Microscope pictures from Gram-positive and negative bacteria, used as reference, and S. marcescens isolate PJ: the fourth attempt was the one making me wonder about the stain influence in the Gram nature results; in fact, even the references presented changed Gram nature.

Gram standards – fourth attempt			
	Gram +	Gram –	<i>S. marcescens</i> (PJ)
t_1		no picture taken	



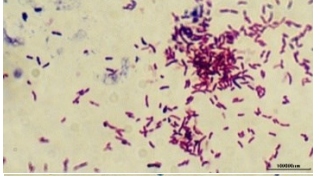

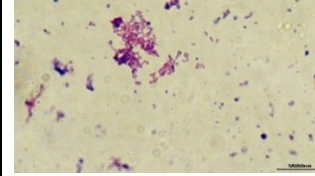
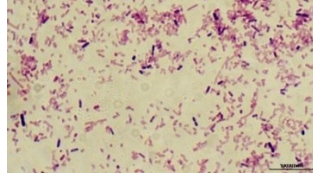
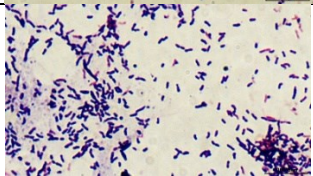
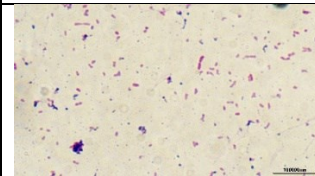
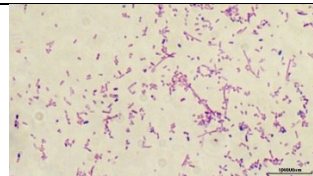
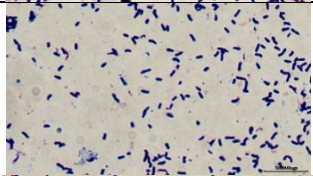
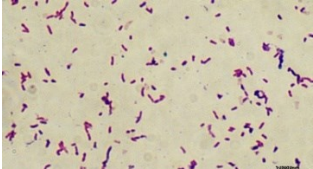
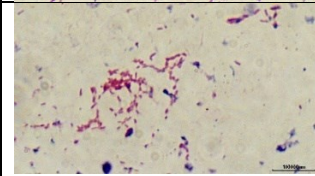
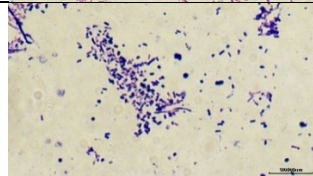
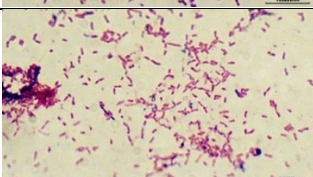
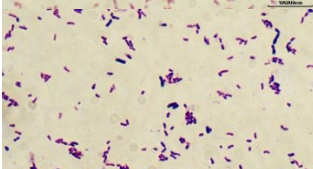
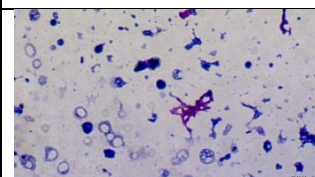
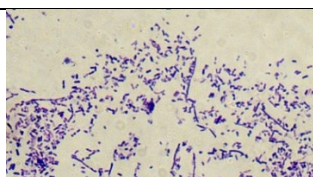
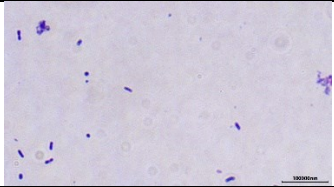
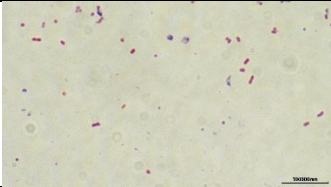
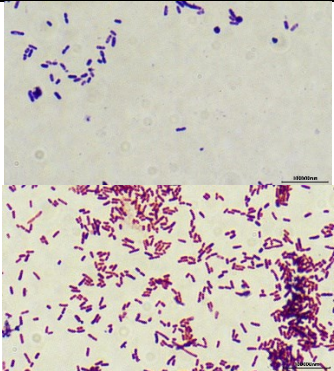
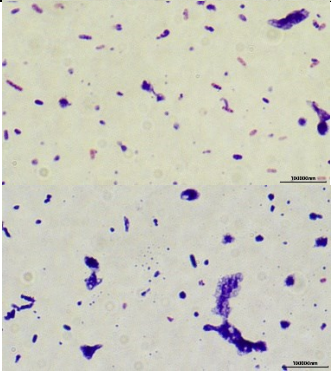
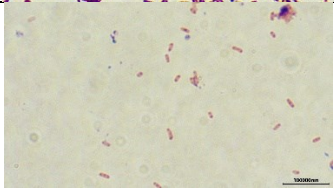
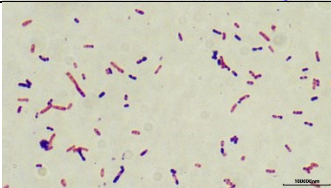
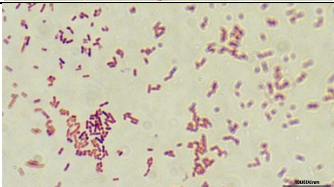
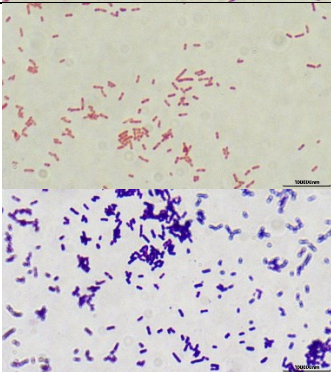
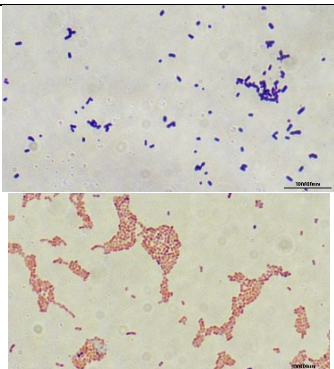
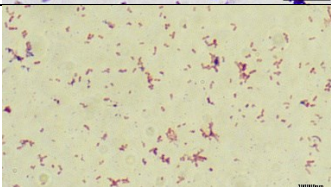
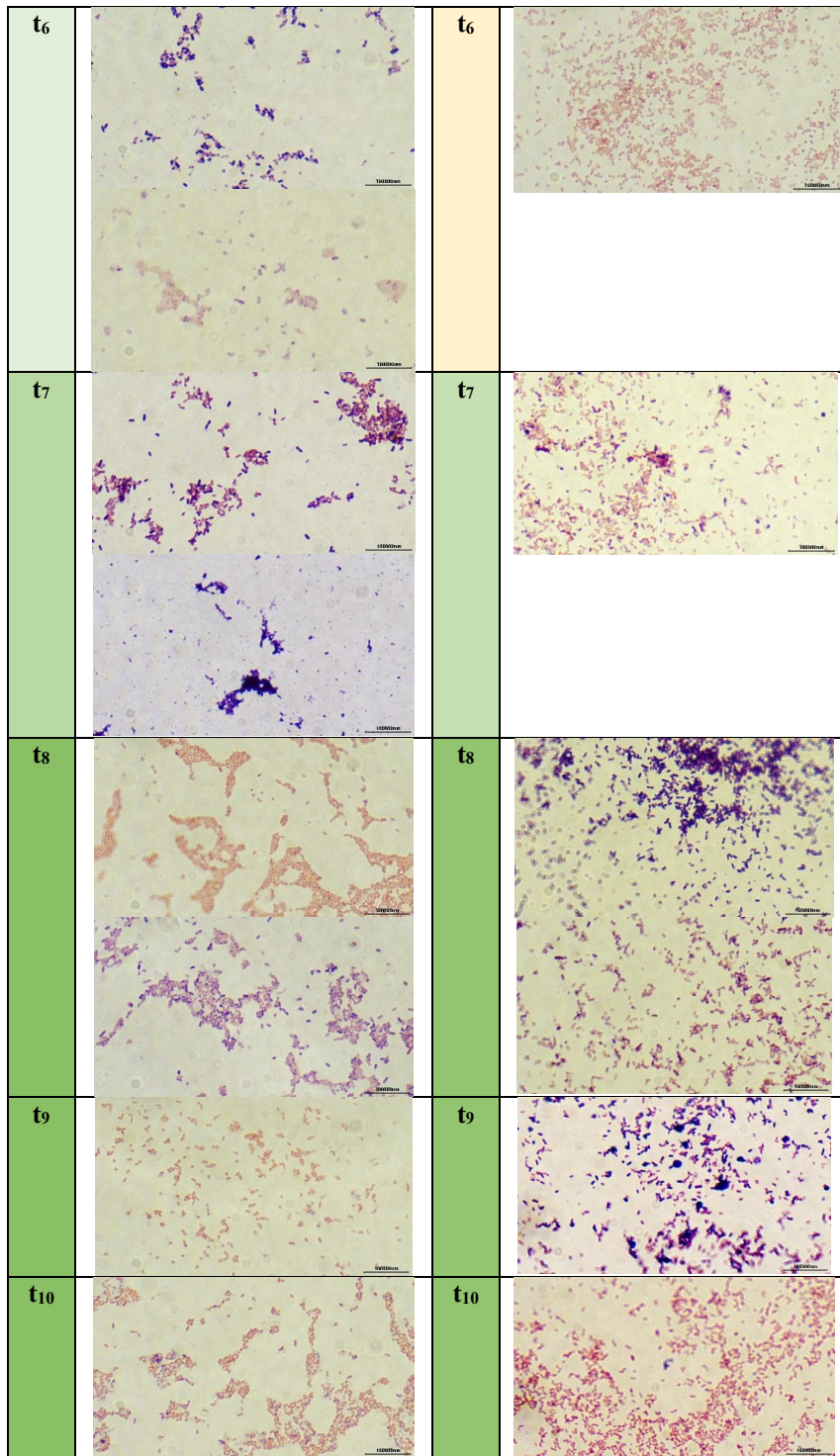
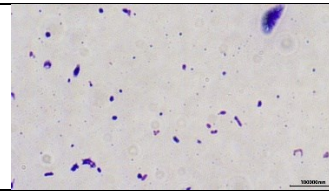
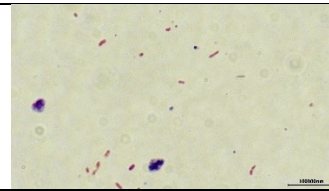
t7	 		
t8			
t9	 		
t10	 		

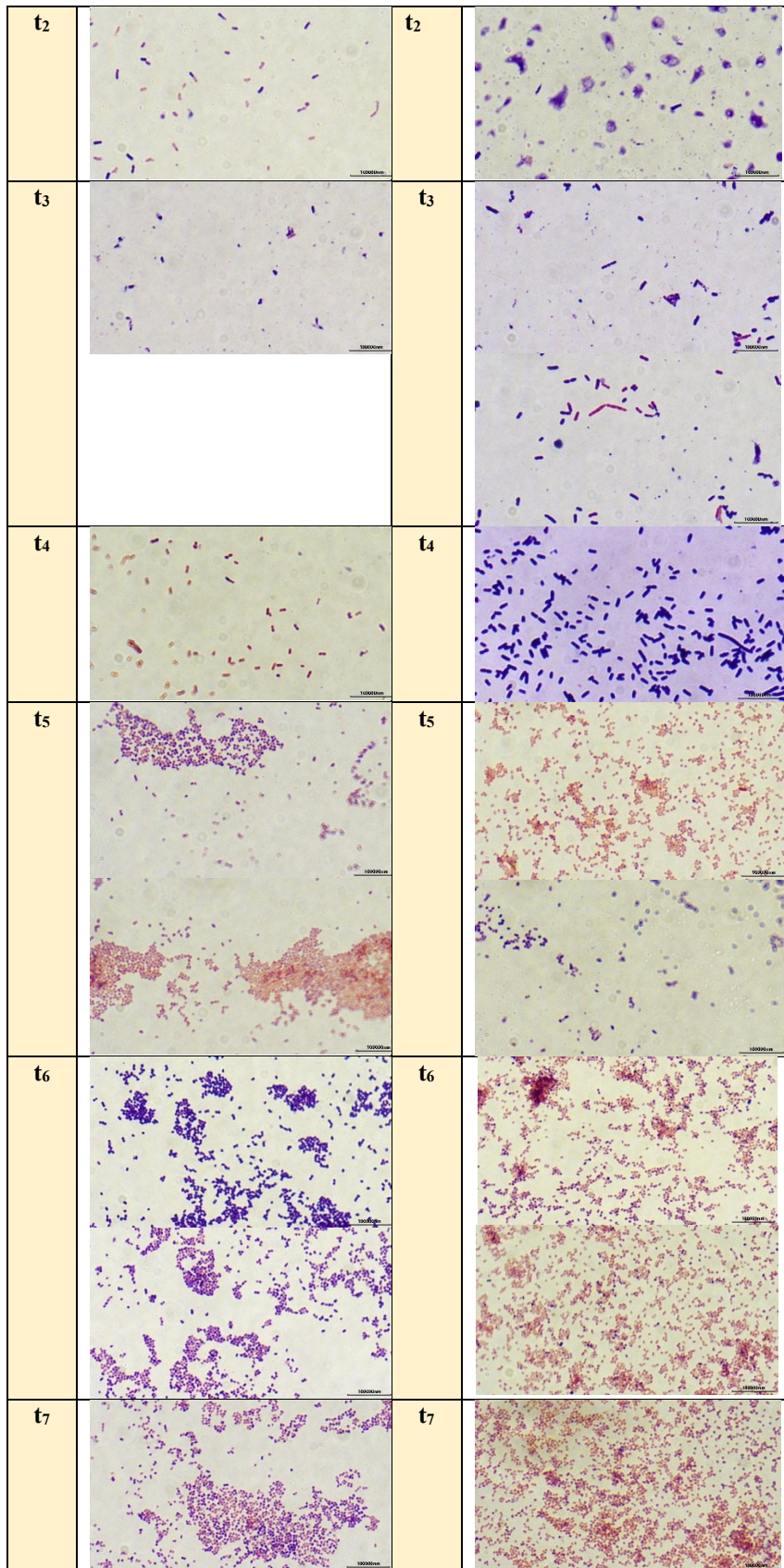
Table 3. Sixth attempt results from microscope visualisation: firstly, “crystalized” samples in both LB and LB + 1% glucose (GL), secondly, “not crystalized” samples in both LB and LB + 1% glucose (GL); below, pH values are reported with the pH colours legend.

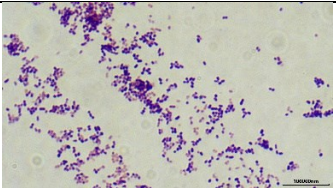
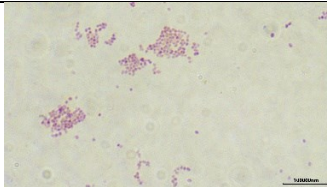
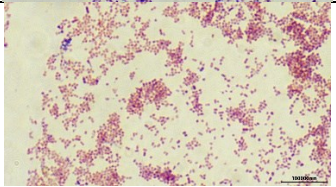
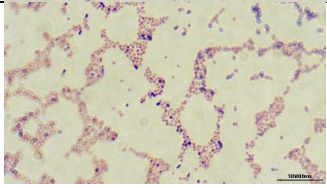
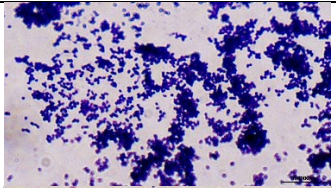
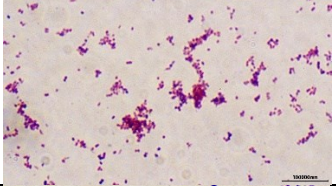
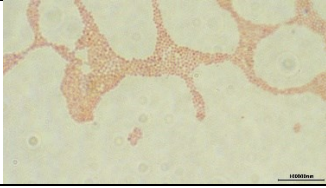
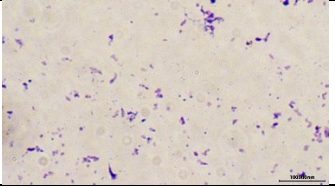
6	6.5	7	7.5	8
---	-----	---	-----	---




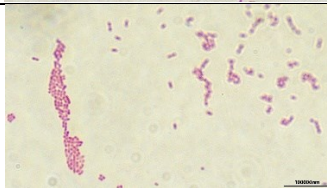

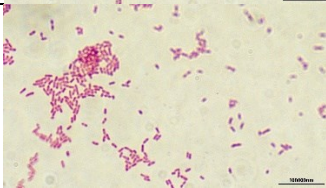
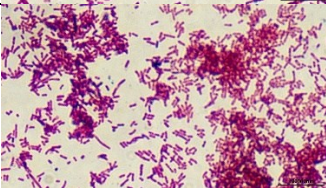
SIXTH ATTEMPT in LB - CRYSTALIZED			
	D6		PJ
t ₁		t ₁	
t ₂		t ₂	
t ₃		t ₃	
t ₄		t ₄	
t ₅		t ₅	

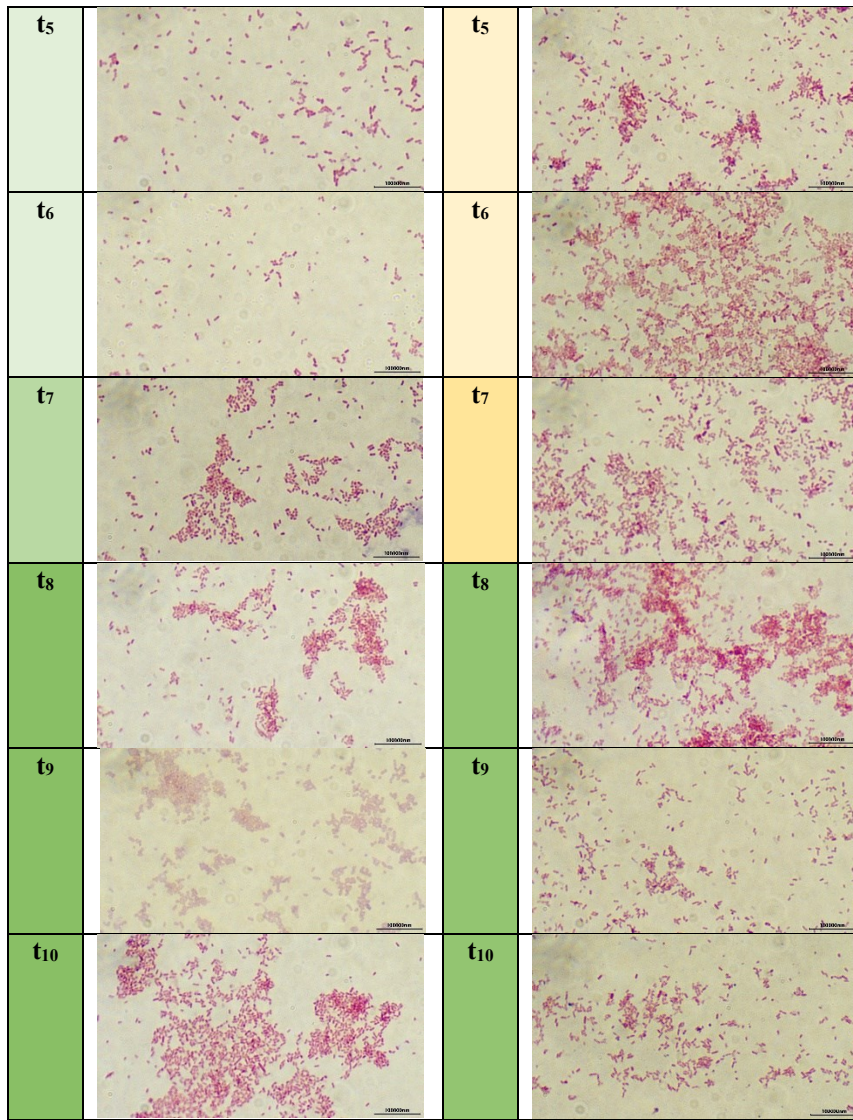


SIXTH ATTEMPT in LB + 1% glucose (GL) - CRYSTALIZED			
	D6		PJ
t1		t1	

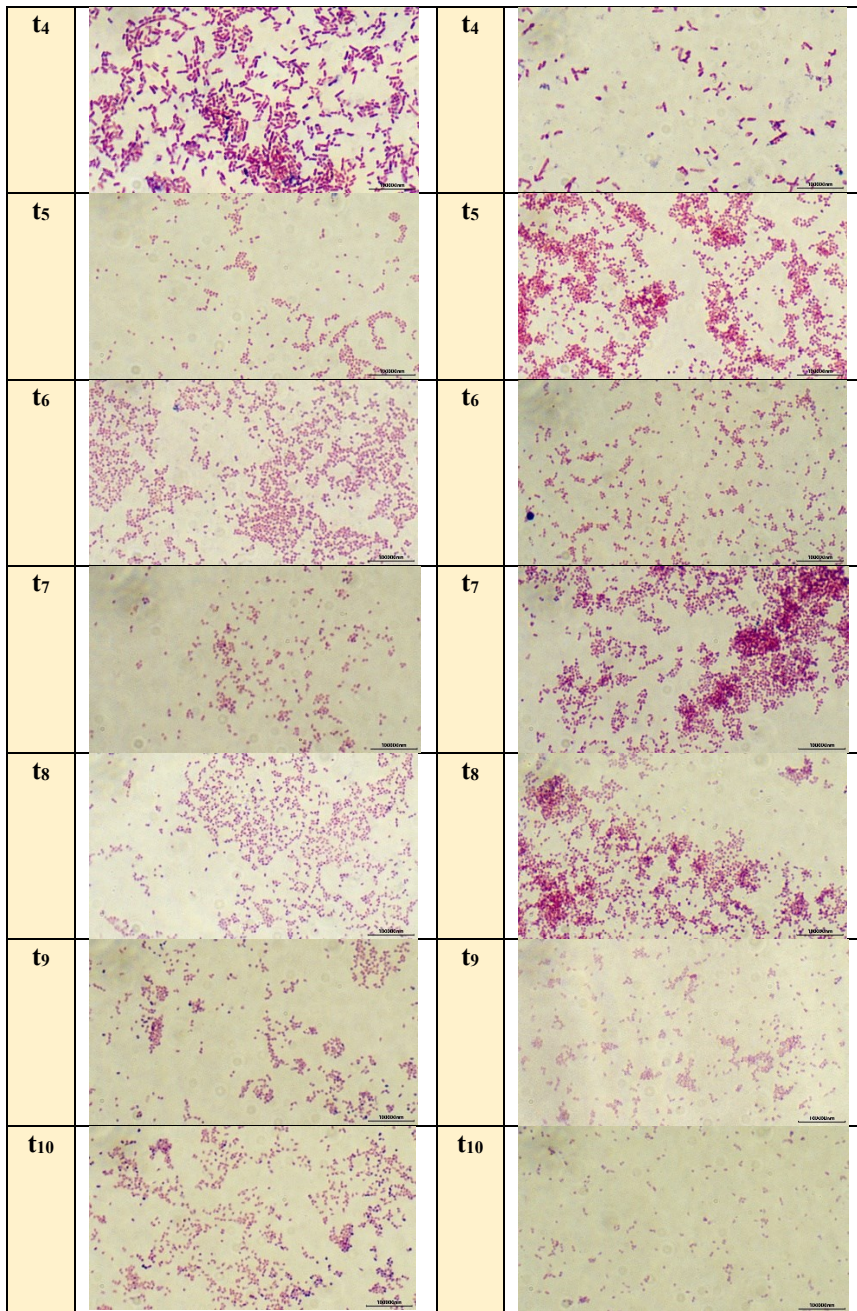


			
t8		t8	
t9		t9	 
t10		t10	

SIXTH ATTEMPT in LB - NOT CRYSTALIZED			
	D6		PJ
t1		t1	no photo taken
t2		t2	
t3		t3	
t4		t4	



SIXTH ATTEMPT in LB + 1% glucose (GL) - NOT CRYSTALIZED			
	D6		PJ
t1	no photo taken	t1	no photo taken
t2	no photo taken	t2	no photo taken
t3		t3	



3.1.4. LPS isolation and HPLC analysis

3.1.4.1. Sugars analysis

The LPS is characteristic of Gram-negative species, and it is not found in the Gram-positive ones: being able to isolate it and analyzing with HPLC its composition, in terms of carbohydrates, helps in the recognition of the isolates' Gram-nature. To analyze the cultures' LPS carbohydrates, PJ sample (120 μ L total volume) was taken from the -80°C freezer: 60 μ L of fresh inoculum were distributed between a 15 mL falcon with 6 mL of LB and a 500 mL flask in a 300 mL LB volume; 100 μ L from the falcon were then used to cultivate a Petri plate with solid LB. After 10 days, 6 flasks with 300 mL of LB each were inoculated respectively with 500 μ L of the culture from the 500 mL flask: 3 bottles were not shaken and labelled as "stable conditions", while the other 3 were shaken at 120 rpm and labelled as "shaking conditions" (Figure 29). In this way, 3 replicates were obtained for each condition of interested, whose difference in prodigiosin production could have been related to the processes of biofilm formation (Slater et al. 2003) and QS (Williamson et al. 2005), that have an important role in the genetic regulation of prodigiosin biosynthesis (Figure 1 and Figure 8).



Figure 29. Pictures of the 3 replicates (n°1,2,3) in stable (on the left) and shaking (on the right) conditions.

After a month from the starting inoculum, the 6 bottles were centrifuged to obtain the pellet used for the LPS isolation (see the procedure in *Methods, paragraph 2.1.6*). From each bottle, 2 phases were obtained, the phenolic and the aqueous one, so samples were named in the following way (Figure 30):

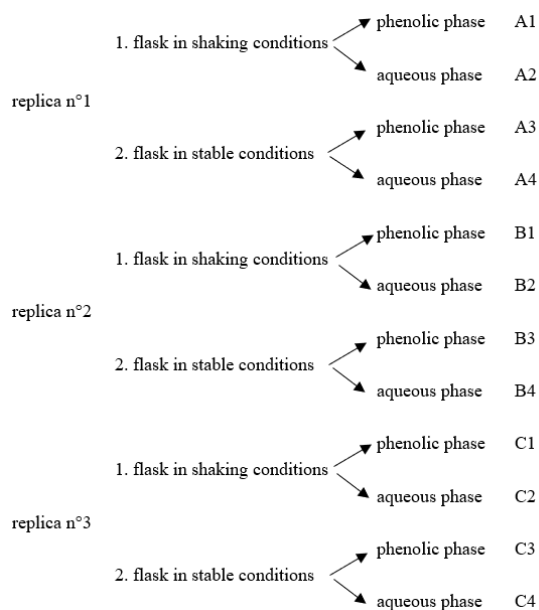


Figure 30. Samples' names from PJ's LPS isolation.

The naming of the samples is important because then it will be used as reference in the HPLC results. It was also important to quantify the final isolated LPS so in the following table (Table 4) the weight of empty Eppendorf tubes (A), the weight of Eppendorf tubes + LPS (B) and the final weight of LPS (B-A) are reported. At the end, samples containing 1 mg of LPS per 200 μ L were obtained thanks to the addition of different amounts of MilliQ ultrapure water (MQ).

	A (g)	B (g)	B-A (g)
A1	0.9701	0.9741	0.0040
A2	0.9759	0.9903	0.0144
A3	0.9715	0.9757	0.0042
A4	0.9734	0.9905	0.0171
B1	0.9755	0.9793	0.0038
B2	0.9712	0.9835	0.0123
B3	0.9756	0.9773	0.0017
B4	0.9788	0.9931	0.0143
C1	0.9763	0.9791	0.0028
C2	0.9754	0.99	0.0146
C3	0.9776	1.0376	0.0600
C4	0.9800	0.9883	0.0083

Table 4. Table with reported weight of empty Eppendorf tubes (A), the weight of Eppendorf tubes + LPS (B) and the final weight of LPS (B-A).

Since the very first steps of the experiment, the tubes containing prodigiosin shown a purple color (Figure 31, picture a), in particular, the phenolic phase, before the dialysis step (Figure 31, picture c); after the lyophilization, the samples still presented the typical pink color, even if more lightly.

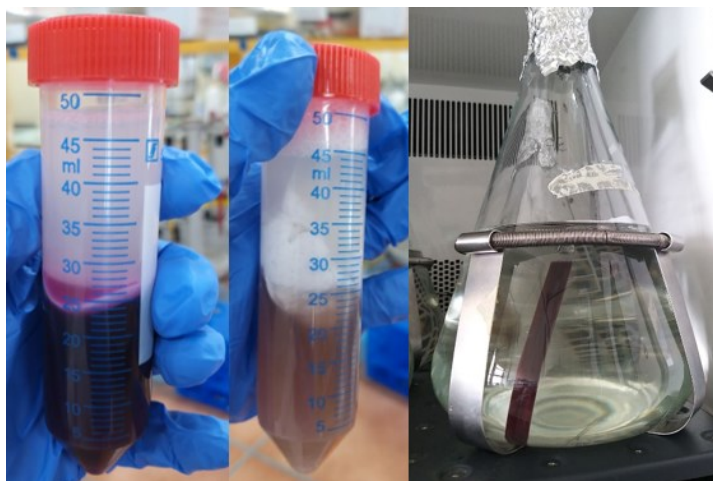


Figure 31. Starting from the left, (a) falcon tube containing the two phases, the phenolic (bottom) and the aqueous (top) one, from the stable-conditions flask; (b) falcon tube containing the aquatic (top) and phenolic phase (bottom) from the shaking conditions flask; (c) membrane containing the phenolic phase from shaking condition flask (the flask had a purple colour because of prodigiosin presence) ready for dialysis.

From the HPLC results, whose output shown the carbohydrates composition of LPS, it was possible to confirm the Gram-negative nature of the culture, because, if Gram-positive, the isolates' HPLC spectra wouldn't have shown any peak. In addition, it seemed that PJ's LPS sugars had a similar distribution among the different replicates, in both phenolic and aqueous phase (*Table 5*). In Bonhomme and collaborators' work, from which this protocol comes, it is said that LPS is expected to be found in the phenolic phase, but, in some cases, like this one, the aqueous phase can present the LPS sugars too (Bonhomme et al 2020); so, both phases were taken into consideration for the carbohydrates type analysis. Particularly, in A1, B1 and C1 (phenolic phase, shaking conditions), mannose, glucose and unprotonic galacturonic acid were present at the same ratio; in A3, B3 and C3 (phenolic phase, stable conditions), the main sugars were mannose, rhamnose, glucose, xylose and unprotonic galacturonic acid. A2, B2 and C2 (aqueous phase, shaking conditions) had in common mannose, rhamnose, glucose, xylose and unprotonic galacturonic acid, but only B2 presented ribose (integral area of about 18.3). On the other hand, A4, B4 and C4 (aqueous phase, stable conditions) had mannose, ribose, rhamnose, glucose, xylose and unprotonic galacturonic acid; so, ribose was present in B4 and C4 in minor amounts (integral area of about 2 and 5, respectively). So, the results obtained from shaking (A1, B1, C1 and A3, B3, C3) and not shaking/stable conditions (A2, B2, C2 and A4, B4, C4) in both phases, the phenolic and aqueous ones, presented the same pattern with slight differences in some sugars that, generally, didn't present high values of integral area, so their contribution to the final LPS carbohydrates' composition was minor than the one of main sugars; but, above all, being able to identifying the different LPS sugars confirmed the Gram-negativity of the isolates.

A1			B1			C1		
time	integral	sugar	time	integral	sugar	time	integral	sugar
10.345	59.453	mannose	10.287	53.658	mannose	10.265	62.845	mannose
\	\	\	\	\	\	11.764	2.359	ribose
\	\	\	\	\	\	13.137	2.366	rhamnose
21.441	35.492	glucose	21.068	42.554	glucose	21.043	22.869	glucose
34.871	2.662	un. galact.	34.204	1.142	un. galact.	34.042	2.045	un. galact.
A2			B2			C2		
10.338	41.797	mannose	10.282	36.285	mannose	10.229	50.285	mannose
\	\	\	12.216	18.326	ribose	\	\	\
12.743	5.057	rhamnose	12.634	4.345	rhamnose	13.209	2.343	rhamnose
21.153	17.609	glucose	20.787	16.401	glucose	20.893	36.799	glucose
24.379	3.301	xylose	24.055	2.055	xylose	22.949	2.053	xylose
34.763	9.671	un. galact.	34.062	12.360	un. galact.	33.775	2.374	un. galact.
A3			B3			C3		
10.318	58.088	mannose	10.260	55.441	mannose	10.233	53.972	mannose
\	\	\	\	\	\	12.566	2.624	ribose
13.337	0.298	rhamnose	13.225	7.297	rhamnose	13.043	2.089	rhamnose
\	\	\	17.039	2.095	unknown	16.928	4.315	unknown
21.333	36.482	glucose	20.990	27.187	glucose	20.795	19.304	glucose
24.430	0.609	xylose	23.921	1.977	xylose	\	\	xylose
34.680	2.426	un. galact.	33.874	3.293	un. galact.	33.745	7.170	un. galact.
A4			B4			C4		
10.292	56.214	mannose	10.262	50.434	mannose	10.263	28.143	mannose
\	\	\	12.910	2.142	ribose	12.607	5.573	ribose
13.264	5.047	rhamnose	13.218	3.175	rhamnose	\	\	\
21.127	26.104	glucose	20.992	26.898	glucose	20.907	20.607	glucose
24.146	1.650	xylose	23.970	2.483	xylose	22.963	5.416	xylose
34.251	3.751	un. galact.	34.001	5.733	un. galact.	33.929	9.588	un. galact.

Table 5. LPS isolation results (type of sugars, retention time and integral area value) from the 3 replicates in shaking and stable conditions, for PJ isolate; "un. galact." stands for unprotonic galacturonic acid.

This experiment was repeated in D6 isolate: 3 replicates in both shaking and not shaking conditions were analyzed, but, in addition, the LPS from both PJ and D6 cultures grown in LB + 1% glucose was taken into consideration. In fact, from the growth curve analysis (*paragraph 3.1.2.*), it was visible how glucose presence changed the shape of bacteria; from the HPLC analysis it was possible to check if the different medium contributed to some differences in LPS composition. A1, A2, A3, A4, B1, B2, B3, B4, C1, C2, C3 and C4 referred to the same sample as before (*Figure 32*), while the samples in glucose have been named in this way:

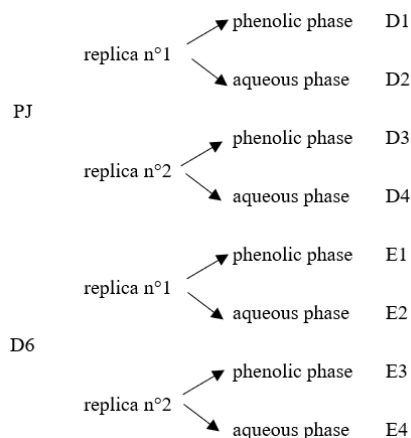


Figure 32. Samples' name from D6's LPS isolation.

The peaks from the second attempt (Table 6), where D6 was used instead of PJ, were more intense, and the quality of the analysis seemed to have improved, in both aqueous and phenolic phase, where LPS was found as in the previous attempt. Also in this case, the fact of having obtained results confirmed the Gram-negativity of the isolates. From A1, B1 and C1 results (phenolic phase, shaking conditions), it was visible that the main sugars were mannose, ribose, rhamnose and glucose, while protonated N-acetylglucosamine was present only in C1 (integral area around 1.2), and B1 had xylose and fucose (integral value of about 1.8 and 0.9). In A3, B3 and C3 (phenolic phase, stable conditions), mannose presented even 2 peaks, the first one at 9 minutes and the other one at 11 minutes, so the area values have been considered together; then, the main sugars were represented by ribose, rhamnose, protonated N-acetylglucosamine, which was present in all three samples, differently from before, as well as xylose. Minor sugars were galactose, visible in A3 (integral area of 0.8), arabinose in B1 (0.6) and fucose in both A3, B3 and C3, but with minor integral values (0.2, 0.4 and 0.6 respectively). The main differences, compared to previous attempt, were the fact that unprotonic galacturonic acid was not present; on the other hand, in the second attempt results, more sugars such as, arabinose, fucose, N-acetylglucosamine and xylose contributed to the LPS carbohydrates composition.

In A2, B2 and C2 results (aqueous phase, shaking conditions), the main carbohydrates were mannose, that presented even in this case two peaks at 9 and 11 minutes, ribose, rhamnose, glucose and xylose. C2 had one peak of protonic galacturonic acid (integral area of about 1.2) at 16 minutes and another small one (integral area of about 0.6) after 31 minutes, while A1 presented the one of galactose (integral area of about 1.6); minor sugars were arabinose and fucose. A4, B4 and C4 shown as major LPS carbohydrates mannose, at both 9 and 11 minutes, ribose, rhamnose, protonated N-acetylglucosamine, glucose and xylose, while minor sugars were fucose and unprotonic galacturonic acid. The main difference between shaking (A2, B2, C2) and stable (A4, B4, C4) aqueous phase was that in the second case fucose, xylose and protonated N-acetylglucosamine had peaks in all 3 samples, while unprotonic galacturonic acid, which was absent in A2, B2 and C2, was present in B4 and C4. The differences between analysis performed using PJ (first attempt) and the

one using D6 (second attempt) was the presence of fucose and protonated N-acetylglucosamine in the last one. In general, from both attempts' results, it can be said that D6 and PJ didn't change Gram nature.

A1			B1			C1		
time	integral	sugar	time	integral	sugar	time	integral	sugar
9.659	13.548	mannose	9.619	13.735	mannose	9.570	17.232	mannose
12.738	27.919	ribose	12.674	26.230	ribose	12.595	26.294	ribose
14.951	7.904	rhamnose	14.924	10.210	rhamnose	14.806	10.917	rhamnose
\	\	\	\	\	\	18.206	1.157	prot. N-ac.
20.004	49.373	glucose	19.902	45.565	glucose	19.698	43.132	glucose
\	\	\	22.621	1.833	xylose	\	\	\
\	\	\	27.577	0.917	fucose	\	\	\
A2			B2			C2		
9.675	13.972	mannose	9.623	18.789	mannose	9.578	36.083	mannose
10.137	18.466	mannose	10.760	16.080	mannose	10.994	2.328	mannose
12.714	2.616	ribose	12.646	2.732	ribose	12.287	5.971	ribose
14.938	16.604	rhamnose	14.843	21.422	rhamnose	14.746	17.680	rhamnose
\	\	\	\	\	\	16.464	1.186	prot. galact.
20.069	43.240	glucose	19.860	38.493	glucose	19.720	31.206	glucose
22.253	2.217	xylose	22.345	1.263	xylose	22.196	1.751	xylose
23.253	1.641	galactose	\	\	\	\	\	\
\	\	\	24.811	1.221	arabinose	24.282	0.776	arabinose
26.253	1.244	fucose	\	\	\	25.849	0.501	fucose
\	\	\	\	\	\	31.890	0.570	un. galact.
A3			B3			C3		
9.631	14.120	mannose	9.601	12.460	mannose	9.552	12.987	mannose
11.679	0.716	mannose	11.678	0.944	mannose	11.628	0.850	mannose
12.700	25.531	ribose	12.628	28.128	ribose	12.529	30.144	ribose
14.927	10.941	rhamnose	14.880	10.651	rhamnose	14.767	9.639	rhamnose
19.948	47.546	prot. N-ac.	19.779	45.452	prot. N-ac.	19.540	44.477	prot. N-ac.
\	\	\	22.529	0.850	xylose	22.333	1.271	xylose
23.083	0.866	galactose	\	\	\	\	\	\
\	\	\	24.798	0.673	arabinose	\	\	\
27.565	0.280	fucose	27.436	0.394	fucose	27.161	0.632	fucose
A4			B4			C4		
9.636	17.888	mannose	9.603	27.936	mannose	9.558	34.181	mannose
10.056	17.663	mannose	10.040	13.955	mannose	10.761	3.127	mannose
12.410	7.070	ribose	12.305	20.565	ribose	12.271	5.341	ribose
14.915	18.581	rhamnose	14.389	2.277	rhamnose	14.766	19.629	rhamnose
20.063	26.562	prot. N-ac.	19.911	20.615	prot. N-ac.	19.754	33.185	prot. N-ac.
22.162	1.481	glucose	22.438	2.792	glucose	21.656	2.464	glucose
24.937	0.757	xylose	23.772	1.036	xylose	23.748	0.834	xylose
\	\	\	30.819	0.202	fucose	\	\	\
\	\	\	32.066	0.163	un. galact.	31.880	0.551	un. galact.

Table 6. LPS isolation results (type of sugars, retention time and integral area value) from the 3 replicates in shaking and stable conditions, for D6 isolate; "un. galact." stands for unprotonic galacturonic acid, while "prot. N-ac." for protonated N-acetylglucosamine.

In LB + 1% glucose medium, where there was just one condition, which was stable, because shaking had no reason to be analysed because there was already no pigment production due to glucose, the results didn't differ that much. In fact, in D1 and E1 (phenolic phase, first repetition for PJ and D6), D3 and E3 (phenolic phase, second repetition for PJ and D6), the major sugars were mannose, ribose, rhamnose, glucose, xylose and arabinose; minor peak was represented by protonic galacturonic acid in E3 (Table 7). D2, E2 (aqueous phase, first repetition for PJ and D6), D4 and E4 (aqueous phase, second repetition for PJ and D6) presented, as main sugars mannose, ribose, rhamnose, glucose, xylose, arabinose and protonic galacturonic acid. The LPS composition of all these samples was almost same, except for protonic galacturonic acid presence or absence; also in this case, the Gram-negativity was confirmed. All the HPLC spectra are reported in *paragraph 7.2.* in the *Appendix.*

D1			E1		
time	integral	sugar	time	integral	sugar
9.509	34.627	mannose	9.516	15.849	mannose
12.285	2.673	ribose	12.505	25.464	ribose
14.696	23.233	rhamnose	14.709	10.396	rhamnose
19.626	33.136	glucose	19.488	45.629	glucose
21.702	1.679	xylose	22.211	1.316	xylose
24.393	1.379	arabinose	25.521	0.480	arabinose
D2			E2		
9.548	25.465	mannose	9.532	33.629	mannose
11.637	2.467	ribose	12.291	8.356	ribose
14.721	20.965	rhamnose	14.743	17.792	rhamnose
19.676	32.341	glucose	19.683	34.749	glucose
21.751	1.473	xylose	21.656	1.451	xylose
24.435	0.988	arabinose	24.408	0.845	arabinose
31.848	0.979	prot. galact.	31.800	0.137	prot. galact.
D3			E3		
9.543	38.947	mannose	9.514	13.348	mannose
\	\	\	12.509	25.635	ribose
14.693	25.620	rhamnose	14.731	10.184	rhamnose
19.644	29.395	glucose	19.485	47.508	glucose
21.934	0.823	xylose	22.714	1.380	xylose
23.268	0.928	arabinose	25.335	0.980	arabinose
31.731	0.387	prot. galact.	\	\	\
D4			E4		
9.541	49.962	mannose	9.556	50.740	mannose
12.295	3.376	ribose	12.255	17.365	ribose
14.703	20.122	rhamnose	14.731	10.511	rhamnose
19.669	24.122	glucose	19.914	12.588	glucose
21.681	1.225	xylose	22.361	2.985	xylose
23.628	0.687	arabinose	24.648	0.625	arabinose
31.751	0.079	prot. galact.	32.134	1.632	prot. galact.

Table 7. LPS isolation results (type of sugars, retention time and integral area value) from the 2 replicates, cultivated in LB +1% glucose, for both PJ and D6; "prot. galact." stands for protonic galacturonic acid.

3.1.4.2. Bradford assay

Bradford assay was performed using some second attempt samples (only A1, A2, A3 and A4 are missing) to quantify the protein amount in both phenolic and aqueous phase, after their separation mediated by phenol and distilled water (see *paragraph 2.1.6. in Methods*). From the standard curve samples' absorption measurements, it was possible to identify the calibration line ($y=0.0006x + 0.3785$), later used to understand the amount of proteins in the LPS isolation samples (*Figure 33*). The protein concentration goes around the value of 0.381 mg/mL in all samples (*Table 8*).

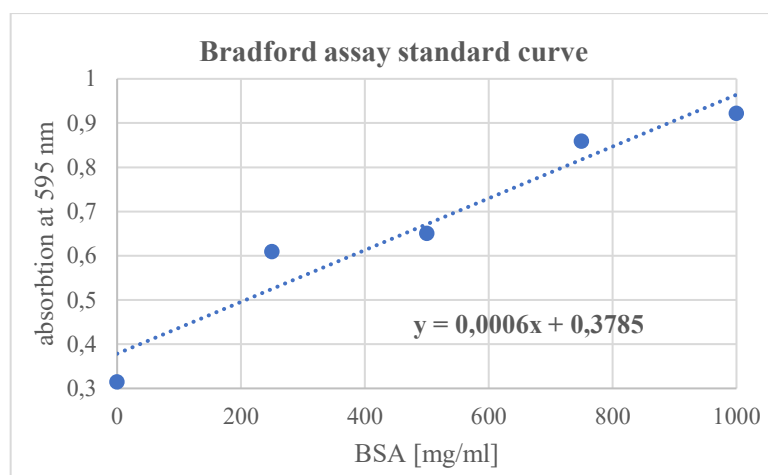


Figure 33. Bradford assay standard curve obtained using the concentrations reported in Table 1.

sample	Abs	protein [mg/mL]	sample	Abs	protein [mg/mL]	sample	Abs	protein [mg/mL]	sample	Abs	protein [mg/mL]
B1	0.482	0.381	C1	0.415	0.381	E1	0.457	0.381	D1	0.458	0.381
B2	0.465	0.381	C2	0.467	0.381	E2	0.477	0.381	D2	0.482	0.381
B3	0.527	0.382	C3	0.514	0.382	E3	0.466	0.381	D3	0.463	0.381
B4	0.507	0.382	C4	0.497	0.381	E4	0.452	0.381	D4	0.487	0.381

Table 8. Absorption values and corresponding protein quantification thank to calibration line found equation.

3.1.5. Glucose inhibition in D6 isolate

Microplates were left in the wardrobe after the end of the experiment and, in few days' time, it was seen that D6 wells were starting to produce pigment in LB + 1% glucose medium. Even during the growth curve experiment, it was visible that in glucose samples seemed pinker than in previous attempts with just PJ. This pigment production, particularly from D6 isolate, was found in LPS isolation process, when cultures in LB + 1% glucose were prepared. So, firstly it was tested if PJ and D6 were able to produce prodigiosin after having grown in glucose: 500 μ L of D6 and PJ from LB +1% glucose medium were used as inoculum for a new liquid LB cultivation (volume of 300 mL) (*Figure 34*).



Figure 34. Liquid LB cultures using PJ inoculum taken from LB + 1% glucose (GL) flasks.

Secondly, PJ and D6 were made grown in bigger volumes of LB + 1% glucose, because previously inhibited prodigiosin production in glucose was just tested in microplates wells. After 16 days, so 10 days later than in LB, D6 started to produce prodigiosin in glucose-rich medium, differently from PJ, that, even after several weeks, didn't show any pigment (Figure 35). Following the obtained results, LB media with glucose in different percentage (1.5%, 2%, 2.5%, 3%, 4%) were prepared, but no pigment was produced (Figure 35). It is hypothesized that once glucose is used for the growth, when in lower concentrations, *S. marcescens* starts to produce prodigiosin, whose process is not inhibited anymore; when the percentage of glucose is too high, sugars are not consumed, and pigment inhibition is still on. Differences in pigment production are normal for different isolates, so this finding could be interesting to better comprehend and characterize those two isolates, PJ and D6.



Figure 35. On the left, D6 cultures in LB + 1% glucose (GL) after 16 days; on the right, different flasks containing PJ and D6 cultures in LB with glucose in different percentages.

3.2. Prodigiosin quantification and assessment

3.2.1. Antioxidant capacity

DPPH (α, α -diphenyl- β -picrylhydrazyl, $C_{18}H_{12}N_5O_6$, MW=394.33) assay is considered a valid accurate, easy, and economic method to evaluate radical scavenging activity of antioxidants, since the radical compound is stable and need not be generated (Sagar et al. 2010). Free radicals, produced by biological systems, are the compounds able to bind free radicals by intervening in the free radical mediated oxidative process. This assay is based on the measurement of the scavenging

capacity of antioxidants species towards it: the odd electron of DPPH nitrogen atom receives a hydrogen atom from antioxidants to the corresponding hydrazine (Sagar et al. 2010).

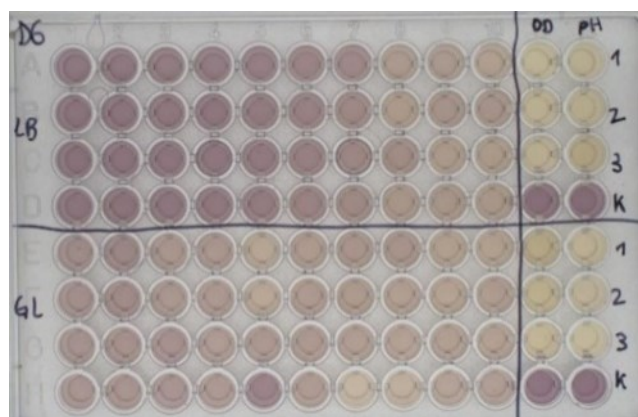


Figure 36. D6 microplate after 24 hours under DPPH (α , α -diphenyl- β -picrylhydrazyl) assay: it is evident how the wells change from purple to yellow with the increase of antioxidant capacity.

Measurements of antioxidant capacity were done for every timepoint sample, in two replicates of each microplates' growth curve experiment. The reported values are the average resulting from each timepoint's two replicates measured twice. The values obtained for the first, second and third attempt were not taken into consideration because of the presence of different and numerous outliers that didn't make the results reliable. As followed, the results for the fifth and sixth growth curve attempt, where both D6 and PJ were analyzed, will be reported, and described. The measurements have been taken after 30 minutes and values should be treated as percentages.

The results from the fifth attempt shown that in both cases (*Table 9*), D6 and PJ, the antioxidant capacity was higher in LB + 1% glucose than in just LB. In fact, even if the highest values were not in t_{10} , that should be shown in the last timepoints because of the theoretical higher amount of pigment, generally the values were higher in glucose medium, highlighted by greener table cells. This evidence was confirmed also in the results from the sixth attempt for both D6 and PJ, where table cells were generally greener (*Table 9*).

D6 and PJ values in LB and LB + 1% glucose after 30 minutes were graphed together to visualize the data from a different point of view: in every graph it was evident how measurements made in LB + 1% glucose had higher antioxidant capacity both in D6 and PJ (*Figure 37* and *Figure 38*). It is also evident how in D6, samples from same timepoints of PJ's ones had higher antioxidant capacity: this was related to the prodigiosin production which was different in the two isolates (it will be highlighted in 3.2.2. paragraph with prodigiosin quantification experiments). Of course, if an isolate grows faster than the other one, it will produce more pigment: it was previously clear how D6 had a faster growth rate compared to PJ.

	sample	t ₁	t ₂	t ₃	t ₄	t ₅	t ₆	t ₇	t ₈	t ₉	t ₁₀	control
LB	PJ 5th	-0.82	-3.350	-2.290	-4.800	-0.690	-0.500	1.043	2.309	1.620	3.414	-1.820
	PJ 6th	-0.24	0.670	1.650	2.160	3.480	3.270	6.700	7.520	7.200	7.500	-0.290
	D6 5th	-1.53	-3.800	-3.250	-0.840	-1.120	0.925	2.047	2.672	3.412	3.040	-1.640
	D6 6th	-0.61	-1.260	0.350	-0.570	1.610	1.310	1.600	3.810	3.940	3.460	-0.790
GL	PJ 5th	-0.7	-3.590	-1.030	0.144	5.575	6.113	9.422	6.569	1.125	5.693	-0.600
	PJ 6th	0.98	1.170	1.470	2.440	9.420	9.210	11.260	15.040	15.970	16.700	-0.700
	D6 5th	2.81	0.470	4.850	4.220	5.510	5.870	6.660	9.290	8.490	8.530	-1.640
	D6 6th	-1.51	0.140	13.980	3.190	6.240	4.640	8.750	9.330	9.490	8.600	-0.790

Table 9. D6 antioxidant capacity values (percentages) from the fifth and sixth attempt; the results are coloured with different shades of red (lower values) and green (higher values) to better perceived the differences. LB stands for the Luria Bertani broth, while GL for LB+ 1% glucose.

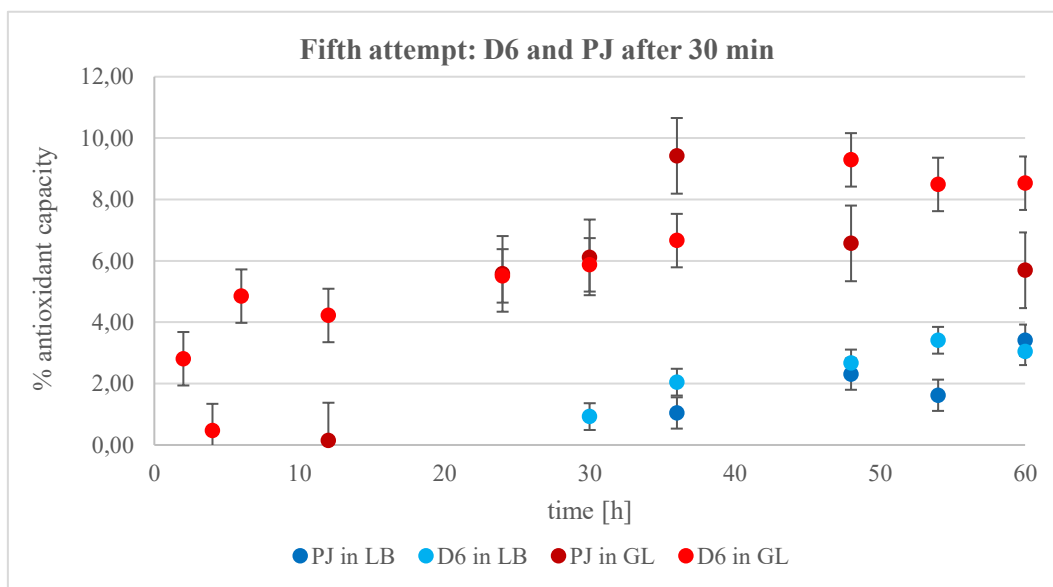


Figure 37. D6 and PJ in LB (in light and dark blue) and LB + 1% glucose (GL, light and dark red) from 5th attempt, after 30 minutes; deviation standard bars are reported, while negative values have been removed.

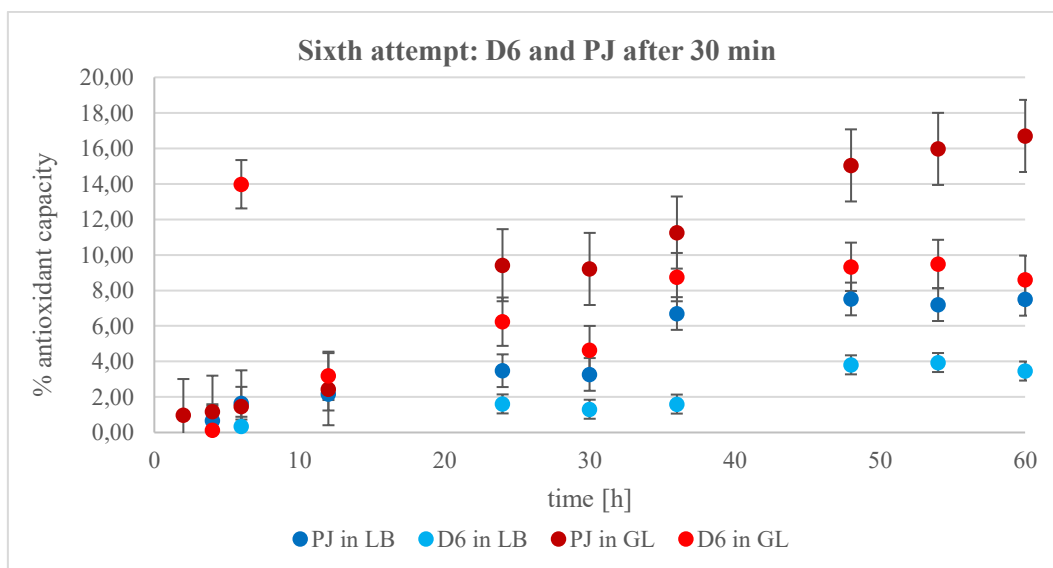


Figure 38. D6 and PJ in LB (in light and dark blue) and LB + 1% glucose (GL, light and dark red) from 6th attempt, after 30 minutes; deviation standard bars are reported, while negative values have been removed.

The higher values, both in D6 and PJ, were present in LB + 1% glucose, where prodigiosin production is, if not completely inhibited, lower than in just LB medium. Therefore, two are the hypothesis: prodigiosin doesn't contribute to the antioxidant capacity as much as thought and reported in previous works or glucose increases that one, even if the LB + 1% glucose control doesn't show much higher values than the LB control, indicating a difference in antioxidant capacity could be influenced by glucose presence. Emad Shalaby and collaborators have hypothesized how in black tea glucose could react with oxidized phenols, becoming scavenger for DPPH radical (*Figure 39*) (Emad Shalaby et al. 2016). So, glucose could possibly bind some molecules present in the isolates' collected supernatant, interfering in the final antioxidant capacity output, but, of course, this phenomenon should be studied apart, and further experimental repetition are needed.

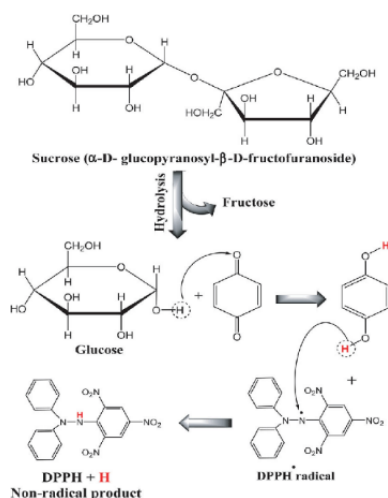


Figure 39. The suggested reaction between sugar and oxidized phenols (e.g., quinones) in black tea and possibility for scavenging of DPPH radical (Emad Shalaby et al. 2016).

3.2.2. Prodigiosin quantification

Prodigiosin was approximately quantified by using absorption spectra: differences in intensities should underline the main discrepancies between PJ and D6 both grown in LB and LB + 1% glucose. As in the DPPH antioxidant assay, also in this case there were problems related to the quantification of the samples from first, second and third attempt, because of some technical problems that will be later discussed; as previously said, for each timepoint two samples were collected for both LB and LB + 1% glucose (for each timepoint there are 4 samples in total for both PJ and D6, that have different microplates).

Absorption spectra were measured in the range of 400 and 700 nm because the microplates reader didn't reach the UV wavelength range; beside that, plastic microplates absorbs the UV light, and it would have been impossible to check the absorption under 400 nm. The solution would be collecting samples from flasks coupled with the usage of quartz cuvettes, but as previously reported in *paragraph 3.1.*, it would be impossible to verify the prodigiosin absorption because the flask opening and closing, necessary to collect the samples, didn't let the pigment accumulation. In fact, quartz cuvettes with path length of 1 cm were the only ones

available, but it would be helpful to have smaller path lengths, for instance 2 mm. For each timepoint there were two replicates, but just the results from one of the two were reported as spectra to make the visual analysis easier.

From the fifth attempt results (*Figure 40* and *Figure 41*), it is evident how D6 presents in LB the characterizing peak around 535 nm, while PJ shows the draft of a peak, but it is not as clear as in D6. Samples in LB + 1% glucose, both from the 5th and 6th attempt (*Figure 42*, *Figure 43*, *Figure 46*, and *Figure 47*), don't present a peak at 535 nm, as confirmation of prodigiosin absence. This technique is good to make first analysis, but it is not very precise. This could be caused by the extraction of the pigment by glass beads is not sufficient and, probably, a better method is needed; as last, the starting amount wasn't enough sometimes to be able to extract sufficient amount of pigment.

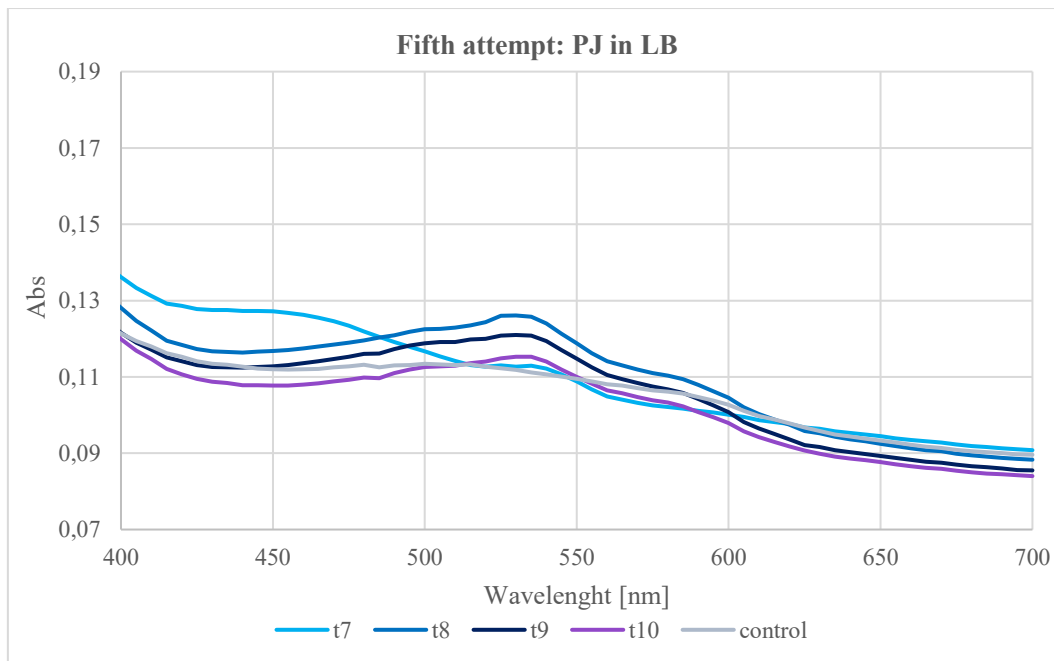


Figure 40. Absorption spectra (range from 400 to 700 nm) of PJ in LB samples taken in different timepoints (t1-t10) during the fifth growth curve attempt, with control (methanol); values that differed were not taken into consideration (corresponding timepoints are not reported).

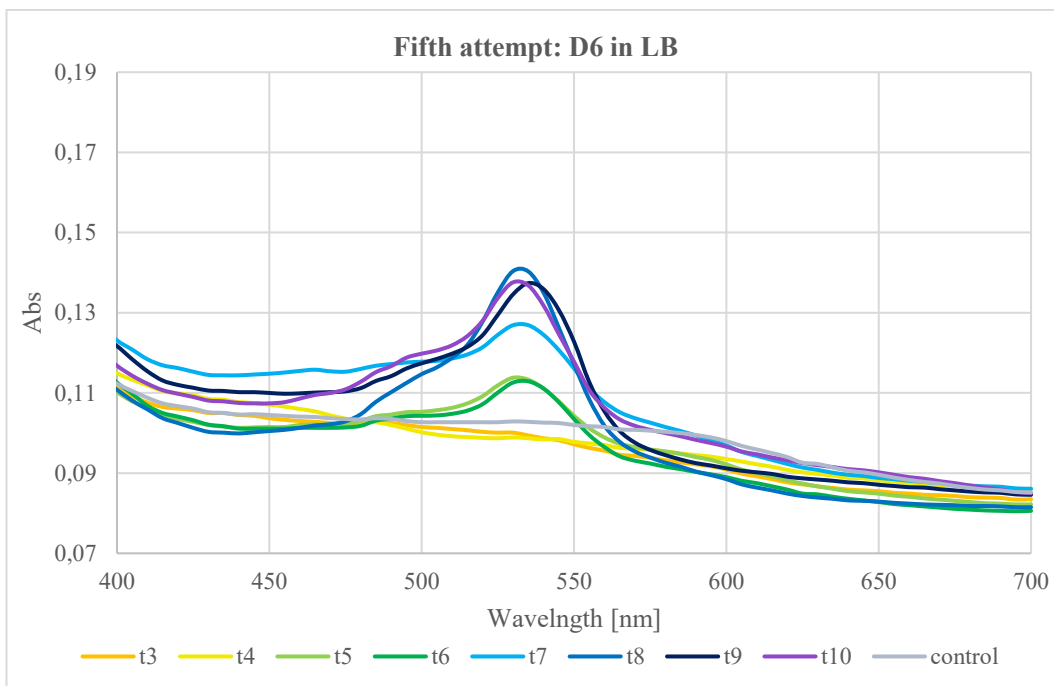


Figure 41. Absorption spectra (range from 400 to 700 nm) of D6 in LB samples taken in different timepoints (t₁-t₁₀) during the fifth growth curve attempt, with control (methanol); values that differed were not taken into consideration (corresponding timepoints are not reported).

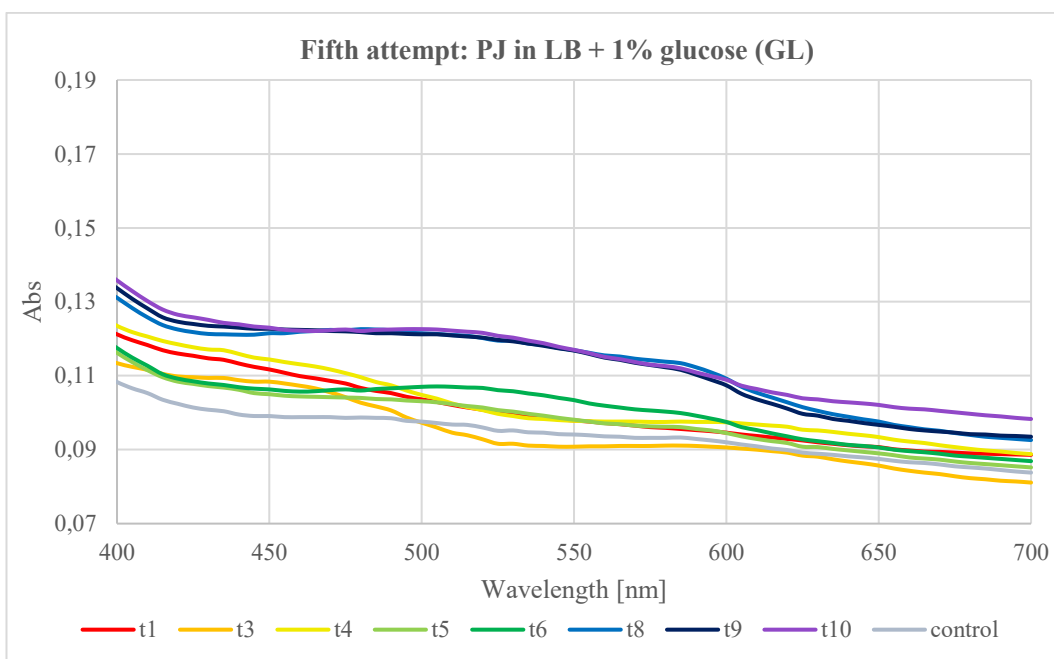


Figure 42. Absorption spectra (range from 400 to 700 nm) of PJ in LB + 1% glucose (GL) samples taken in different timepoints (t₁-t₁₀) during the fifth growth curve attempt, with control (methanol); values that differed were not taken into consideration (corresponding timepoints are not reported).

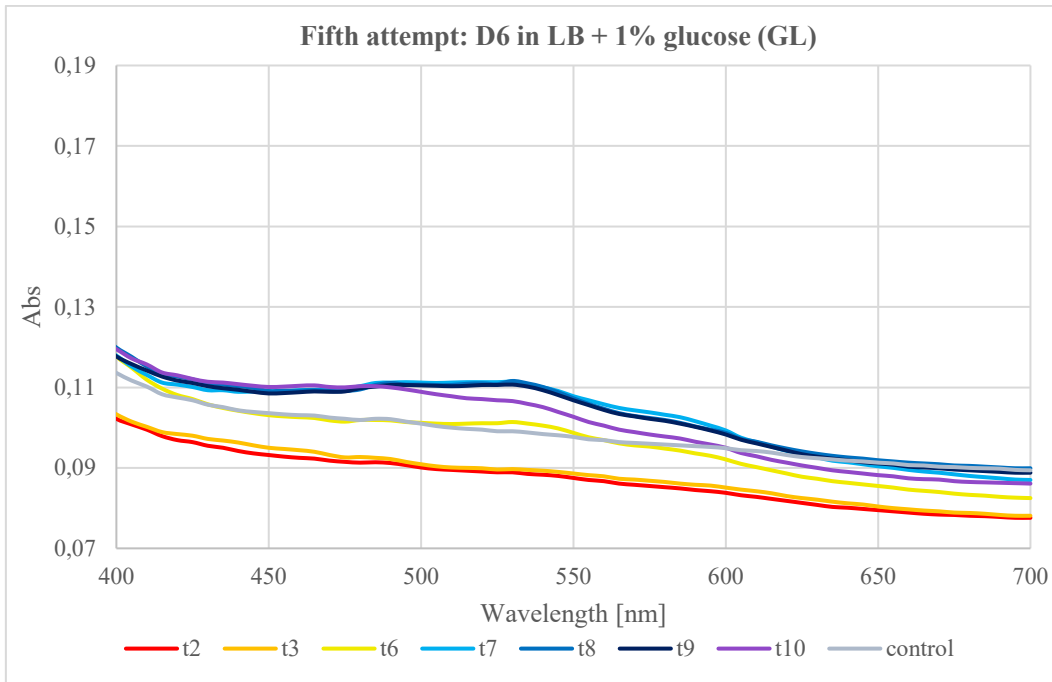


Figure 43. Absorption spectra (range from 400 to 700 nm) of D6 in LB + 1% glucose (GL) samples taken in different timepoints (t_1 - t_{10}) during the fifth growth curve attempt, with control (methanol); values that differed were not taken into consideration (corresponding timepoints are not reported).

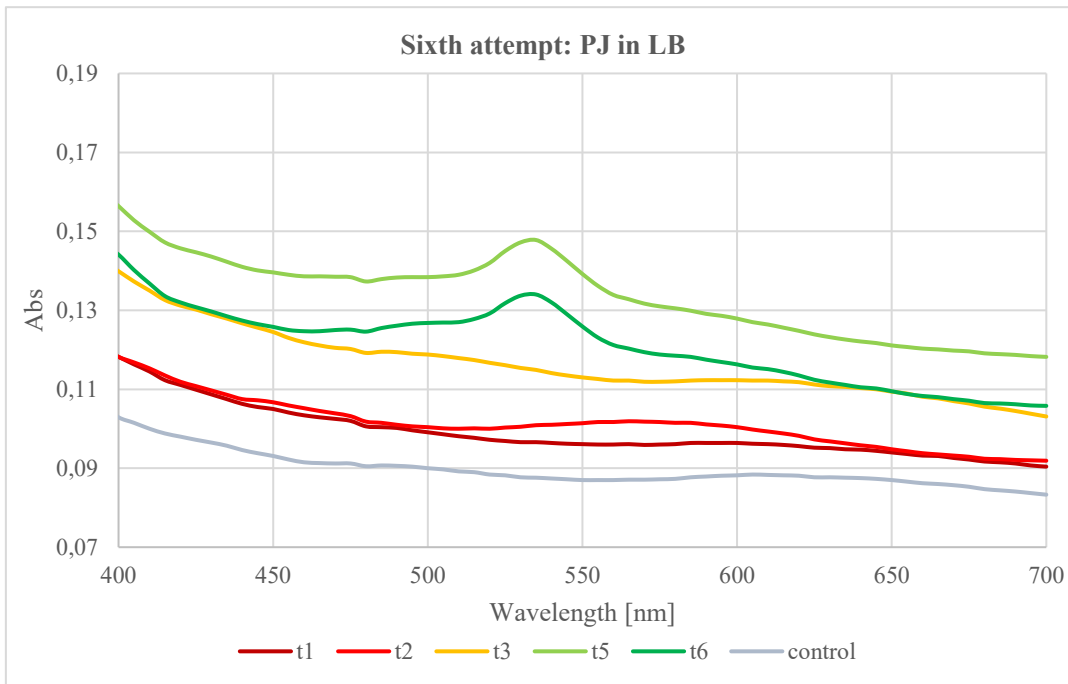


Figure 44. Absorption spectra (range from 400 to 700 nm) of PJ in LB samples taken in different timepoints (t_1 - t_{10}) during the sixth growth curve attempt, with control (methanol); values that differed were not taken into consideration (corresponding timepoints are not reported).

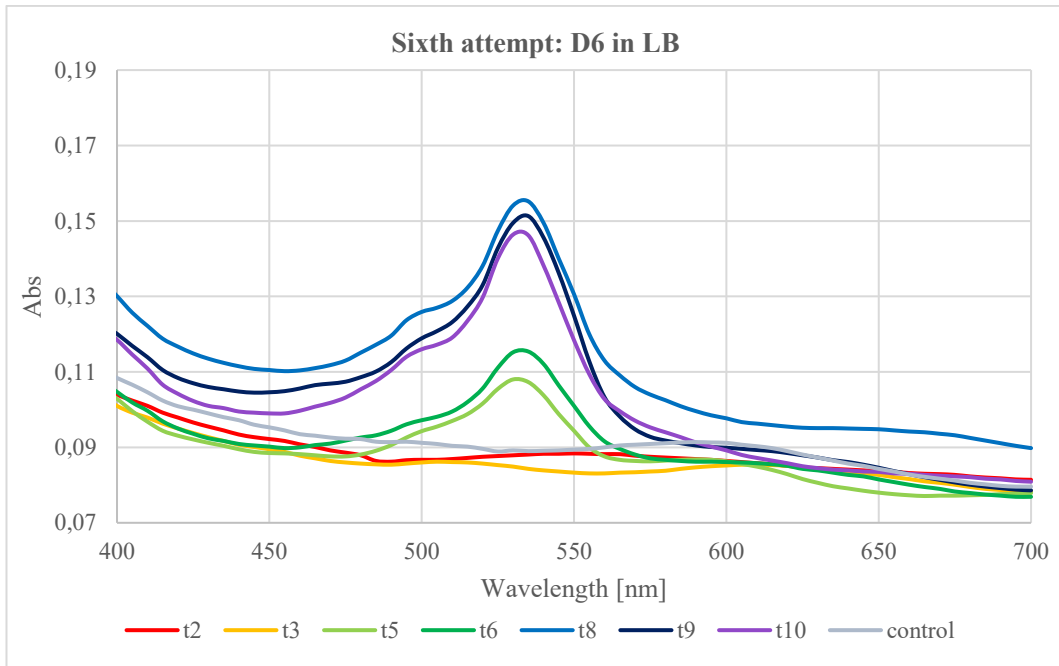


Figure 45. Absorption spectra (range from 400 to 700 nm) of D6 in LB samples taken in different timepoints (t1-t10) during the sixth growth curve attempt, with control (methanol); values that differed were not taken into consideration (corresponding timepoints are not reported).

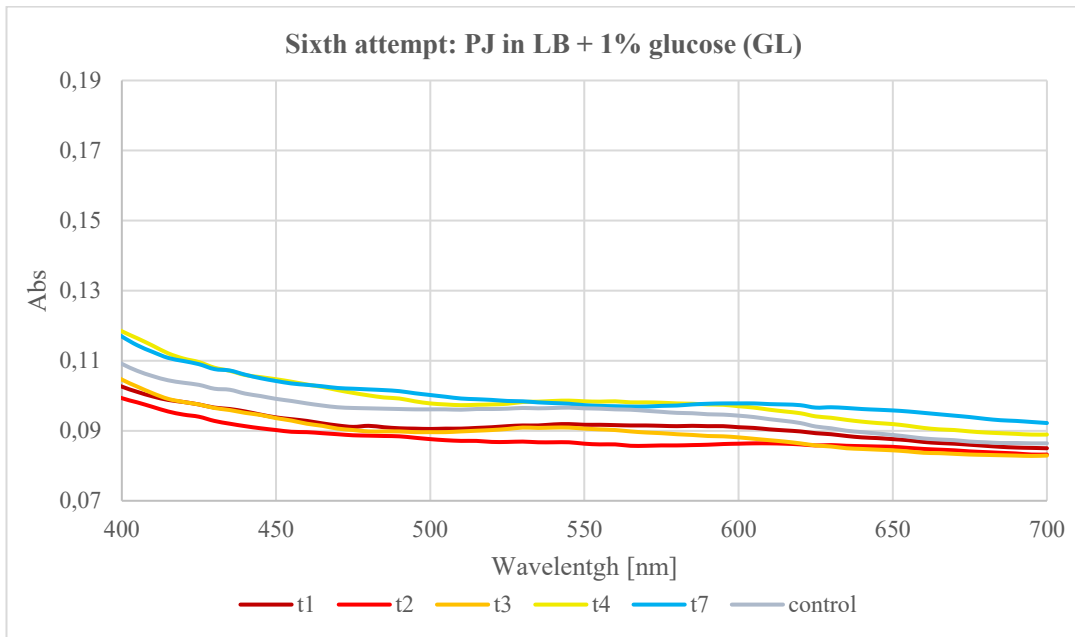


Figure 46. Absorption spectra (range from 400 to 700 nm) of PJ in LB + 1% glucose (GL) samples taken in different timepoints (t1-t10) during the sixth growth curve attempt, with control (methanol); values that differed were not taken into consideration (corresponding timepoints are not reported).

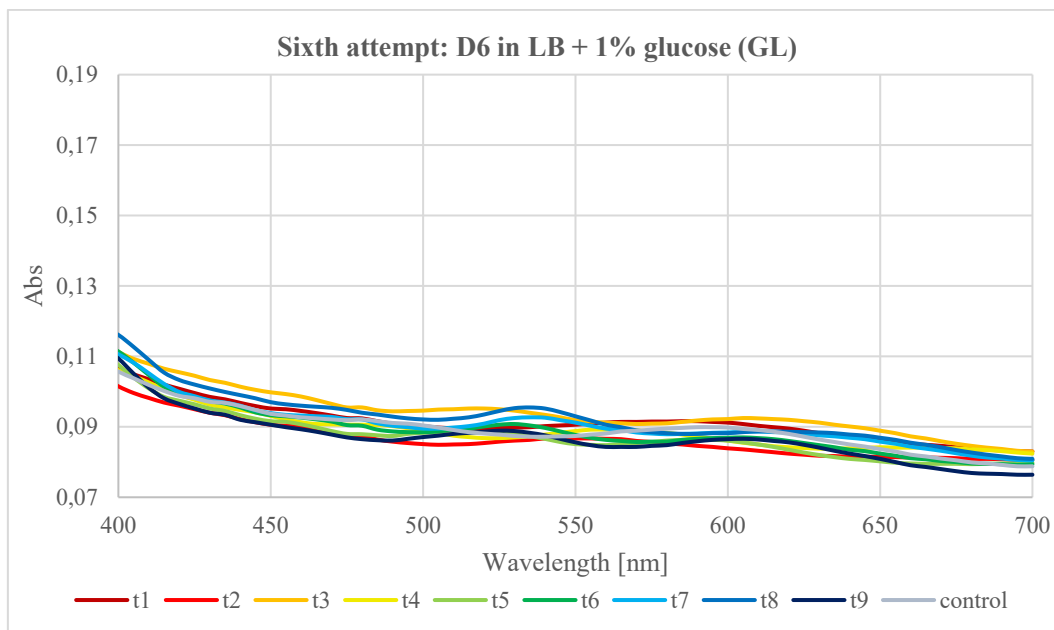


Figure 47. Absorption spectra (range from 400 to 700 nm) of D6 in LB + 1% glucose (GL) samples taken in different timepoints (t_1 - t_{10}) during the sixth growth curve attempt, with control (methanol); values that differed were not taken into consideration (corresponding timepoints are not reported).

3.3. Spectrophotometric characterization

Spectra analysis wanted to highlight the interaction of prodigiosin with the solvent where it is dissolved to comprehend its composition and to characterize its structure. In fact, experiments were done with ethanol and methanol and many different solvents will be used in next analysis (spectra in the *Appendix, paragraph 7.2.1.*).

3.3.1. Absorption and fluorescence spectra

As previously said, early analysis were performed using ethanol and, later, methanol, whose properties don't differ that much from one another, differing only for a methilenic group, so spectra results were expected to present similar patterns and peaks. Besides the used solvent, absorption spectra were measured from 240 nm to 700 nm: in literature (*paragraph 1.1.3.*), generally, the reported spectra start from 300 nm, while in our case, because we were interested in the UV interactions, the range was broadened to 240 nm. Regarding the fluorescence spectra, it was decided to use as excitation wavelengths the peaks values from the absorbance results. This means that the individuated peaks wavelengths at around 260, 330, 390, 400, 470, 500 and 537 nm were used to excite the samples in the fluorescence analysis, whose range extended from 240 and 800. As last step, excitation spectra were later done in the range of 250-554 nm to make comparisons between the interactions in ethanol and methanol. Two things should be underlined: first, the experiments were performed once a week, for this reason the week number will be reported in the graphs and mentioned; secondly, the sample freshness and the measurements timing, that will be later discussed, caused aggregates formation and, hence, the results. Therefore, to not let the solvent to influence the spectra analysis, samples in both ethanol and methanol were made evaporating with gaseous nitrogen and prodigiosin was later resuspended the in fresh solvent.

Starting from ethanol, the first absorption spectrum, which will be referred as first sample (first week), was performed using 2-years-old sample: 4 peaks were identified, at 266 nm, 328 nm, 387 nm, and 500 nm. In all fluorescence spectra there was a so-called “ghost peak”, due to some unspecific light scattering, which means a peak that changes in intensity and wavelength depending on the excitation, so this wavelength was not taken into consideration; as solution, filters or correction programs should be used. The spectrum with excitation at 390 nm was, during this first measurement, discarded, because there was no signal, if not only the one caused by the ghost peak.

The second measurement in ethanol, which will be referred as second sample (second week), was done with PJ's fresh isolated pigment (100 μ L) eluted in 3 mL of ethanol: the absorption spectrum was measured, and the peaks were at 262, 336, 390, 470, 500 and 537 nm. For fluorescence analysis, the peak at 390 nm was the only one not used as excitation wavelength; from the fluorescence spectra, it was noticeable that the peaks were less intense than the ones from first measurement and this could have been caused by pigment aggregation or differences in concentration. A third measurement was done with the same sample used in the second measurement (second sample, third week), which was, at the time of the experiment, 2 weeks old. The absorption spectra revealed that the peaks having the same pattern of previous measurements, but the values were slightly shifted. What was different in the fluorescence spectra was the presence of a peak at 670 nm, when sample was excited at 440 nm. This discrepancy was seen also in the 390 nm spectrum, and it could have been caused by aggregation phenomenon. Therefore, 5 samples of 100 μ L of prodigiosin in ethanol were made evaporating with gaseous nitrogen, to obtain pure pigment. A fourth measurement was done (fourth week), with the second sample that was made evaporating and then prodigiosin was diluted with 3 mL of ethanol. In the absorption spectra, the only difference was represented by the greater intensity of the peak at 470 nm, meaning that there could have been the coexistence of two species. So, fluorescence spectra were done and the peak at 670 nm that was identified in the previous analysis wasn't present, meaning that there were no aggregates or contamination, so the results of the second measurement wasn't take into consideration.

Concerning samples in methanol, they were prepared twice in 4 weeks' time (named first and fourth measurement): in the first analysis 2 mL of methanol and 50 μ L of prodigiosin were used, while in the second attempt 3 mL and 100 μ L, respectively. From the absorption and fluorescence spectra, it was evident that besides differences in concentration, the peaks' distribution were similar to one another and the ethanol ones.

A fifth measurement was done, both with ethanol and methanol to confirm all the results obtained: for the first one, 250 μ L of fresh evaporated prodigiosin were used (to reach the appropriate intensity of 0,2) in 3 mL of ethanol, while for the second one, 100 μ L of fresh evaporated prodigiosin were used in 3 mL of 100% methanol (*Figure 48*). From a comparison between methanol and ethanol fluorescence spectra from the 4th and 5th measurements for methanol and 2nd measurement for ethanol,

all the results are the same, but differences are present in the 265 and 470 nm spectra (*Figure 49*). In fact, ethanol presented peaks with higher intensity around at 350 and 700-750 nm, while methanol had the major peaks at 300 and 600 nm. It was evident that both absorption and fluorescence spectra from the first analysis changed and this is unexpected because the two solvents have similar properties, so spectra should not differ that much. To understand these differences in the fluorescence spectra, excitation spectra were taken, and lifetime of the excited states measured (*paragraph 2.3.2*). The excitation spectra were performed with emission wavelength fixed at 554, because it was the value of the highest peak in 470 nm spectrum, and excitation range from 250 to 540 nm.

Because of the probable presence of two species or impurities in the ethanol samples, absorption, fluorescence, and excitation spectra were performed starting from 250 μ L of fresh prodigiosin, that was made evaporated with gaseous nitrogen and dissolved in 3 mL of 100% ethanol (*Figure 50*). The absorption spectra results (sixth measurement) shown the presence of two species, because in pure ethanol the peak at 470 nm was the most intense (*Figure 48*). There are differences among the impure ethanol, 100% pure ethanol and 100% pure methanol spectra: regardless of the concentration differences, the peaks have a different evolution and pattern, so the presence of two different species is probable and should be investigated. To do that, pigment should be purified and studied in different pH buffer to understand the behaviour of those two species. Down below, peaks' values are reported (*Table 10*).

Table 10. Starting from the column on the left, samples' names in ethanol (above) and methanol (below) and experimental week, peaks values in the absorption spectra, excitation wavelength used for fluorescence spectra and peaks values obtained in the excitation spectra. The different attempts are reported in different colours to help in the data visualization; in red, unique values are highlighted.

Samples measured in ethanol			
attempt	peaks ab. (nm)	excitation λ (nm)	peaks fl. (nm)
First sample (2 years old)	266	260	300, 350, 530, 630, 700-750
–	387	390	350, 700-750
first week	500	500	500
Second sample (fresh)	262	265	360, 650-800
–	336	336	360, 700-800
–	470	440	550
second week	500	440	/
–	537	537	550
Second sample (2 weeks old)	265	265	360, 650-800
–	330	330	370, 700-800
–	470	440	550, 670 , 725
third week	500	440	/
–	537	537	550
Second sample (evaporated)	264	265	330
–	341	341	375, 700-800
–	470	440	550
fourth week	537	537	550
Third sample (evaporated)	265	265	330,
–	344	340	375, 700-800
–	470	470	550
fifth week	537	537	550

Samples measured in methanol			
attempt	peaks ab.(nm)	excitation λ (nm)	peaks fl. (nm)
First sample (fresh)	265	260	300, 350, 530, 630, 700-800
- first week	356	328	350, 650, 700-800
	465	450	500
	503	/	/
	536	/	/
First sample (evaporated)	260	265	300
- fourth week	328	356	-
	500	440	550
Second sample (evaporated)	264	265	300
- fifth week	355	-	-
	470	470	550
	500	/	/
	537	/	/

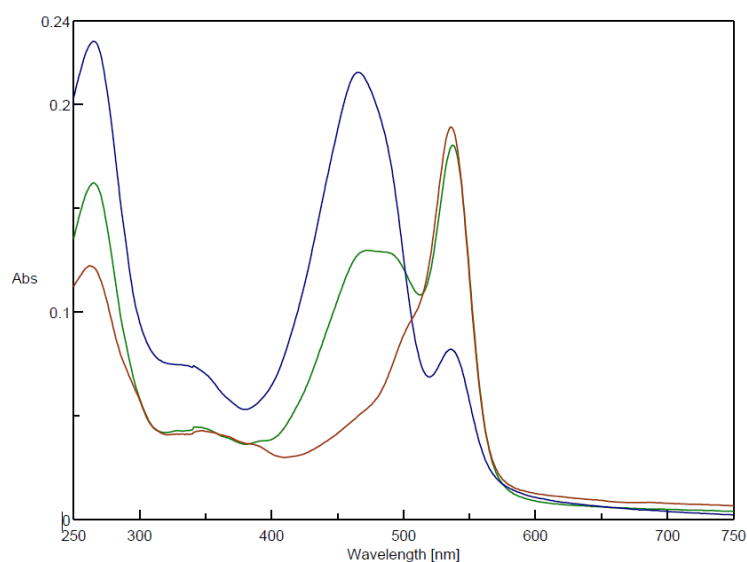


Figure 48. Comparison between the absorption spectrum done in impure ethanol as fifth measurement (in green), in 100% ethanol as sixth measurement (in blue) and in 100% methanol as fifth measurement (in red).

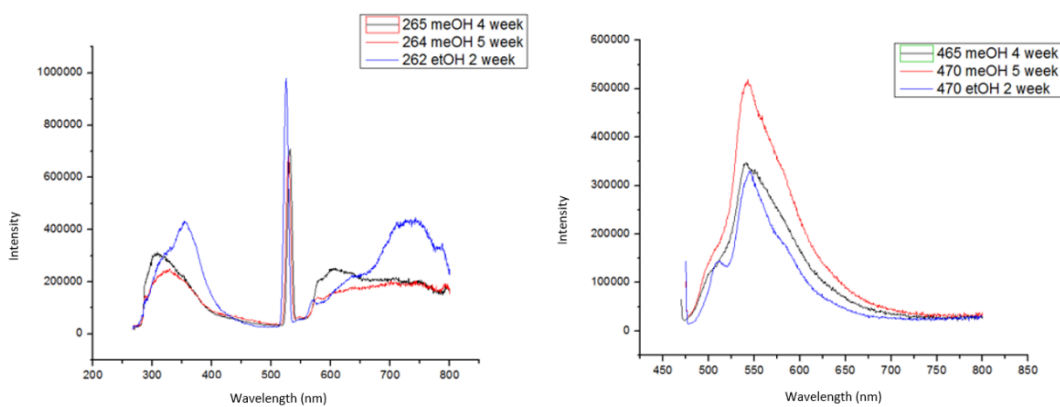


Figure 49. On the left, the comparison between methanol spectra at 265 and 264 nm from the fourth and fifth measurements and ethanol spectra at 262 nm from the second measurement; on the right, the comparison between methanol spectra at 465 and 470 nm from the fourth and fifth measurements and ethanol spectra at 470 nm from the second measurement.

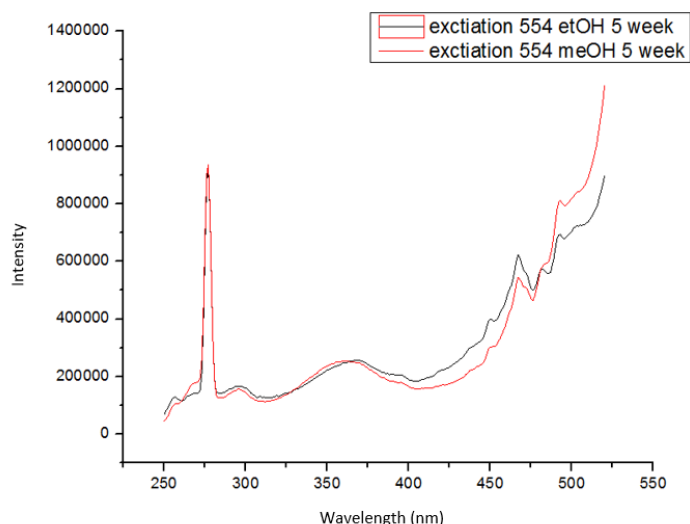


Figure 50. Comparisons of excitation spectra (excitation at 554 nm) in ethanol, in black, and methanol, in red.

3.3.2. Lifetime measurements

Lifetime measurements were performed based on the evidence obtained by the previous fluorescence spectra. Particularly, the quality of the spectra results was directly correlated to the freshness of the samples, so the pigment was made evaporating and dissolved in ethanol or methanol right before the lifetime measurements. In addition, lifetime measurements should underline the presence or absence of aggregates, whose hypothesis was thought from the changes in absorption spectra.

wavelength	n°	τ_1	f_1	τ_2	f_2	χ^2
etOH 265	1	2.58 ± 0.9	0.243 ± 0.1	8.69 ± 1	0.757 ± 0.1	1.54
	2	3.34 ± 1	0.39 ± 0.2	10.3 ± 2	0.61 ± 0.2	0.623
etOH 270	1	3.02 ± 0.4	0.41 ± 0.08	11.5 ± 1	0.59 ± 0.08	1.07
	2	2.93 ± 0.4	0.401 ± 0.08	11.3 ± 1	0.599 ± 0.08	1.11
etOH 280	1	3.46 ± 0.2	0.581 ± 0.05	14.7 ± 1	0.419 ± 0.05	1.77
meOH 270	1	1.3 ± 0.5	0.184 ± 0.08	6.61 ± 0.7	0.816 ± 0.08	1.38

Table 11. Lifetime measurements in ethanol and methanol at 265, 270 and 280 nm; τ_1, τ_2, f_1 and f_2 are reported together with the error value, which is the same and fixed for f_1 and f_2 .

From the results (Table 11) it is evident that for measurements made in ethanol (etOH 265, 270 and 280), the short component (τ_1) doesn't change with the excitation wavelength, while the long one (τ_2) increase with the increase of the excitation wavelength. Fractional intensity, which is the fractional proportion of total fluorescence signal from a given component, of τ_1 increases, while the one of τ_2 decreases, indicating that both components are characteristic of prodigiosin. In methanol (meOH 270), both components were shorter compared to those found in ethanol. Repeated measurements should be done again in the future using purified prodigiosin, to be sure not to have the contribution of impurities. In fact, this technique is highly sensitive to dirtiness.

3.3.3. Prodigiosin extraction and purification by TLC

The results from absorption, fluorescence, and excitation spectra shown that a more specific method of purification is needed, because the spectra had some peaks around 220-300 nm that were caused by the presence of some bacterial impurities (*paragraph 2.3.1*). According to the procedure from Tejasvini and collaborators' paper, in our attempts, the pigment was purified by two techniques (Tejasvini et al. 2016). Firstly, a small amount of water was added to improve phase separation between ethanol-water and chloroform (*Figure 51*). After 3 hours, the elution solvent was isolated and analysed: the absorption spectrum presented a peak at 265 nm that in the original paperwork is not present both because the spectrum shown in the article extends from 300 to 600 nm and the obtained sample has a lot of impurities (*Figure 51*). The method was not sufficient to purify the pigment.

Secondly, an elution solvent (*paragraph 1.3.4*) with the following proportions was used: 6 methanol: 3 ethyl acetate: 1 chloroform. Silica gel TLC papers immersed in the solution helped in the purification and from a first attempt it was evident that this second technique worked, for this reason, the following day, the second procedure was repeated, and the absorption spectrum didn't show the peak at 265 nm, indicating the absence of impurities from bacterial pellet. The article reported that the Rf value is 0.84; the values obtained from different repeats were 0.89, 0.85, 0.83, 0.83, 0.91 and 0.93. Later attempts were done using the Linomat machine to better distribute the sample on the plates and silica gel glass plates were used instead of the paper ones (see details in *paragraph 1.3.4*). Because the plates were old, they were baked for 2 hours at 120°C, to take off the humidity. The powder obtained from the papers was dissolved in 20 mL of methanol and the absorption spectrum was done: it was full of dirty, and it was evident even from the samples that presented an orange shade. The same experiment was performed using the solvent in different ratio on the TLC papers (and not glasses, that are in limited number) and the samples in ethanol used from past spectra; the list of the different ratio is reported with the respectively obtained Rf values, that can be two in case the pigment separation wasn't clear:

- 1) 4:5:1 → 0.73/0.76
- 2) 4:3:3 → 0.7
- 3) 5:4:1 → 0.76/0.83
- 4) 5:3:2 → 0.67/0.76
- 5) 7:2:1 → 0.44
- 6) 3:5:2 → 0.87

From the results, the best ratio seemed to be the number 1 and 3, so the experiment was repeated on glass papers. The results were not satisfying because the pigment was not well separated and in too low amount to perform an absorption spectrum.

Because another extraction method was needed, after having isolated the pigment from the lyophilized samples of D2, D4 and D6 the same way it was done before, the prodigiosin in chloroform solution (volume of 2 mL) was diluted in 12 mL of acidified methanol with HCl and pH at 2.47 (Heinemann et al. 1970). After the

extraction it was evident how the solutions, coming from different isolates, that previously had different shades of pink (*Figure 52*), presented the same colour (*Figure 53*). So, absorption spectra were performed and it seems that the contribution of bacterial residues and impurities, around 250 and 400 nm, was less than the one obtained in previous extractions with chloroform or TLC (*Figure 51*), but it seems that this method used alone is not sufficient (*Figure 52*).

The solution was later purified with the same TLC silica gel sheet used before (around 500 μL of pigmented solution were placed per plate after having made the methanol solution evaporating and transferring that in chloroform). The amount of purified pigment wasn't a lot, but in higher amounts compared to the previously obtained; the solution presented an orange colour (*Figure 53*), typical of the pigment in alkaline pH (Hubbard et al. 1956). Absorption spectra were performed (*Figure 53*) and the impurities contribution, from both TLC plate and bacteria, was still relevant after extraction and purification, meaning that more methods should be tried or different plates, but there was still a reduction of it compared to the first attempts. It is very interesting to see how the spectrum changes due to alkalinity, underlining that something on the TLC papers is changing the properties of prodigiosin. More experimental photos are reported in *paragraph 7.2.2* in the *Appendix*.

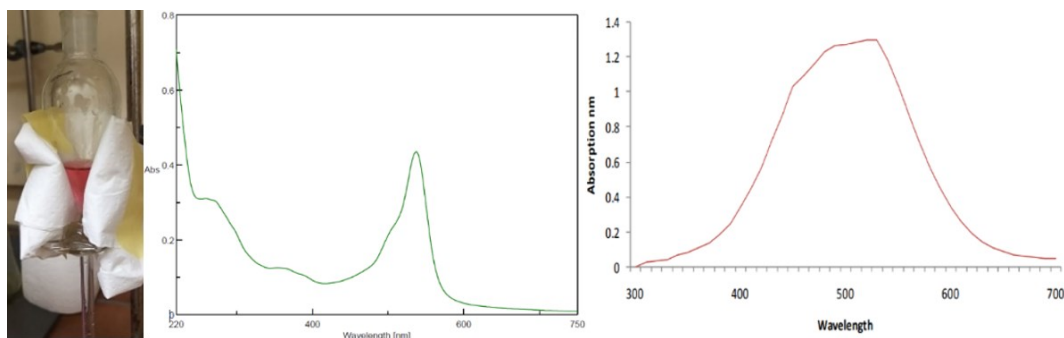


Figure 51. Starting from the left, a picture of the separating funnel; in the middle the absorption spectrum obtained after the purification with chloroform in the funnel, whose peaks from 220 to 440 nm were caused by impurities; on the right, there is the spectrum reported in the paperwork (Tejasvini et al. 2016).

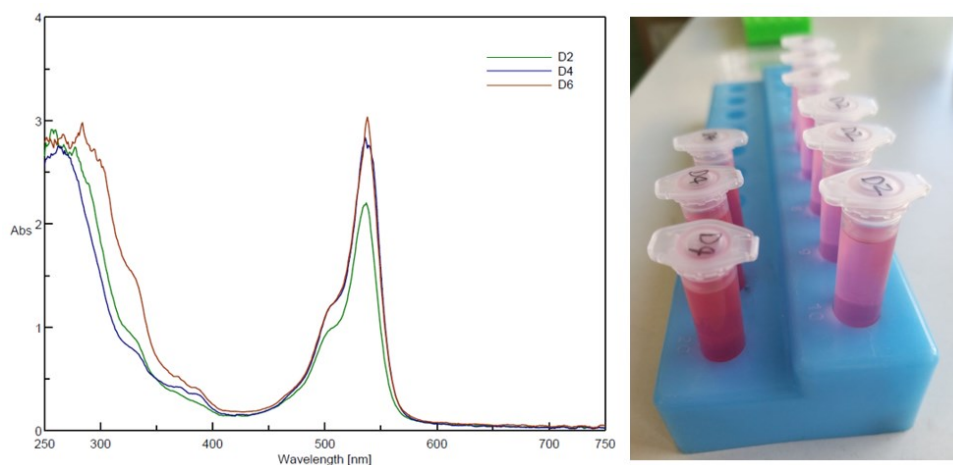


Figure 52. On the left, absorption spectra of prodigiosin from D2 (in green), D4 (in blue) and D6 (in red) isolates in methanol after the extraction in acidified methanol (Heinemann et al. 1970): all samples presented still impurities, whose contribution extends from 250 to 400 nm, as in the previous figure; on the left, samples before the extraction treatment, presenting different shades of pink/purple.

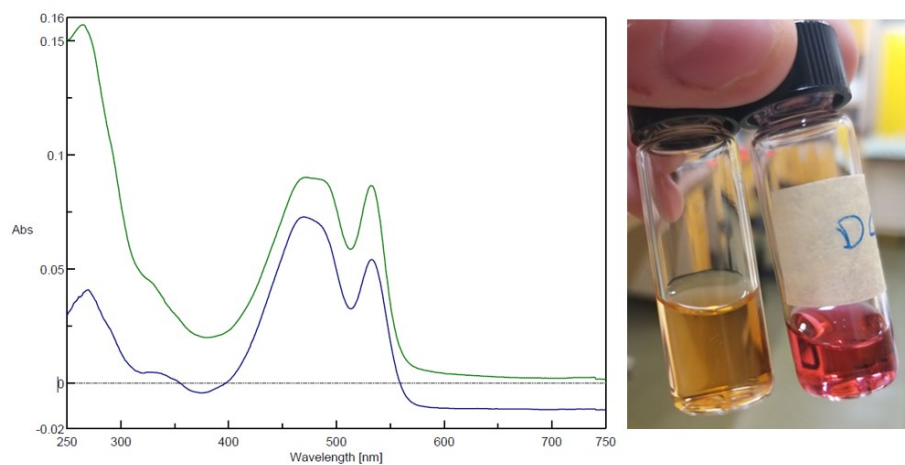


Figure 53. On the left, absorption spectra of D2 samples after TLC purification (both green and blue samples are from D2, but two different TLC plate runs): it is evident from the previous figure, how the impurities are still present (peak from 250 to 350 nm), but their contribution seems having lowered; on the right, orange prodigiosin sample after TLC and pink sample after the acidified methanol, but before the TLC).

4. DISCUSSION

4.1. Gram variability

Gram staining has been one of the most used and diffused techniques to differentiate Gram-negative from Gram-positive bacteria, whose differences in the cell wall could affect many aspects of the cell, including the way it takes up and retains stains. The mechanism is very easy: first, the crystal violet penetrates the cell walls of both Gram-positive and negative, then iodine forms complexes with it in the inner and outer layers, preventing that to be removed; later, the decolorization leaves the Gram-positive cells purple, while the Gram-negative ones lose their color, so, safranin can stain these cells. In fact, due to the ethanol, Gram-negative bacteria lose their outer lipopolysaccharide membrane, while the Gram-positive cells, because of their multilayers, have the crystal violet-iodine complexes trapped. Some species can present a mix of both pink and purple cells, for example, some *Bacillus*, *Butyvirio* and *Clostridium* strains present a decrease in peptidoglycan thickness during the growth, causing the increasing of purple Gram-negative bacteria within the time (Beveridge TJ, 1990). In this last case we talk about Gram variability, while Gram-indeterminate species, as *Mycobacteria* and *Mycoplasma*, don't present stable Gram stain, so every experiment can show different outputs; this is also related to antibiotics resistance (Reynolds et al. 2009).

Even if the Gram staining technique is quite easy, many problems can change the results. Particularly, the final output can be influenced by inadequate specimen or smear preparation (Samuel et al. 2016). For example, if decolourizer is left too long on the sample, both Gram-positive and negative species lose the stain (Beveridge TJ 1983): this phenomenon was seen even during some of our experiments, when, not on purpose, ethanol was left more time than necessary.

Because the Gram variability, shown in Aleksandra Odrobina's thesis work (Odrobina 2021) was not easy to see and reproduce, it is not possible to confirm the double nature of *S. marcescens* isolates. Particularly, some Gram-negative and positive species, used as controls, also changed in Gram nature when the crystal violet solution wasn't shaken before its application. In fact, slides that were treated with centrifuged and not-centrifuged crystal violet solution presented differences in the staining results: it seems that the crystallization of violet solution altered the staining process of Gram-negative bacteria that shown purple colour instead of red one. Normally, in Gram-positive bacteria, the decolorising dehydrates and shrinks the cell walls, causing the pores closing and stain retention; on the contrary, in Gram negative bacteria, decolourizer doesn't retain the stain. So, it can be hypothesized that, because of the size of crystals and their high concentration in not-centrifuged solution, even if Gram-positive bacteria shouldn't keep the purple stain when decolorized, the crystals are too big and too concentrated to exit the membrane. On the other hand, Gram-negative bacteria changing in positive can be explained with overuse of decolourizer, that, when left too long, causes in both Gram species the loosing of stain. This phenomenon is not easy to explain, but an alternative could be to verify if the Gram variability happens in stress-conditions, such as nutrients

deprivation, different temperature, pH, or electrolyte content (Beveridge TJ, 1990). This could be particularly interesting starting from the fact that in Fatimah and collaborators' work, the isolate of *S. marcescens*, able to change from Gram-negative to positive, came from slaughterhouses waste, rich in lipids and proteins (Fatimah et al. 2019). In fact, the high concentration of nitrogen, fatty acids or mineral salts could have contributed somehow to this cell wall thinning phenomenon, that was, on the other hand, reproducible in simple Luria Bertani broth, differently from my studying case.

The HPLC shown the carbohydrates composition of isolates' LPS, which is identifying of Gram-negative bacteria's membrane, and whose presence confirmed the isolates' Gram-negativity: in fact, it was possible to verify the type of the characterizing sugars, whose distribution was constant between both samples and the two different growing conditions, as well as to confirm the probable absence of Gram variability. If isolates had changed from Gram-negative to Gram-positive, HPLC analysis would have not reported such intense peaks, meaning that the isolated LPS carbohydrates were in high amounts. The method used is valuable if applied in other species than *Leptospira* (Bonhomme et al. 2020) and the results confirmed the necessity to analyse the LPS, in the case of *S. marcescens*, both aqueous and phenolic phase. In fact, the Bradford assay results should be considered satisfying, considering the fact that the technique was performed on a species different from *Leptospira*. In addition, the protein concentration was measured just after the first separation of organic and aqueous phase, but other samples after dialysis should be taken into consideration to follow the decreasing of protein amount, that should diminish even more, step after step. The protocol used takes from two to three weeks of work, so repetitions are very useful and necessary, not only to confirm the results, but to have less differences in obtained values, in fact, peaks were greater in the second attempt spectra rather than in the first one's. The LPS isolation was a key experiment because it represented the confirmation about the probable absence of Gram variability phenomenon, that it couldn't have been analysed only starting based on Gram staining results. This last technique, even if very simple, is subjected to many factors and variables, so HPLC was essential.

4.2. Prodigiosin quantification and assessment

As reported before in the *Results* section (*chapter 3*), the difficulties in the extraction of the pigment by glass beads and the low amount of pigment obtained at each timepoint didn't make the quantification easy and precise. Even if the used techniques didn't help in the exact quantification of prodigiosin, some conclusions can be made. In fact, higher amounts of pigment production were registered in LB than LB + 1% glucose, confirming the prodigiosin inhibition. The presence of more pigment in D6 rather than PJ can be explained by a natural difference between the two isolates in prodigiosin production or by the faster growth of D6; in fact, faster is the bacteria to reach the stationary phase, higher the amount of pigment earlier produced would be. This analysis is still very superficial and hypothesis confirmations should be obtained by using more sensitive techniques.

Regarding the DPPH assay results for the antioxidant capacity description, higher values, both in D6 and PJ, are present in LB + 1% glucose, where prodigiosin production should be absent. Even if the pigment production wouldn't be completely inhibited in glucose, such result is unexpected. It can be hypothesized that, despite the well-described antioxidant properties in literature, prodigiosin doesn't contribute to the antioxidant capacity as much as thought, or that glucose can alter the final output (Emad Shalaby et al. 2016). Even in this case, results should be verified by more experimental repetitions and discussed.

4.3. Prodigiosin spectrophotometric characterization

Results from absorption spectra underlined the probable co-existence of two prodigiosin species and the formation of aggregates, when pigment is left in solvent (e.g., ethanol) for a longer period. On the other hand, excitation spectra shown different results than the fluorescence spectra's ones: when molecules are excited at a certain wavelength, you expect them to decay to the ground state always in the same way every time the excitation happens, but, if excitation changes, aggregates or different species could be involved and responsible for the differences in de-excitation.

Lifetime measurements confirmed what just said. In fact, χ^2 values were reliable, but because of the inability to distinguish with confidence if the two components were caused by two co-existing prodigiosin species (one component for each of the species) or impurities (one of the two components is caused by bacterial residues), which the technique is very sensitive to, the experiment should be reproduced by using purified pigment. In addition, probable forming aggregates, that were highlighted by absorption spectra, could shorten the lifetime of these components, so freshness is an important requirement in time-dependending analysis.

The extraction with acidified methanol (Xu et al. 2011) and the TLC purification (Vu Trong Luong et al. 2018), that were lastly done, seem not to be sufficient for the total removal of bacterial impurities, but to be sure about that, the obtained purified samples should be used, not only for spectrophotometric analysis, but also for lifetime measurements to check any difference between the old results. Regardless the presence of two different species, once purified, prodigiosin should be also analyzed in different solutions to see how it interacts with certain molecules and to understand its properties. It should be interesting also to understand how the spectra change increasing or decreasing the pH.

5. CONCLUSIONS

Prodigiosin is a pigment and a second bioactive metabolite that was firstly discovered in *S. marcescens*, but it is produced by both Gram-positive and negative bacteria. During the last decades, research has been interested in its characterization, particularly because of its antioxidant and antitumoral properties, but its value and marketability go further (Khanafari et al. 2006). In fact, microbial molecules, such as pigments, have been exploited not only in the pharmaceutical industry, but also as substitutes of the synthetic ones, being safer in human products (Darshan et al. 2015). In fact, natural pigments own, generally, beneficial outcomes and stability to light, heat, and pH (Joshi et al. 2003): food industry has been adopting them for their potential as food colorants, while bioengineering has made comparisons with the synthetic ones to find the reasons of their adverse effects (Darshan et al. 2015). Considering the many advantages of natural microbial pigments, natural colours are also more environment-friendly and visually appealing.

Considering prodigiosin benefits, it has been demonstrated that the pink pigment is a proapoptotic factor towards different multi-drug resistant cancer cell lines, as well as antifungal and immunosuppressive. Antitumoral activities were registered against some remarkable aggressive type of tumours, like acute human T-cell leukemia, promyelocytic leukemia, and human and rat hepatocellular cancer, human breast cancer and TNF-stimulated human cervix carcinoma (Darshan et al. 2015).

It could be also used as colorant for both food, like yogurt and carbonated drinks (Namazkar et al. 2013), and polymers as polyolefins (Ryazantseva et al. 2014), as well as sun protection factor in sunscreen creams (Suryawanshi et al. 2014). For all these reasons, the discovery and study of new species or isolates producing prodigiosin is very important: the characterization of isolates' pigment could help in the comprehension of not only its metabolic role, but also in the exploitation of its properties. For example, in cycloprodigiosins, the study of the promotion of H⁺/Cl⁻ symport activity, that acidifies the cytosol, inducing the apoptosis, could explain the targets and help in the design of more potent proapoptotic agents (Darshan et al. 2015). The prodigiosin family is noteworthy for their diversified biological effects, but their mode of action needs to be deepened to obtain a more reliable and conclusive picture: prodigiosin group presents a common mechanism towards selected molecular targets, which is relevant for the development of anticancer drugs (Darshan et al. 2015).

This thesis represents the first steps for the isolates' prodigiosin characterization, whose properties could represent a new starting point for further research. On the other hand, the Gram variability topic, whose hypothesis was, in this case, not confirmed, is also very interesting to deepen into, for example, testing the bacterial growth in stress-conditions. In fact, many Gram-variable or Gram-indetermined microorganisms are resistant to antibiotics, which is a relevant problem particularly in the healthcare system. Because the used LPS isolation technique, firstly thought for *Leptospira* (Bonhomme et al. 2020), worked quite well in *S. marcescens*, it could

be interesting to check it in Gram-variable species: in this way, we are setting a new method for the studying of this unique and rare phenomenon.

APPENDICES

APPENDIX A

A.1. Growth curve measurements in 96-wells-microplates

		LB					GL				
	hours	1	2	3	average	dev. st.	1	2	3	average	dev. st.
t₀	0	0.120	0.115	0.131	0.264	0.008	0.116	0.124	0.145	0.096	0.015
t₁	2	0.152	0.153	0.151	0.114	0.001	0.168	0.158	0.181	0.127	0.012
t₂	4	0.363	0.212	0.202	0.194	0.090	0.182	0.172	0.220	0.143	0.025
t₃	6	0.276	0.273	0.259	0.202	0.009	0.353	0.231	0.460	0.261	0.114
t₄	12	0.534	0.584	0.517	0.409	0.035	0.514	0.327	0.501	0.336	0.104
t₅	24	0.601	0.605	0.621	0.457	0.011	0.620	0.410	0.731	0.440	0.163
t₆	32	0.678	0.722	0.755	0.539	0.039	0.646	0.487	0.910	0.511	0.213
t₇	36	0.685	0.729	0.738	0.538	0.028	0.674	0.380	0.927	0.495	0.274
t₈	48	0.671	0.676	0.686	0.508	0.008	0.724	0.503	0.897	0.531	0.197
t₉	54	0.719	0.774	0.765	0.565	0.030	0.792	0.546	0.828	0.542	0.154
t₁₀	60	0.797	0.848	0.813	0.614	0.026	0.861	0.685	0.917	0.616	0.121

Table A1. Table reporting the PJ OD₆₀₀ values measured at each timepoint for each well from the first attempt, referred as “not aerated conditions”; the control wells have been cross-contaminated.

		LB					GL				
	hours	1	2	3	average	dev. st.	1	2	3	average	dev. st.
t₀	0	0.088	0.087	0.086	0.087	0.001	0.084	0.085	0.086	0.085	0.001
t₁	2	0.118	0.120	0.125	0.121	0.004	0.113	0.118	0.110	0.113	0.004
t₂	4	0.176	0.152	0.170	0.166	0.013	0.161	0.159	0.153	0.158	0.004
t₃	6	0.255	0.231	0.255	0.247	0.014	0.262	0.248	0.237	0.249	0.012
t₄	12	0.620	0.597	0.646	0.621	0.024	0.483	0.475	0.454	0.470	0.015
t₅	24	0.780	0.783	0.812	0.792	0.018	0.712	0.685	0.670	0.689	0.021
t₆	32	0.817	0.812	0.821	0.817	0.005	0.744	0.710	0.700	0.718	0.023
t₇	36	0.880	0.854	0.874	0.869	0.014	0.773	0.738	0.726	0.746	0.024
t₈	48	0.946	0.917	0.949	0.937	0.018	0.806	0.761	0.753	0.773	0.029
t₉	54	0.992	0.977	0.996	0.988	0.010	0.823	0.759	0.754	0.779	0.038
t₁₀	60	1.039	1.025	1.040	1.035	0.008	0.831	0.763	0.760	0.785	0.040

Table A2. Table reporting the PJ OD₆₀₀ values measured at each timepoint for each well from the second attempt, referred as “aerated conditions”.

		LB					GL				
	hours	1	2	3	average	dev. st.	1	2	3	average	dev. st.
t₁	2	0.181	0.121	0.116	0.139	0.036	0.102	0.120	0.125	0.116	0.012
t₂	4	0.206	0.129	0.122	0.152	0.047	0.107	0.125	0.132	0.121	0.013
t₃	6	0.327	0.196	0.172	0.232	0.084	0.162	0.179	0.194	0.178	0.016
t₄	12	0.508	0.393	0.362	0.421	0.077	0.332	0.397	0.416	0.382	0.044
t₅	24	0.915	0.876	0.848	0.880	0.034	0.691	0.654	0.627	0.657	0.032
t₆	32	0.939	0.902	0.907	0.916	0.020	0.645	0.659	0.708	0.671	0.033
t₇	36	0.961	0.929	0.925	0.938	0.019	0.680	0.703	0.721	0.701	0.020
t₈	48	0.900	0.954	0.946	0.933	0.029	0.711	0.780	0.793	0.762	0.044
t₉	54	0.915	0.993	0.987	0.965	0.043	0.713	0.795	0.822	0.777	0.057
t₁₀	60	0.949	1.015	0.993	0.986	0.033	0.710	0.794	0.814	0.773	0.055

Table A3. Table reporting the PJ OD₆₀₀ values measured at each timepoint for each well from the fourth attempt.

Gram -					Gram +				
1	2	3	average	dev. st.	1	2	3	average	dev. st.
0.103	0.108	0.107	0.106	0.003	0.092	0.092	0.090	0.091	0.001
0.142	0.131	0.140	0.137	0.006	0.099	0.102	0.094	0.098	0.004
0.205	0.223	0.204	0.211	0.011	0.110	0.103	0.102	0.105	0.004
0.314	0.322	0.303	0.313	0.010	0.145	0.134	0.127	0.135	0.009
0.412	0.405	0.387	0.402	0.013	0.271	0.252	0.254	0.259	0.010
0.463	0.451	0.433	0.449	0.015	0.319	0.297	0.302	0.306	0.011
0.475	0.493	0.469	0.479	0.012	0.356	0.340	0.344	0.347	0.008
0.548	0.540	0.561	0.549	0.010	0.516	0.501	0.513	0.510	0.008
0.582	0.602	0.605	0.596	0.012	0.560	0.552	0.562	0.558	0.005
0.596	0.614	0.619	0.610	0.012	0.581	0.580	0.586	0.582	0.003

Table A4. Table reporting the Gram negative and positive bacteria OD_{600} values measured at each timepoint for each well from the fourth attempt; the table is the continuity of the third one.

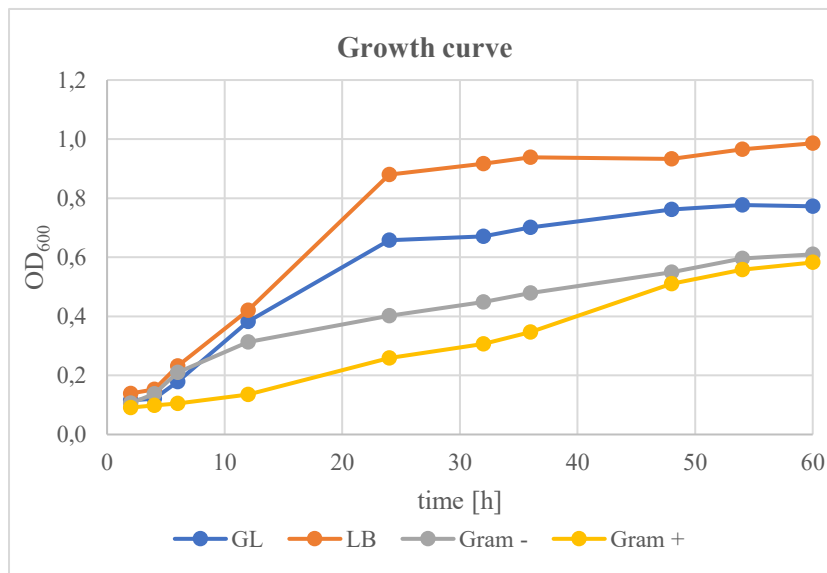


Table A5. Graph reporting the PJ in LB and LB + 1% glucose (GL), Gram-negative and positive bacteria OD_{600} values measured at each timepoint for each well from the fourth attempt.

hours	LB					GL					
	1	2	3	average	dev. st.	1	2	3	average	dev. st.	
t₁	2	0.119	0.116	0.110	0.115	0.005	0.113	0.113	0.119	0.115	0.003
t₂	4	0.189	0.186	0.173	0.183	0.009	0.136	0.136	0.140	0.138	0.003
t₃	6	0.268	0.243	0.249	0.253	0.013	0.210	0.211	0.211	0.211	0.001
t₄	12	0.475	0.483	0.489	0.482	0.007	0.384	0.419	0.419	0.407	0.020
t₅	24	0.776	0.734	0.749	0.753	0.021	1.102	1.086	1.093	1.094	0.008
t₆	32	0.828	0.778	0.790	0.799	0.026	1.153	1.130	1.137	1.140	0.012
t₇	36	0.855	0.797	0.816	0.823	0.029	1.167	1.153	1.158	1.159	0.007
t₈	48	0.981	0.877	0.876	0.911	0.061	1.161	1.164	1.174	1.166	0.007
t₉	54	1.031	0.933	0.934	0.966	0.056	1.168	1.151	1.157	1.159	0.009
t₁₀	60	1.077	0.963	0.966	1.002	0.065	1.176	1.163	1.172	1.170	0.006

Table A6. reporting the PJ OD_{600} values measured at each timepoint for each well from the fifth attempt.

		LB					GL				
hours		1	2	3	average	dev. st.	1	2	3	average	dev. st.
t ₁	2	0.116	0.121	0.115	0.117	0.003	0.123	0.122	0.126	0.124	0.002
t ₂	4	0.169	0.174	0.170	0.171	0.003	0.155	0.159	0.169	0.161	0.007
t ₃	6	0.240	0.253	0.263	0.252	0.011	0.273	0.261	0.302	0.279	0.021
t ₄	12	0.403	0.412	0.408	0.408	0.005	0.508	0.510	0.528	0.515	0.011
t ₅	24	0.766	0.766	0.767	0.766	0.000	1.138	1.144	1.110	1.131	0.018
t ₆	32	0.820	0.807	0.811	0.813	0.006	1.179	1.169	1.158	1.169	0.011
t ₇	36	0.842	0.822	0.826	0.830	0.011	1.176	1.176	1.150	1.167	0.015
t ₈	48	0.931	0.914	0.921	0.922	0.008	1.220	1.211	1.214	1.215	0.005
t ₉	54	0.951	0.957	0.956	0.955	0.004	1.244	1.225	1.229	1.233	0.010
t ₁₀	60	1.004	0.981	0.985	0.990	0.012	1.249	1.233	1.233	1.238	0.009

Table A7. reporting the D6 OD₆₀₀ values measured at each timepoint for each well from the fifth attempt.

		LB					GL				
hours		1	2	3	average	dev. st.	1	2	3	average	dev. st.
t ₁	2	0.130	0.115	0.118	0.121	0.008	0.141	0.138	0.133	0.137	0.004
t ₂	4	0.142	0.128	0.129	0.133	0.008	0.141	0.140	0.130	0.137	0.006
t ₃	6	0.180	0.181	0.177	0.179	0.002	0.202	0.205	0.206	0.204	0.002
t ₄	12	0.375	0.348	0.343	0.355	0.018	0.372	0.378	0.372	0.374	0.004
t ₅	24	0.760	0.737	0.754	0.750	0.012	1.089	1.096	1.064	1.083	0.017
t ₆	32	0.826	0.785	0.788	0.800	0.023	1.147	1.143	1.149	1.146	0.003
t ₇	36	0.821	0.786	0.790	0.799	0.019	1.164	1.146	1.162	1.157	0.010
t ₈	48	0.925	0.915	0.904	0.915	0.011	1.145	1.223	1.216	1.195	0.043
t ₉	54	0.972	0.941	0.932	0.948	0.021	1.260	1.269	1.244	1.258	0.013
t ₁₀	60	0.999	0.975	0.959	0.978	0.020	1.199	1.196	1.202	1.199	0.003

Table A8. reporting the PJ OD₆₀₀ values measured at each timepoint for each well from the sixth attempt.

		LB					GL				
hours		1	2	3	average	dev. st.	1	2	3	average	dev. st.
t ₁	2	0.143	0.145	0.150	0.146	0.003	0.142	0.137	0.137	0.139	0.003
t ₂	4	0.181	0.182	0.191	0.185	0.005	0.171	0.167	0.163	0.167	0.004
t ₃	6	0.241	0.253	0.261	0.252	0.010	0.278	0.256	0.270	0.268	0.011
t ₄	12	0.445	0.434	0.457	0.445	0.011	0.629	0.592	0.585	0.602	0.024
t ₅	24	0.775	0.767	0.764	0.769	0.005	1.138	1.146	1.137	1.140	0.005
t ₆	32	0.859	0.827	0.817	0.834	0.022	1.188	1.203	1.185	1.192	0.010
t ₇	36	0.853	0.823	0.817	0.831	0.019	1.199	1.212	1.195	1.202	0.009
t ₈	48	0.949	0.914	0.914	0.926	0.020	1.239	1.240	1.242	1.240	0.001
t ₉	54	0.991	0.965	0.969	0.975	0.014	1.254	1.249	1.246	1.249	0.004
t ₁₀	60	1.042	1.010	1.021	1.024	0.016	1.262	1.252	1.247	1.254	0.008

Table A9. reporting the D6 OD₆₀₀ values measured at each timepoint for each well from the sixth attempt.

		t ₁	t ₂	t ₃	t ₄	t ₅	t ₆	t ₇	t ₈	t ₉	t ₁₀	Legend pH colours	
1° attempt	LB											6	
	GL											6.5	
2° attempt	LB											7	
	GL											7.5	
3° attempt	LB											8	
	GL												
4° attempt	LB												
	GL												

Table A10. Prodigiosin production differences between LB and LB + 1% glucose from the first, second, third and fourth attempt; pigment production is testified also by pH changes (on the right the legend is reported).

Table A11. 96-wells-microplate configuration used in the first attempt ("not aerated conditions").

Table A12. 96-wells-microplate configuration used in the second, third, fourth, fifth and sixth attempt.

A.2. Growth and size analysis

SECOND ATTEMPT: average length of PJ in LB										
	t ₁	t ₂	t ₃	t ₄	t ₅	t ₆	t ₇	t ₈	t ₉	t ₁₀
	2	4	6	12	24	30	36	48	54	60
1	0.017	0.020	0.017	0.020	0.008	0.010	0.010	0.015	0.010	0.012
2	0.020	0.022	0.020	0.011	0.013	0.013	0.012	0.018	0.013	0.015
3	0.017	0.019	0.021	0.018	0.015	0.012	0.015	0.014	0.010	0.012
4	0.017	0.019	0.020	0.011	0.011	0.014	0.012	0.016	0.011	0.013
5	0.019	0.019	0.016	0.013	0.011	0.010	0.012	0.014	0.011	0.012
6	0.014	0.025	0.018	0.016	0.010	0.014	0.013	0.019	0.010	0.015
7	0.012	0.016	0.019	0.017	0.013	0.010	0.011	0.014	0.016	0.015
8	0.019	0.019	0.019	0.024	0.015	0.013	0.012	0.014	0.014	0.014
9	0.010	0.025	0.018	0.014	0.010	0.008	0.014	0.012	0.012	0.012
10	0.009	0.028	0.011	0.011	0.010	0.014	0.015	0.016	0.009	0.012
average mm	0.016	0.021	0.018	0.015	0.012	0.012	0.013	0.015	0.012	0.013
average µm	1.643	2.073	1.763	1.525	1.163	1.180	1.253	1.485	1.163	1.324
dev.st.	0.004	0.004	0.003	0.004	0.002	0.002	0.001	0.002	0.002	0.001

Table A13. Average bacterial length from 2nd attempt in LB; deviation standard is reported.

SECOND ATTEMPT: average width of PJ in LB

	t ₁	t ₂	t ₃	t ₄	t ₅	t ₆	t ₇	t ₈	t ₉	t ₁₀
	2	4	6	12	24	30	36	48	54	60
1	0.007	0.008	0.005	0.008	0.008	0.006	0.004	0.003	0.004	0.006
2	0.006	0.008	0.007	0.006	0.005	0.006	0.005	0.002	0.005	0.007
3	0.006	0.008	0.005	0.005	0.004	0.004	0.005	0.007	0.004	0.008
4	0.004	0.008	0.005	0.007	0.005	0.005	0.005	0.008	0.010	0.006
5	0.005	0.007	0.007	0.006	0.005	0.008	0.005	0.007	0.005	0.007
6	0.004	0.007	0.008	0.010	0.005	0.004	0.004	0.004	0.003	0.005
7	0.006	0.005	0.009	0.006	0.003	0.002	0.007	0.005	0.004	0.005
8	0.010	0.005	0.008	0.005	0.005	0.004	0.004	0.004	0.006	0.004
9	0.006	0.006	0.005	0.006	0.004	0.007	0.005	0.004	0.003	0.004
10	0.005	0.008	0.006	0.003	0.004	0.003	0.005	0.007	0.004	0.006
average mm	0.006	0.007	0.006	0.006	0.005	0.005	0.005	0.005	0.005	0.006
average µm	0.576	0.697	0.633	0.590	0.500	0.490	0.483	0.485	0.490	0.550
dev.st.	0.002	0.001	0.002	0.002	0.001	0.002	0.001	0.002	0.002	0.001

Table A13. Average bacterial width from 2nd attempt in LB; deviation standard is reported.

SECOND ATTEMPT: average length of PJ in LB + 1% (GL)

	t ₁	t ₂	t ₃	t ₄	t ₅	t ₆	t ₇	t ₈	t ₉	t ₁₀
	2	4	6	12	24	30	36	48	54	60
1	0.019	0.014	0.018	0.016	0.010	0.015	0.013	0.008	0.010	0.010
2	0.020	0.021	0.020	0.015	0.011	0.009	0.018	0.011	0.007	0.010
3	0.022	0.019	0.021	0.013	0.011	0.009	0.016	0.013	0.012	0.013
4	0.016	0.019	0.015	0.012	0.014	0.014	0.011	0.014	0.008	0.009
5	0.021	0.020	0.020	0.008	0.010	0.008	0.009	0.011	0.010	0.009
6	0.017	0.022	0.019	0.011	0.008	0.011	0.009	0.015	0.011	0.008
7	0.016	0.015	0.016	0.010	0.009	0.010	0.012	0.014	0.010	0.012
8	0.021	0.021	0.017	0.009	0.011	0.012	0.007	0.006	0.012	0.010
9	0.018	0.017	0.018	0.012	0.011	0.014	0.012	0.011	0.010	0.009
10	0.019	0.019	0.019	0.011	0.011	0.011	0.012	0.011	0.010	0.010
average mm	0.019	0.019	0.018	0.012	0.011	0.011	0.012	0.011	0.010	0.010
average µm	1.880	1.862	1.823	1.155	1.066	1.133	1.167	1.120	1.001	0.997
dev.st.	0.002	0.003	0.002	0.003	0.002	0.002	0.003	0.003	0.001	0.002

Table A14. Average bacterial length from 2nd attempt in LB + 1% glucose (GL); dev. standard is reported.

SECOND ATTEMPT: average width of PJ in LB + 1% (GL)

	t ₁	t ₂	t ₃	t ₄	t ₅	t ₆	t ₇	t ₈	t ₉	t ₁₀
	2	4	6	12	24	30	36	48	54	60
1	0.006	0.007	0.007	0.006	0.005	0.004	0.005	0.005	0.003	0.006
2	0.006	0.006	0.005	0.006	0.004	0.004	0.005	0.004	0.005	0.006
3	0.006	0.008	0.006	0.004	0.003	0.005	0.004	0.004	0.003	0.006
4	0.005	0.006	0.004	0.006	0.004	0.005	0.006	0.004	0.003	0.004
5	0.006	0.007	0.006	0.004	0.003	0.004	0.005	0.002	0.003	0.004
6	0.004	0.007	0.007	0.004	0.006	0.004	0.004	0.006	0.004	0.004
7	0.005	0.007	0.008	0.005	0.005	0.004	0.004	0.002	0.003	0.003
8	0.006	0.007	0.008	0.004	0.004	0.005	0.006	0.005	0.004	0.004
9	0.007	0.006	0.005	0.004	0.004	0.004	0.005	0.005	0.003	0.004
10	0.006	0.007	0.005	0.005	0.004	0.005	0.003	0.003	0.003	0.005
average mm	0.006	0.007	0.006	0.005	0.004	0.004	0.004	0.004	0.004	0.005
average µm	0.573	0.663	0.600	0.455	0.410	0.447	0.445	0.365	0.350	0.460
dev.st.	0.001	0.001	0.001	0.001	0.001	0.001	0.001	0.001	0.001	0.001

Table A15. Average bacterial width from 2nd attempt in LB + 1% glucose (GL); dev. standard is reported.

THIRD ATTEMPT: average length of PJ in LB

	t ₁	t ₂	t ₃	t ₄	t ₅	t ₆	t ₇	t ₈	t ₉	t ₁₀
	2	4	6	12	24	30	36	48	54	60
1	0.016	0.020	0.021	0.008	0.012	0.005	0.010	0.009	0.008	0.010
2	0.010	0.021	0.017	0.011	0.010	0.006	0.011	0.007	0.006	0.008
3	0.015	0.020	0.020	0.010	0.008	0.006	0.009	0.007	0.010	0.009
4	0.011	0.018	0.022	0.017	0.012	0.008	0.009	0.005	0.008	0.010
5	0.014	0.021	0.019	0.010	0.010	0.007	0.005	0.008	0.003	0.010
6	0.011	0.021	0.018	0.011	0.009	0.005	0.006	0.006	0.008	0.006
7	0.018	0.019	0.015	0.014	0.008	0.004	0.006	0.006	0.007	0.009
8	0.013	0.015	0.017	0.009	0.010	0.003	0.005	0.008	0.007	0.012
9	0.018	0.016	0.014	0.010	0.010	0.007	0.005	0.007	0.010	0.010
10	0.015	0.019	0.016	0.012	0.008	0.003	0.007	0.006	0.009	0.010
average mm	0.014	0.019	0.018	0.011	0.010	0.005	0.007	0.007	0.008	0.009
average µm	1.380	1.893	1.760	1.137	0.970	0.537	0.707	0.690	0.767	0.930
dev.st.	0.003	0.002	0.003	0.003	0.001	0.002	0.002	0.001	0.002	0.002

Table A16. Average bacterial length from 3rd attempt in LB; deviation standard is reported.

THIRD ATTEMPT: average width of PJ in LB

	t ₁	t ₂	t ₃	t ₄	t ₅	t ₆	t ₇	t ₈	t ₉	t ₁₀
	2	4	6	12	24	30	36	48	54	60
1	0.005	0.006	0.005	0.005	0.003	0.003	0.003	0.003	0.004	0.002
2	0.004	0.006	0.006	0.004	0.004	0.003	0.004	0.004	0.003	0.002
3	0.005	0.006	0.008	0.003	0.003	0.004	0.003	0.002	0.003	0.002
4	0.004	0.006	0.007	0.004	0.003	0.004	0.004	0.003	0.002	0.002
5	0.005	0.006	0.006	0.004	0.003	0.004	0.004	0.003	0.002	0.003
6	0.004	0.006	0.005	0.004	0.002	0.002	0.002	0.002	0.002	0.002
7	0.005	0.005	0.006	0.005	0.003	0.003	0.003	0.003	0.003	0.003
8	0.005	0.008	0.006	0.003	0.004	0.002	0.003	0.002	0.002	0.003
9	0.004	0.006	0.004	0.004	0.003	0.003	0.002	0.002	0.003	0.003
10	0.006	0.005	0.005	0.003	0.003	0.003	0.003	0.003	0.002	0.003
average mm	0.005	0.006	0.006	0.004	0.003	0.003	0.003	0.003	0.003	0.003
average µm	0.455	0.593	0.550	0.387	0.320	0.317	0.297	0.283	0.270	0.260
dev.st.	0.001	0.001	0.001	0.001	0.000	0.001	0.001	0.001	0.001	0.001

Table A17. Average bacterial width from 3rd attempt in LB; deviation standard is reported.

THIRD ATTEMPT: average length of PJ in LB + 1% (GL)

	t ₁	t ₂	t ₃	t ₄	t ₅	t ₆	t ₇	t ₈	t ₉	t ₁₀
	2	4	6	12	24	30	36	48	54	60
1	0.013	0.020	0.018	0.010	0.009	0.005	0.005	0.005	0.006	0.006
2	0.018	0.016	0.024	0.010	0.007	0.006	0.006	0.005	0.006	0.005
3	0.016	0.023	0.014	0.014	0.005	0.007	0.007	0.005	0.007	0.005
4	0.013	0.022	0.015	0.010	0.008	0.006	0.007	0.004	0.003	0.005
5	0.012	0.020	0.018	0.009	0.006	0.006	0.008	0.004	0.004	0.007
6	0.011	0.016	0.010	0.010	0.011	0.005	0.006	0.006	0.005	0.006
7	0.015	0.017	0.014	0.010	0.010	0.004	0.006	0.005	0.004	0.004
8	0.008	0.017	0.018	0.010	0.011	0.006	0.006	0.004	0.004	0.005
9	0.030	0.015	0.016	0.014	0.008	0.006	0.007	0.004	0.006	0.006
10	0.012	0.017	0.011	0.009	0.005	0.008	0.002	0.003	0.005	0.003
average mm	0.015	0.018	0.016	0.011	0.008	0.006	0.006	0.005	0.005	0.005
average µm	1.478	1.790	1.570	1.070	0.780	0.590	0.575	0.457	0.497	0.523
dev.st.	0.006	0.003	0.004	0.002	0.002	0.001	0.002	0.001	0.001	0.001

Table A18. Average bacterial length from 3rd attempt in LB + 1% glucose (GL); deviation standard is reported.

THIRD ATTEMPT: average width of PJ in LB + 1% (GL)

	t ₁	t ₂	t ₃	t ₄	t ₅	t ₆	t ₇	t ₈	t ₉
	2	4	6	12	24	30	36	48	54
1	0.005	0.005	0.008	0.005	0.002	0.005	0.004	0.003	0.003
2	0.005	0.006	0.006	0.004	0.006	0.004	0.004	0.003	0.004
3	0.006	0.006	0.006	0.004	0.005	0.003	0.006	0.002	0.003
4	0.005	0.005	0.003	0.004	0.003	0.004	0.003	0.003	0.002
5	0.005	0.007	0.003	0.004	0.003	0.005	0.003	0.003	0.003
6	0.007	0.005	0.004	0.004	0.004	0.003	0.004	0.003	0.002
7	0.006	0.006	0.003	0.003	0.003	0.007	0.004	0.003	0.003
8	0.006	0.004	0.006	0.004	0.004	0.003	0.004	0.002	0.003
9	0.005	0.007	0.004	0.004	0.004	0.004	0.003	0.003	0.002
10	0.004	0.006	0.005	0.005	0.003	0.003	0.004	0.003	0.003
average mm	0.005	0.006	0.005	0.004	0.003	0.004	0.004	0.003	0.003
average μm	0.537	0.555	0.475	0.410	0.335	0.410	0.365	0.280	0.283
dev.st.	0.001	0.001	0.002	0.001	0.001	0.001	0.001	0.001	0.001

Table A19. Average bacterial width from 3rd attempt in LB + 1% glucose (GL); deviation standard is reported.**FOURTH ATTEMPT: average length of PJ in LB**

	t ₁	t ₂	t ₃	t ₄	t ₅	t ₆	t ₇	t ₈	t ₉	t ₁₀
	2	4	6	12	24	30	36	48	54	60
1	0.029	0.020	0.026	0.022	0.019	0.015	0.015	0.011	0.010	0.012
2	0.019	0.020	0.018	0.022	0.013	0.013	0.022	0.012	0.011	0.013
3	0.020	0.023	0.025	0.020	0.014	0.016	0.017	0.010	0.013	0.011
4	0.021	0.022	0.023	0.018	0.011	0.014	0.015	0.012	0.012	0.010
5	0.021	0.026	0.020	0.015	0.012	0.013	0.010	0.011	0.009	0.014
6	0.026	0.020	0.026	0.017	0.011	0.017	0.011	0.016	0.011	0.015
7	0.026	0.017	0.028	0.017	0.010	0.012	0.020	0.015	0.014	0.011
8	0.032	0.022	0.024	0.020	0.011	0.012	0.016	0.016	0.009	0.010
9	0.031	0.031	0.022	0.019	0.015	0.011	0.013	0.016	0.009	0.011
10	0.036	0.025	0.027	0.014	0.011	0.013	0.014	0.013	0.009	0.013
average mm	0.026	0.022	0.024	0.018	0.013	0.014	0.015	0.013	0.011	0.012
average μm	2.607	2.225	2.410	1.830	1.267	1.367	1.523	1.323	1.073	1.210
dev.st.	0.006	0.004	0.003	0.003	0.003	0.002	0.004	0.002	0.002	0.002

Table A20. Average bacterial length from 4th attempt in LB; deviation standard is reported.**FOURTH ATTEMPT: average width of PJ in LB**

	t ₁	t ₂	t ₃	t ₄	t ₅	t ₆	t ₇	t ₈	t ₉	t ₁₀
	2	4	6	12	24	30	36	48	54	60
1	0.005	0.007	0.006	0.004	0.004	0.004	0.004	0.004	0.002	0.003
2	0.005	0.007	0.006	0.004	0.004	0.005	0.004	0.003	0.003	0.003
3	0.005	0.007	0.006	0.004	0.003	0.005	0.004	0.003	0.004	0.003
4	0.005	0.008	0.005	0.004	0.003	0.003	0.004	0.003	0.003	0.003
5	0.006	0.006	0.006	0.005	0.004	0.004	0.004	0.003	0.003	0.003
6	0.004	0.007	0.006	0.004	0.004	0.004	0.003	0.003	0.003	0.003
7	0.005	0.006	0.006	0.004	0.003	0.004	0.003	0.003	0.003	0.003
8	0.006	0.006	0.006	0.005	0.003	0.003	0.003	0.003	0.003	0.003
9	0.006	0.007	0.006	0.005	0.003	0.004	0.004	0.003	0.003	0.003
10	0.005	0.007	0.007	0.004	0.003	0.003	0.003	0.003	0.003	0.003
average mm	0.005	0.006	0.006	0.004	0.003	0.004	0.003	0.003	0.003	0.003
average μm	0.517	0.640	0.597	0.430	0.343	0.397	0.347	0.317	0.300	0.300
dev.st	0.001	0.001	0.001	0.001	0.001	0.001	0.001	0.001	0.001	0.001

Table A21. Average bacterial width from 4th attempt in LB; deviation standard is reported.

FOURTH ATTEMPT: average length of PJ in LB + 1% glucose (GL)										
	t ₁	t ₂	t ₃	t ₄	t ₅	t ₆	t ₇	t ₈	t ₉	t ₁₀
	2	4	6	12	24	30	36	48	54	60
1	/	0.025	0.023	0.019	0.014	0.011	0.011	0.006	0.010	0.008
2	/	0.022	0.025	0.016	0.018	0.010	0.010	0.007	0.009	0.008
3	/	0.017	0.025	0.020	0.016	0.009	0.009	0.009	0.006	0.014
4	/	0.027	0.027	0.019	0.021	0.010	0.010	0.009	0.007	0.009
5	/	0.039	0.024	0.022	0.015	0.013	0.010	0.011	0.012	0.009
6	/	0.025	0.022	0.019	0.013	0.009	0.012	0.008	0.011	0.009
7	/	0.022	0.024	0.025	0.017	0.013	0.009	0.013	0.010	0.011
8	/	0.021	0.022	0.017	0.019	0.014	0.011	0.012	0.011	0.009
9	/	0.022	0.018	0.026	0.012	0.010	0.012	0.008	0.009	0.010
10	/	/	0.026	0.022	0.012	0.013	0.007	0.012	0.010	0.008
average mm	/	0.024	0.024	0.020	0.016	0.011	0.010	0.009	0.010	0.009
average µm	/	2.417	2.377	2.042	1.560	1.113	0.985	0.940	0.958	0.943
dev.st.	/	0.006	0.003	0.003	0.003	0.002	0.002	0.002	0.002	0.002


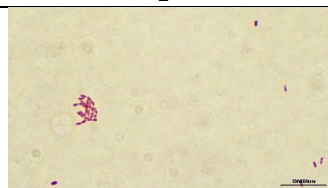

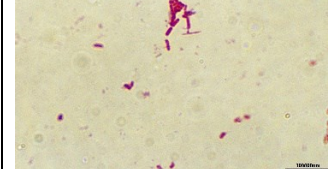
Table A22. Average bacterial length from 4th attempt in LB + 1% glucose (GL); dev. stand. is reported.

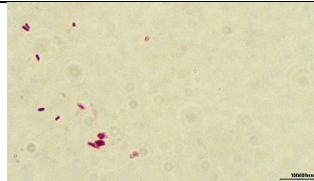
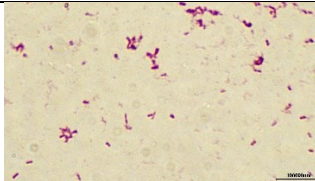
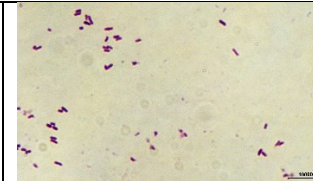

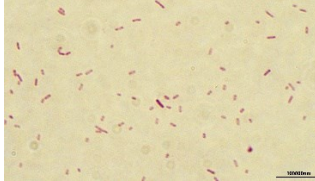
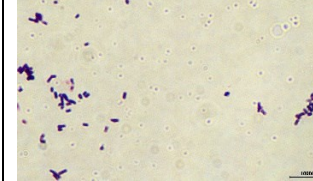
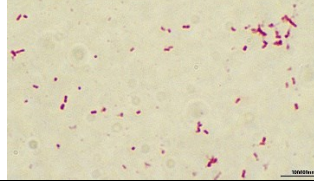
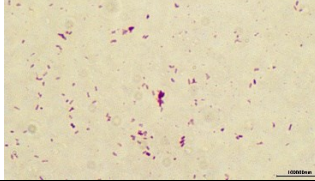
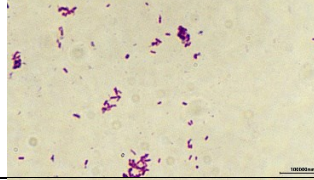
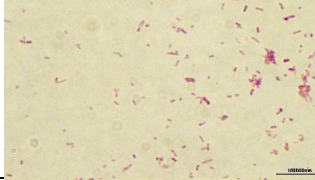
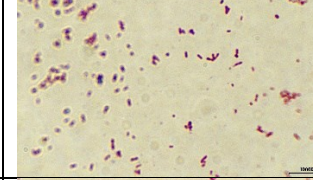




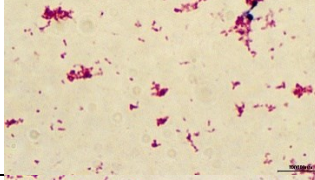
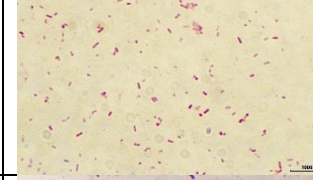
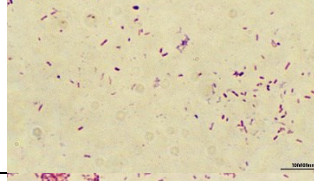
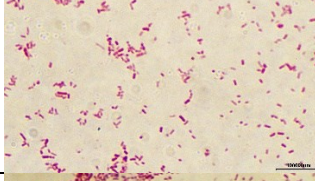
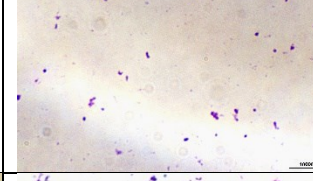
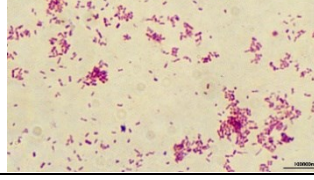
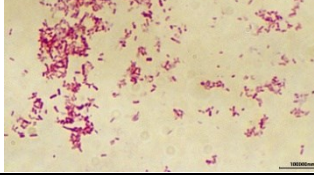
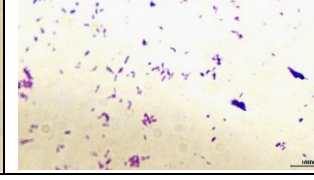
FOURTH ATTEMPT: average width of PJ in LB + 1% glucose (GL)										
	t ₁	t ₂	t ₃	t ₄	t ₅	t ₆	t ₇	t ₈	t ₉	t ₁₀
	2	4	6	12	24	30	36	48	54	60
1	/	0.007	0.007	0.005	0.004	0.006	0.006	0.005	0.006	0.005
2	/	0.006	0.006	0.005	0.004	0.004	0.007	0.005	0.005	0.006
3	/	0.005	0.006	0.004	0.004	0.005	0.005	0.005	0.006	0.005
4	/	0.007	0.007	0.005	0.005	0.004	0.005	0.005	0.005	0.005
5	/	0.007	0.007	0.005	0.005	0.005	0.004	0.005	0.005	0.005
6	/	0.007	0.007	0.005	0.004	0.004	0.006	0.005	0.005	0.005
7	/	0.006	0.008	0.005	0.005	0.005	0.006	0.005	0.006	0.005
8	/	0.006	0.006	0.004	0.005	0.004	0.006	0.006	0.006	0.006
9	/	0.007	0.006	0.005	0.004	0.004	0.006	0.005	0.005	0.005
10	/	/	0.005	0.006	0.004	0.004	0.005	0.005	0.006	0.005
average mm	/	0.006	0.007	0.005	0.004	0.005	0.005	0.005	0.005	0.005
average µm	/	0.622	0.653	0.493	0.440	0.457	0.540	0.490	0.547	0.530
dev.st	/	0.001	0.001	0.001	0.000	0.001	0.001	0.000	0.000	0.001

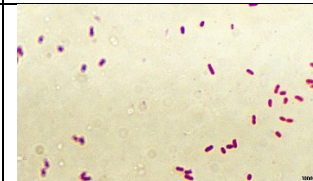
Table A23. Average bacterial width from 4th attempt in LB + 1% glucose (GL); deviation standard is reported.

A.3. Gram staining and microscope analysis

Table A24. Microscope pictures from PJ first attempt ("not aerated conditions") both in LB and LB + 1% glucose (GL); for each timepoint there are three repetitions and pH colours are reported.

FIRST ATTEMPT: PJ in LB			
	1	2	3
t ₁			no picture taken
t ₂	no picture taken		

t3			
t4			
t5			no picture taken
t6			
t7			
t8			
t9			
t10			

FIRST ATTEMPT: PJ in LB + 1% glucose (GL)			
	1	2	3
t1	no picture taken	no picture taken	

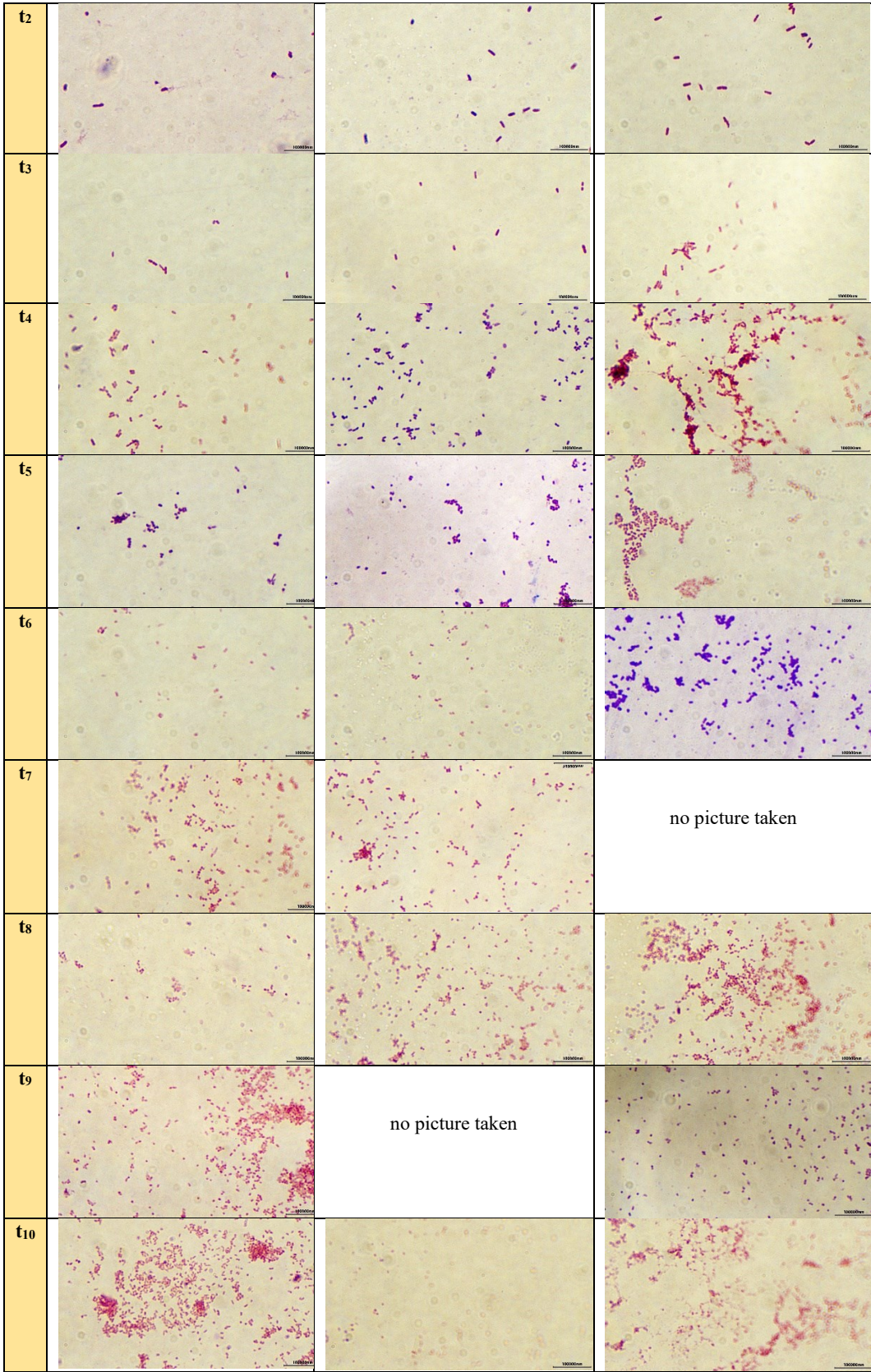
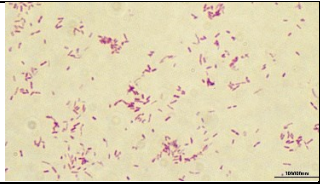
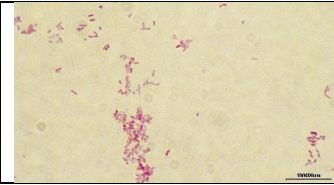
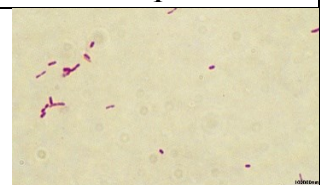
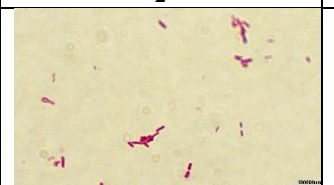

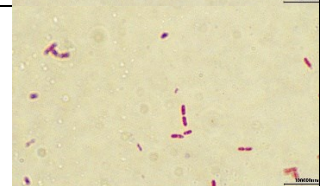
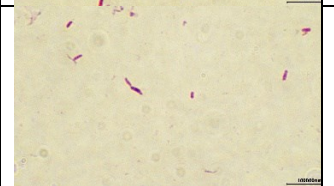
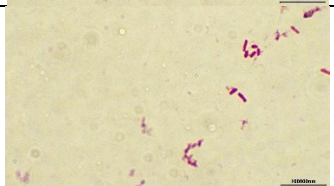


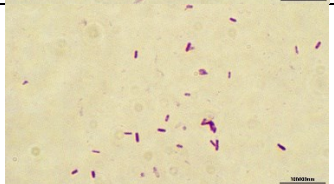

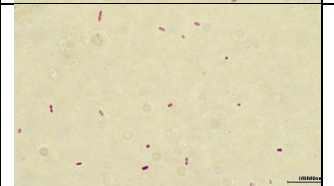
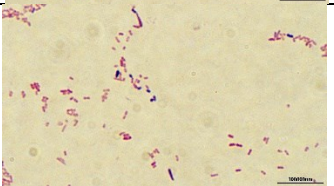
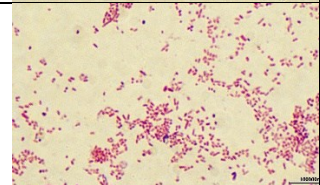
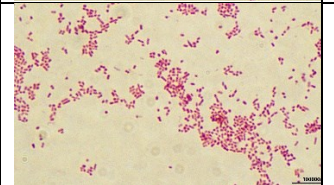
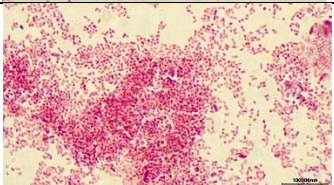
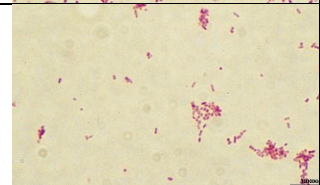
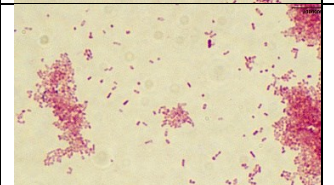
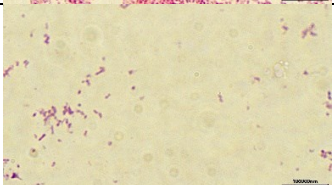
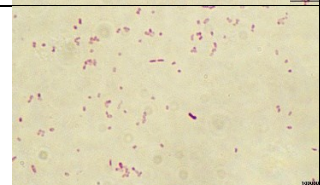
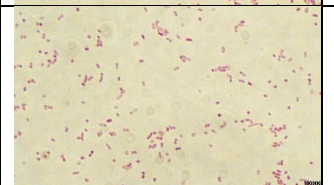

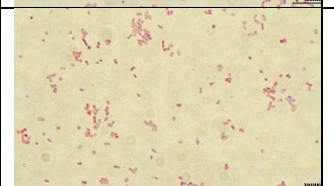
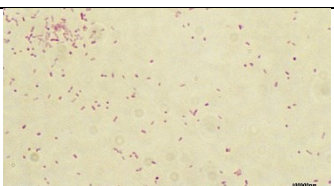


Table A25. Microscope pictures from PJ second attempt ("aerated conditions") both in LB and LB + 1% glucose (GL); for each timepoint there are three repetitions and pH colours are reported.

SECOND ATTEMPT: PJ in LB			
	1	2	3
t1			
t2			
t3			
t4			no picture taken
t5			
t6			
t7			
t8		no picture taken	
t9			

t10			no picture taken
------------	---	---	------------------

SECOND ATTEMPT: PJ in LB + 1% glucose (GL)			
	1	2	3
t1			
t2			
t3			
t4			
t5			
t6			
t7			no picture taken
t8			

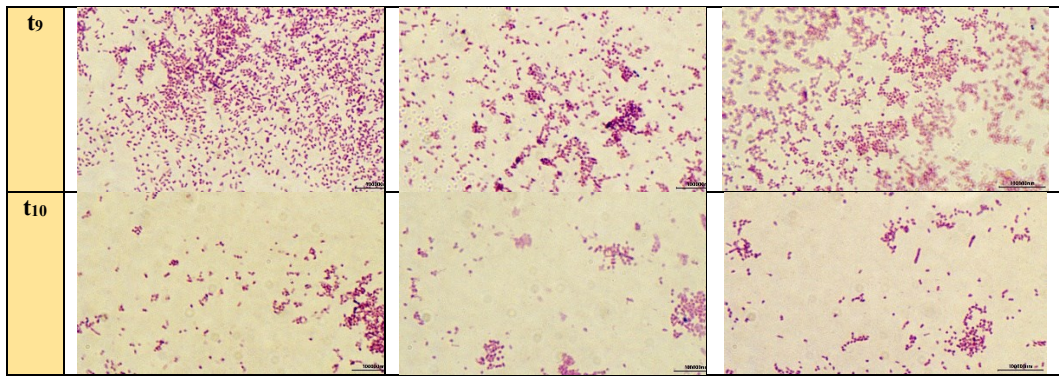
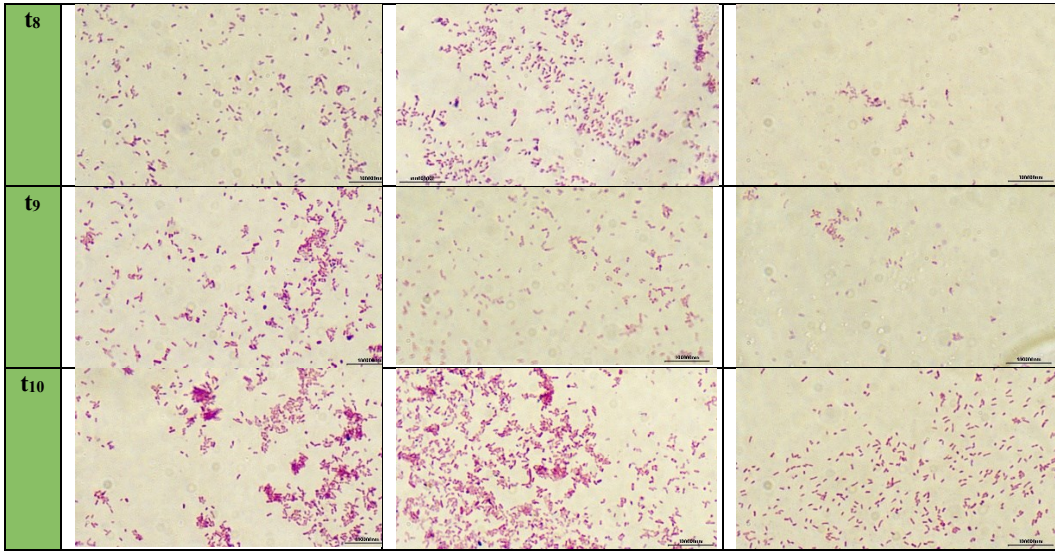


Table A26. Microscope pictures from PJ third attempt (“fresh sample”) both in LB and LB + 1% glucose (GL); for each timepoint there are three repetitions and pH colours are reported.

THIRD ATTEMPT: PJ in LB			
	1	2	3
t1	no picture taken		
t2			
t3			no picture taken
t4			
t5			
t6			
t7			



THIRD ATTEMPT: PJ in LB + 1% glucose (GL)			
	1	2	3
t1			
t2			no picture taken
t3		no picture taken	
t4			
t5		no picture taken	
t6			

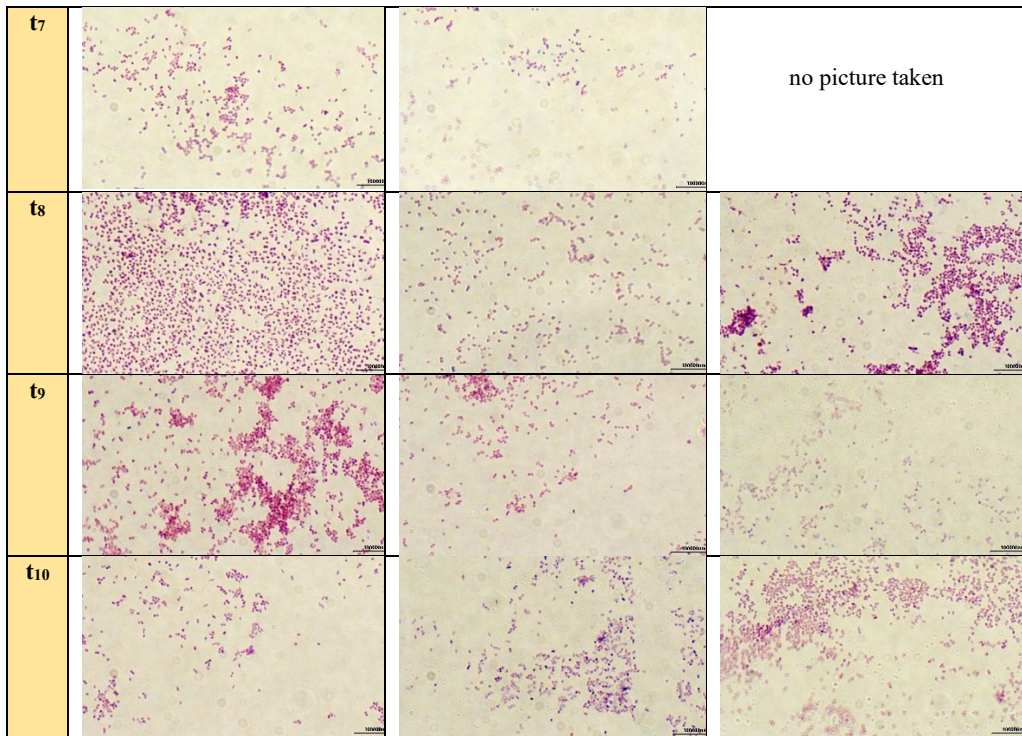
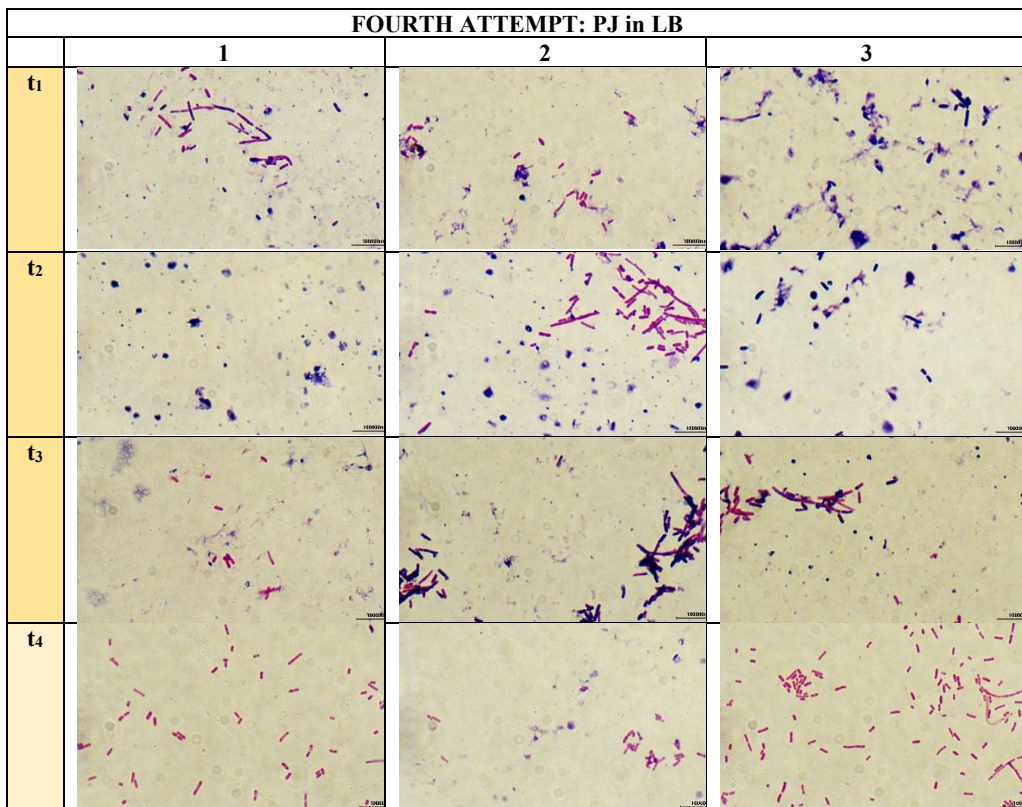
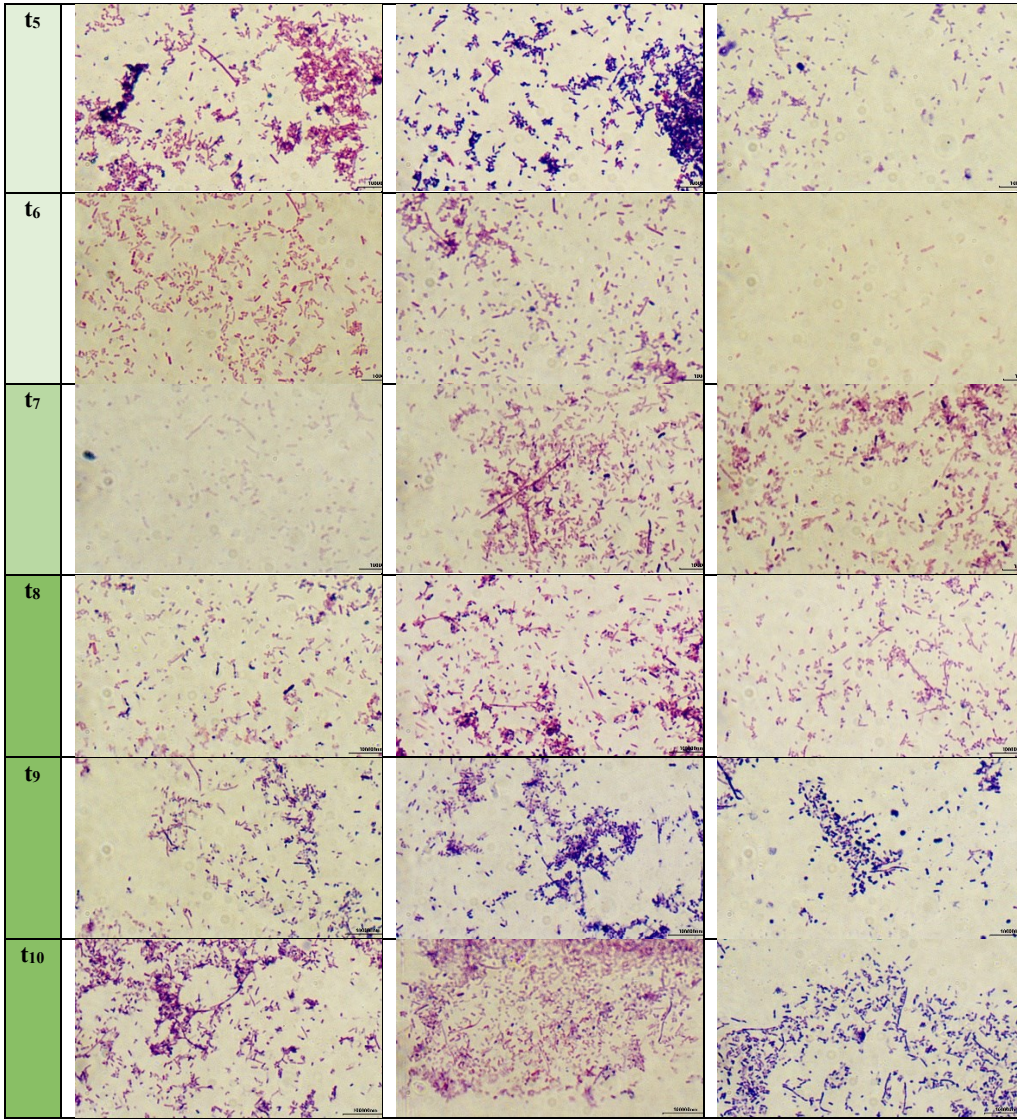


Table A27. Microscope pictures from PJ fourth attempt both in LB and LB + 1% glucose (GL); for each timepoint there are two repetitions and pH colours are reported.





FOURTH ATTEMPT: PJ in LB + 1% glucose (GL)			
	1	2	3
t1	no picture taken	no picture taken	no picture taken
t2			no picture taken
t3			

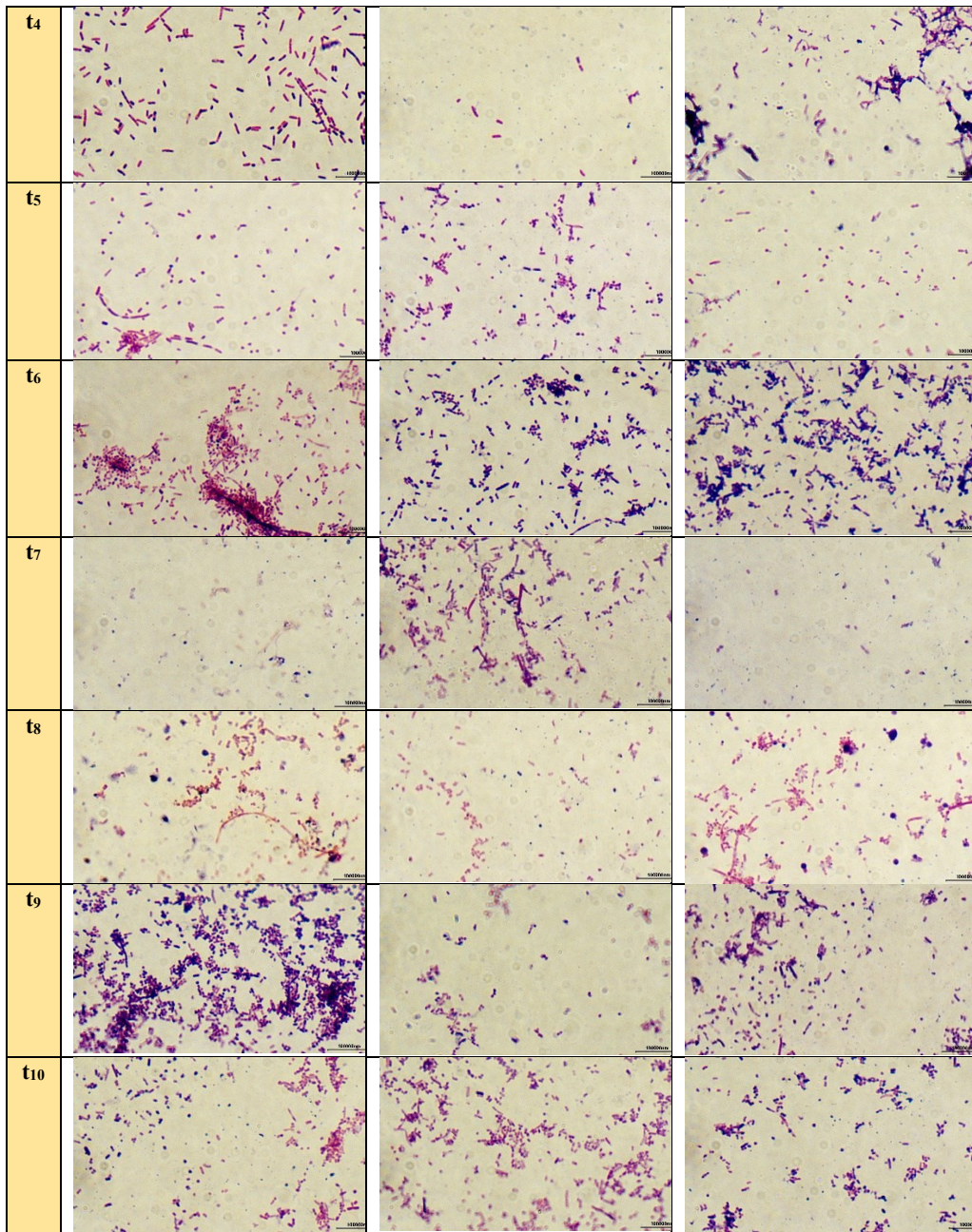
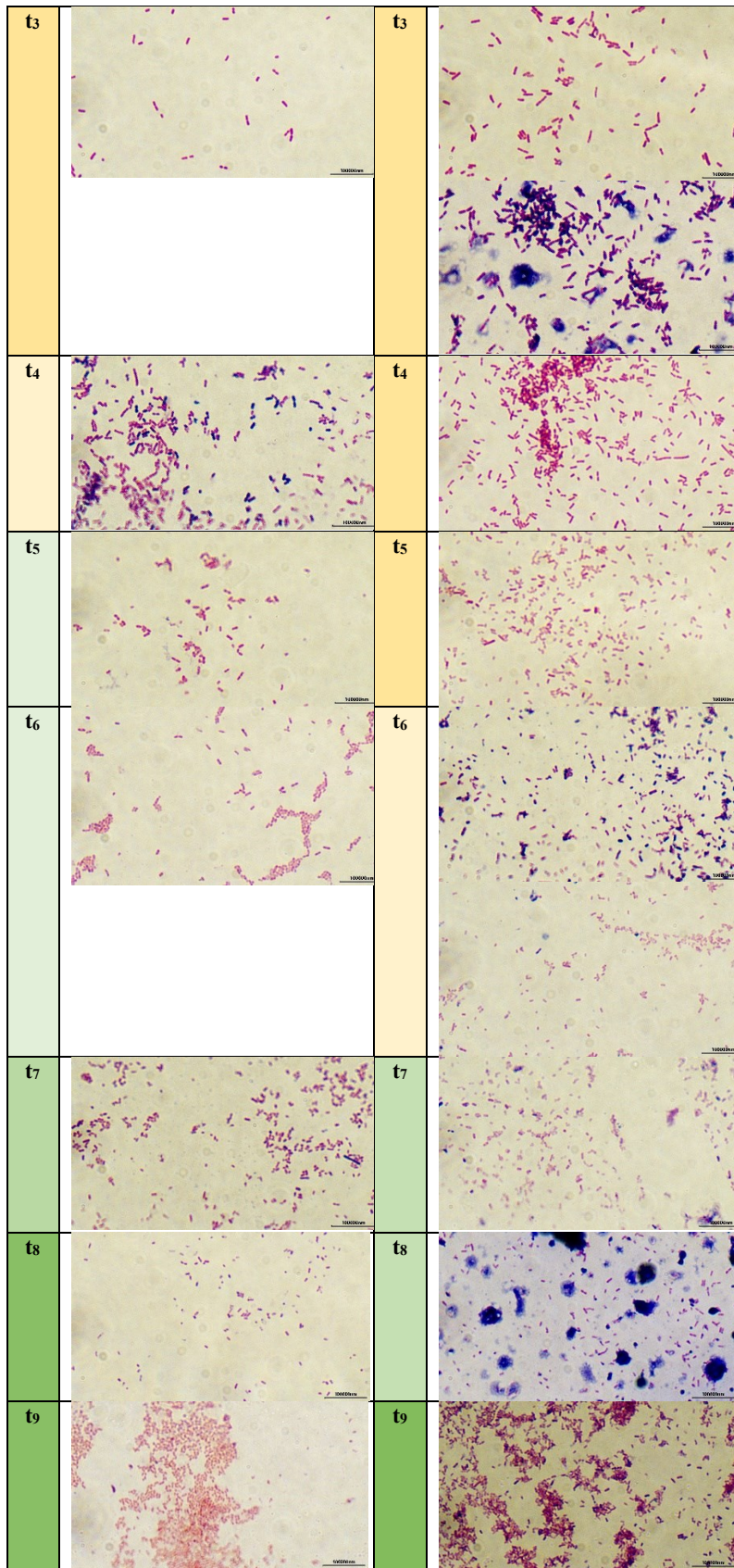
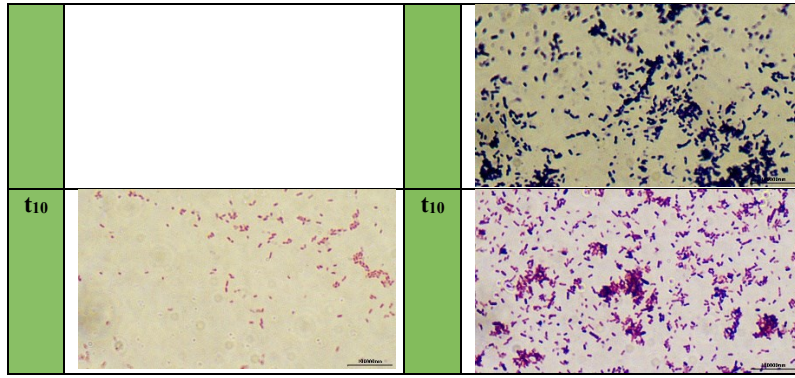


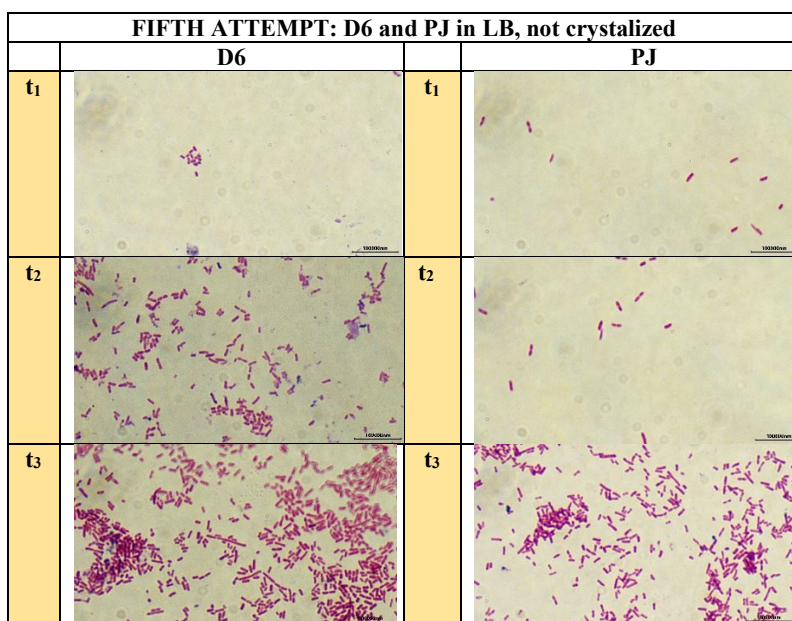
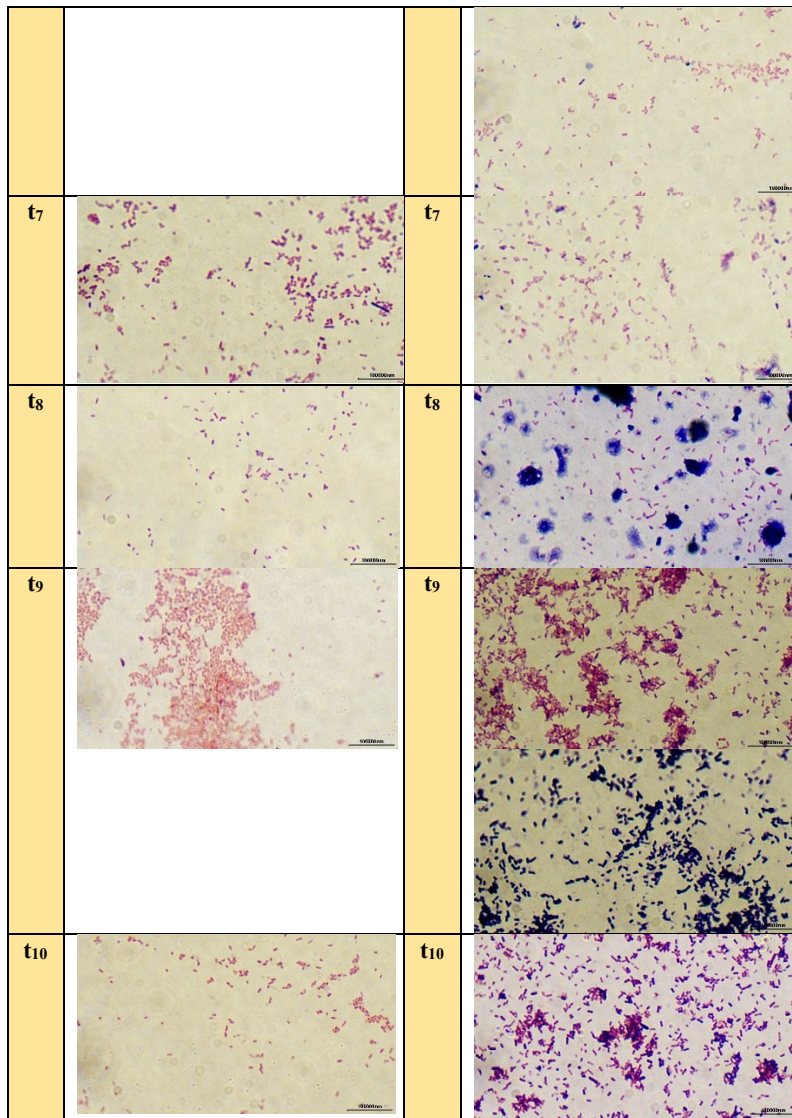
Table A28. Microscope pictures from PJ and D6 fifth attempt (“crystalized” and “not crystalized”) both in LB and LB + 1% glucose (GL); for each timepoint there is one repetition and pH colours reported.

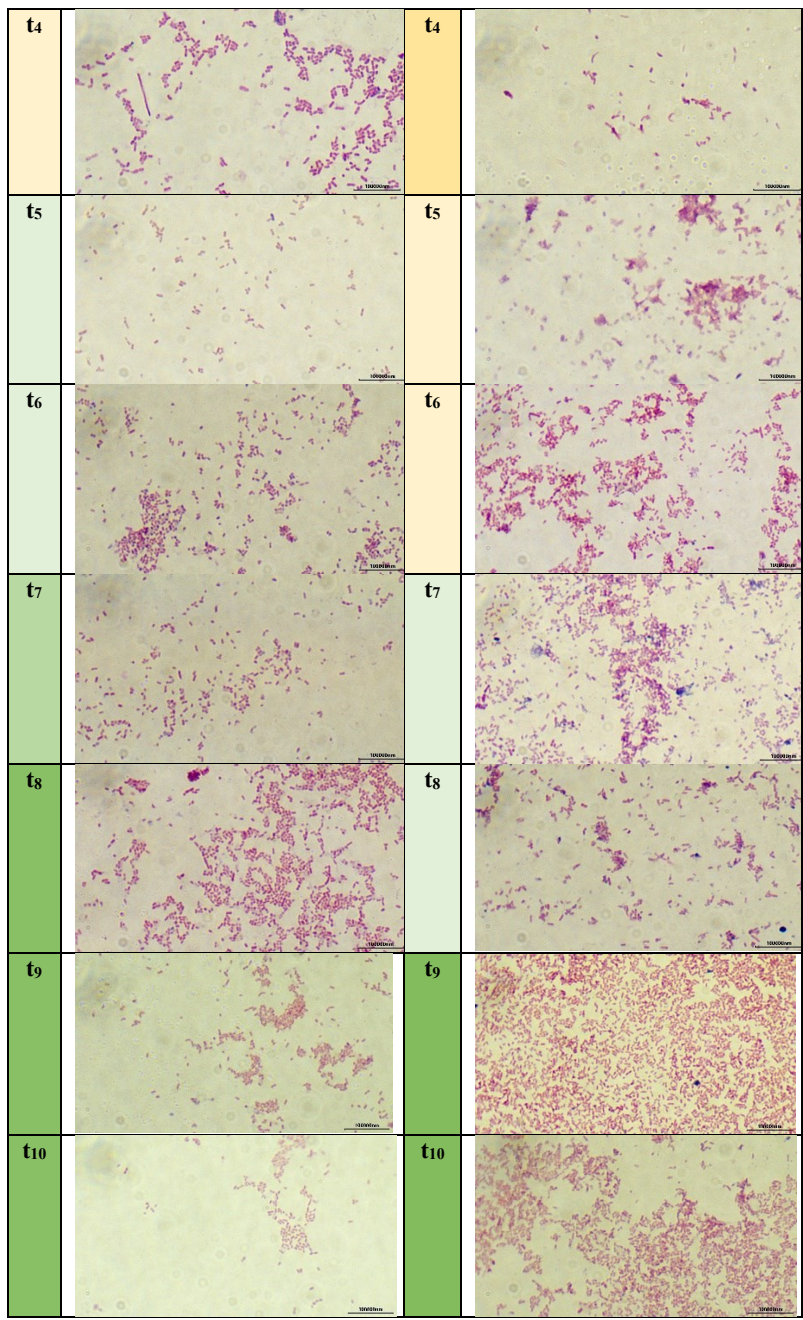
FIFTH ATTEMPT: D6 and PJ in LB, crystalized			
	D6		PJ
t1		t1	
t2		t2	

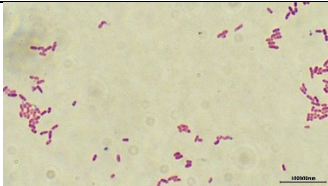

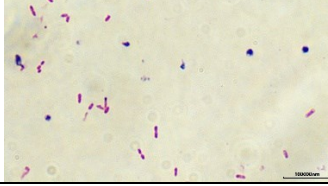


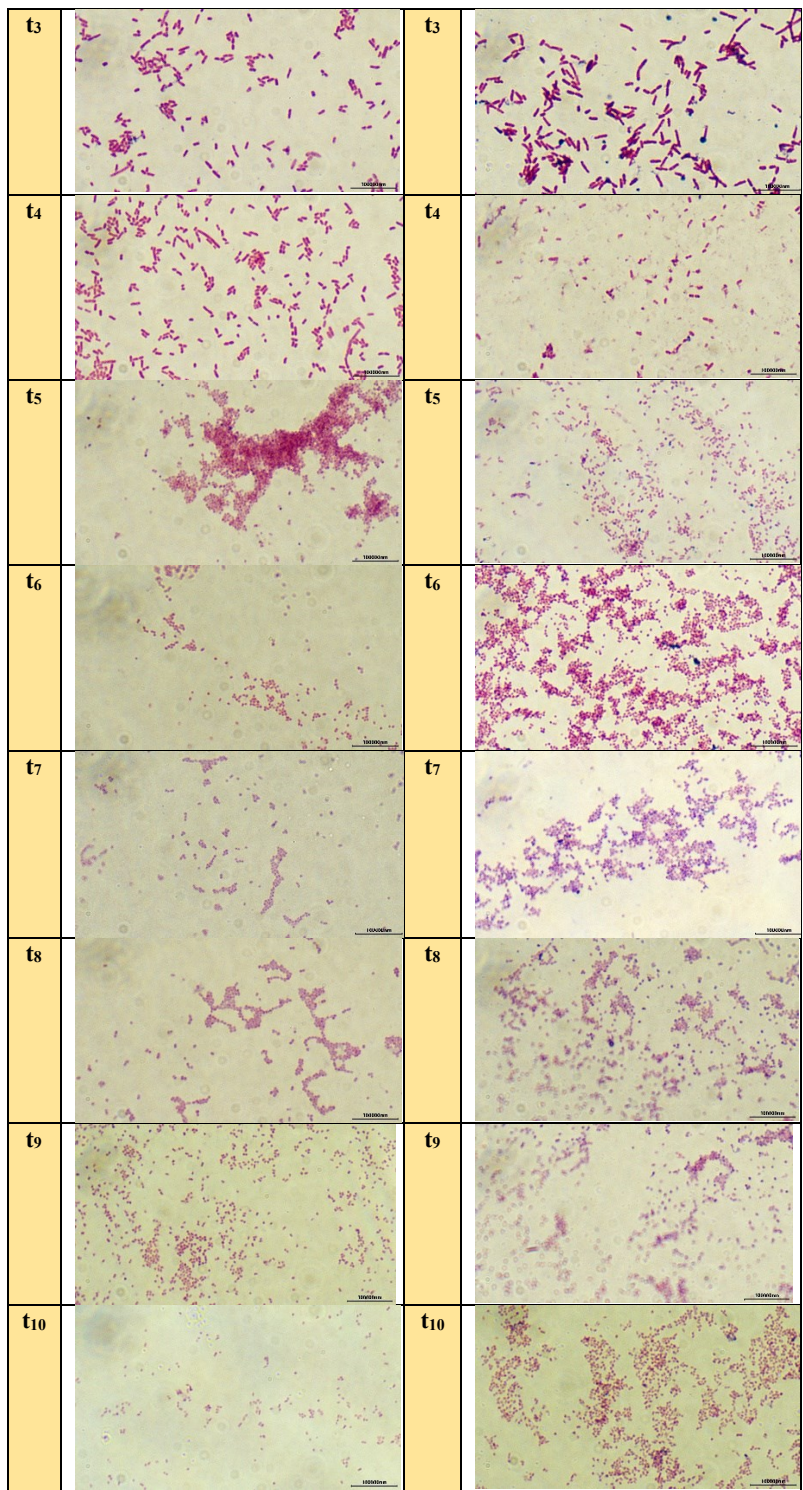


FIFTH ATTEMPT: D6 and PJ in LB + 1% glucose (GL), crystalized			
	D6		PJ
t1		t1	
t2		t2	
t3		t3	
t4		t4	
t5		t5	
t6		t6	





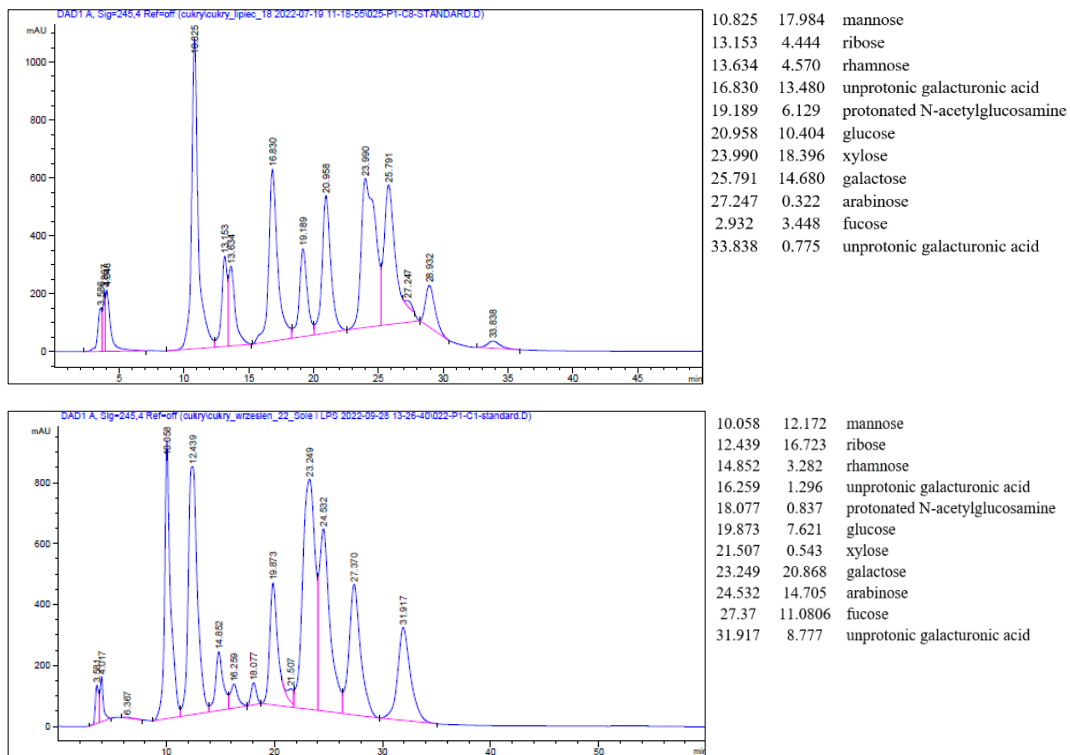
FIFTH ATTEMPT: D6 and PJ in LB + 1% glucose (GL), not crystalized			
	D6		PJ
t1		t1	no photo taken
t2		t2	



APPENDIX B

B.1. Sugars analysis

Table B1. Standard HPLC spectra on the right, retention time values with corresponding sugars on the left; the upper spectrum is from the first experiment, the below one from the second attempt.



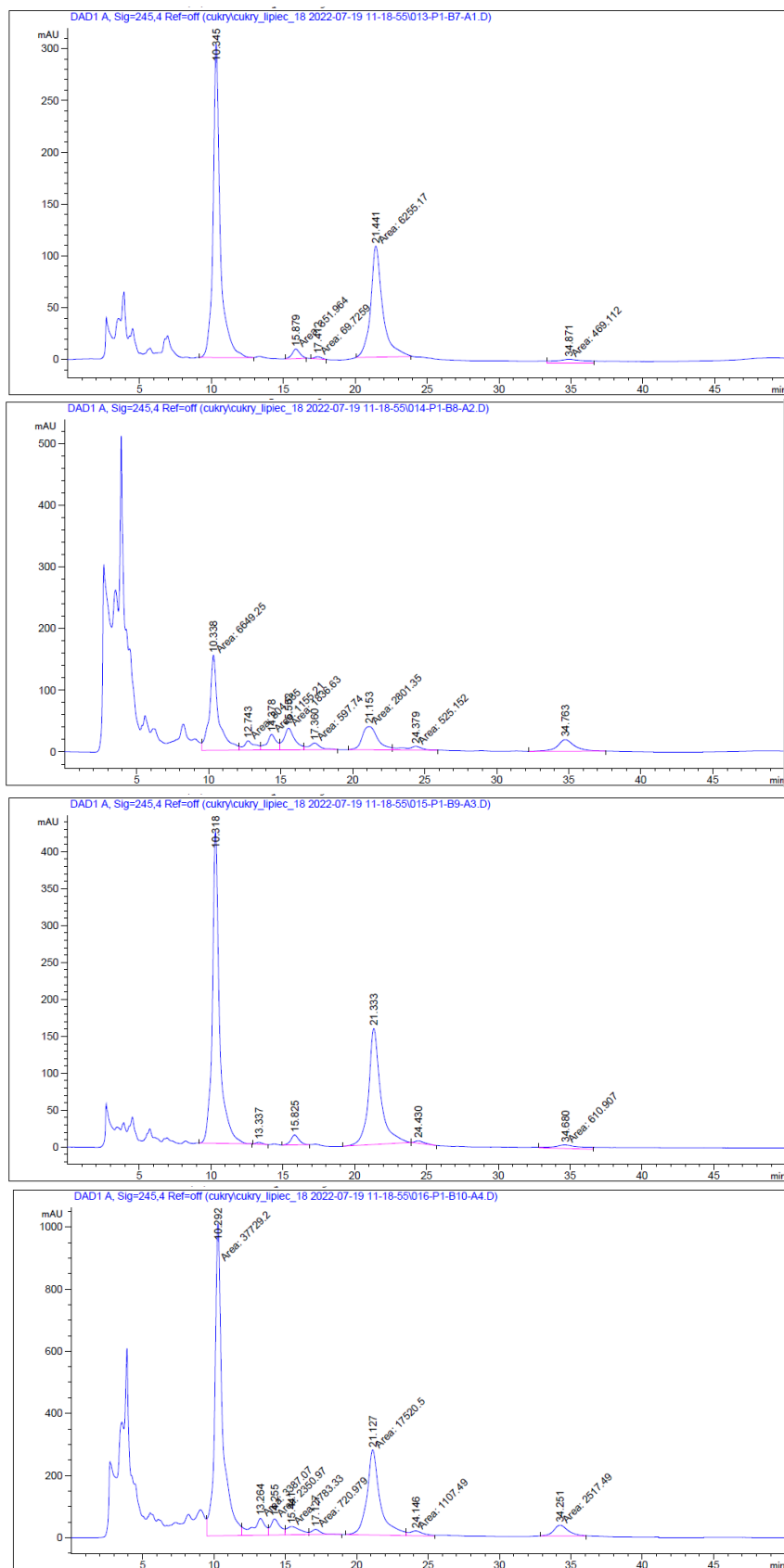


Table B2. Starting from above, A1, A2, A3 and A4 results from first attempt of HPLC analysis (names are also reported in the upper part of the spectra, in blue); peaks retention time is reported with value of integral (area).

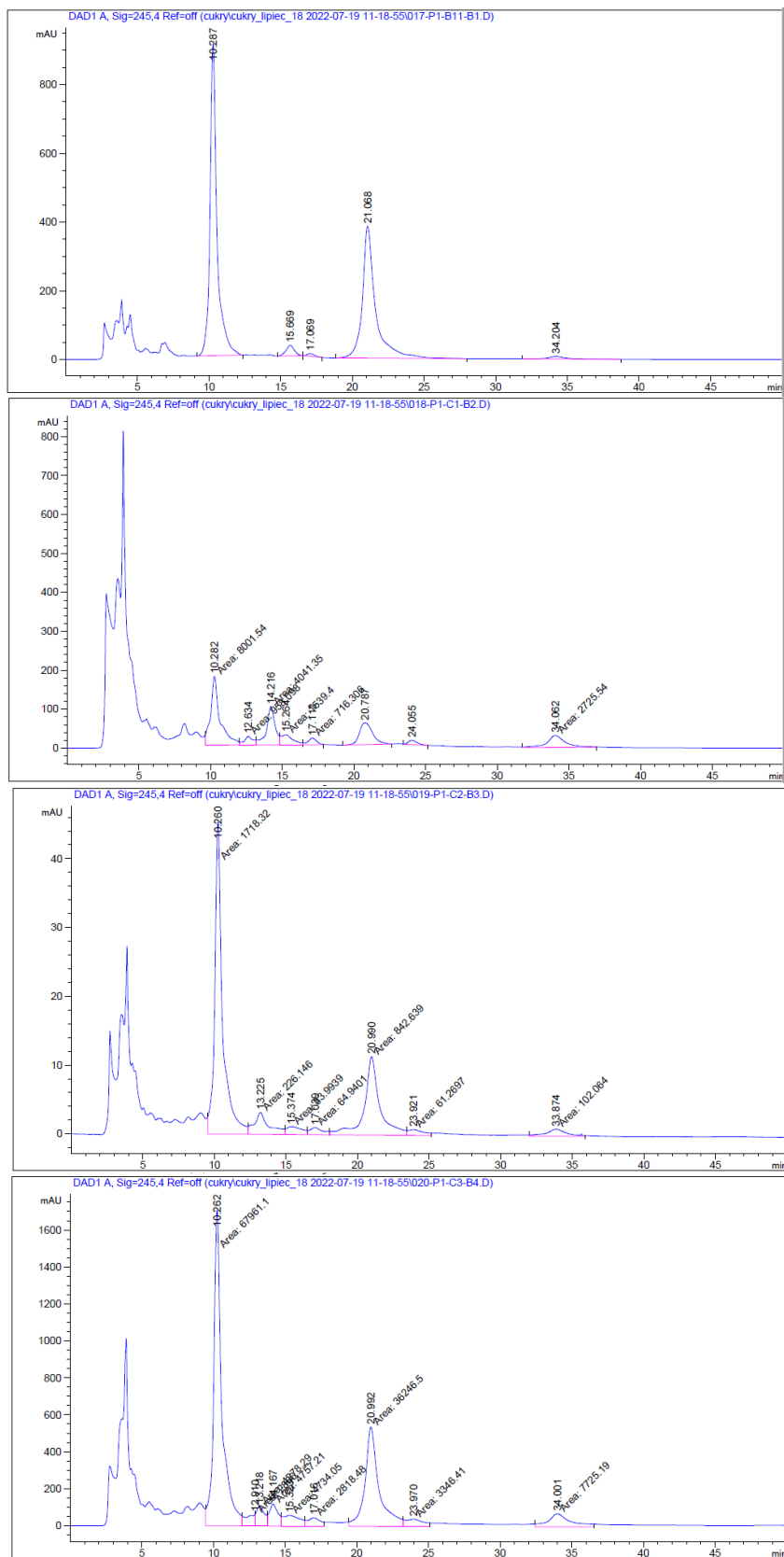


Table B3. Starting from above, B1, B2, B3, B4 results from first attempt for HPLC analysis (names are also reported in the upper part of the spectra, in blue); peaks' retention time is reported with value of integral (area).

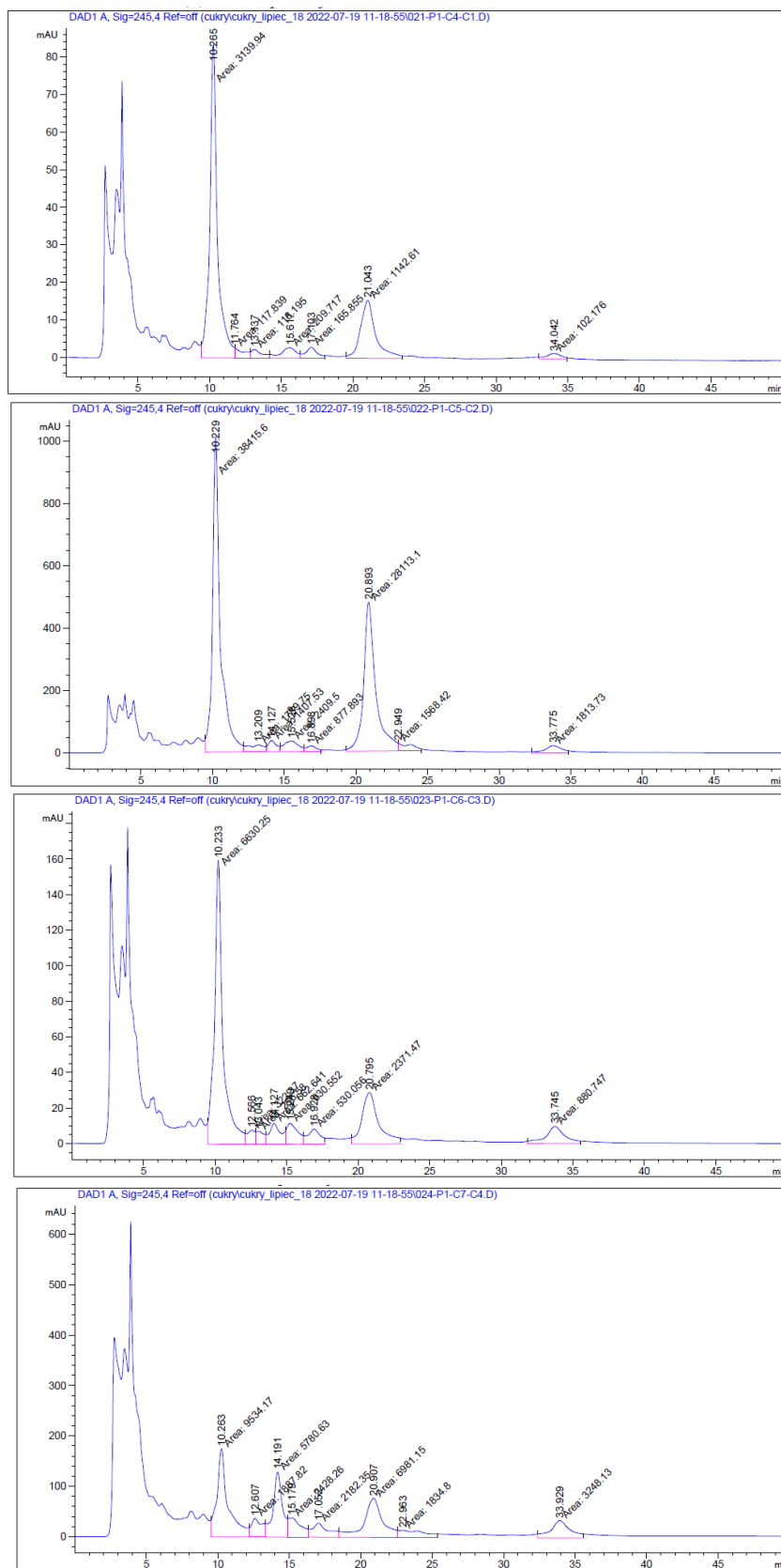


Table B4. Starting from above, C1, C2, C3 and C4 results from first attempt of HPLC analysis (names are also reported in the upper part of the spectra, in blue); peaks' retention time is reported with value of integral (area).

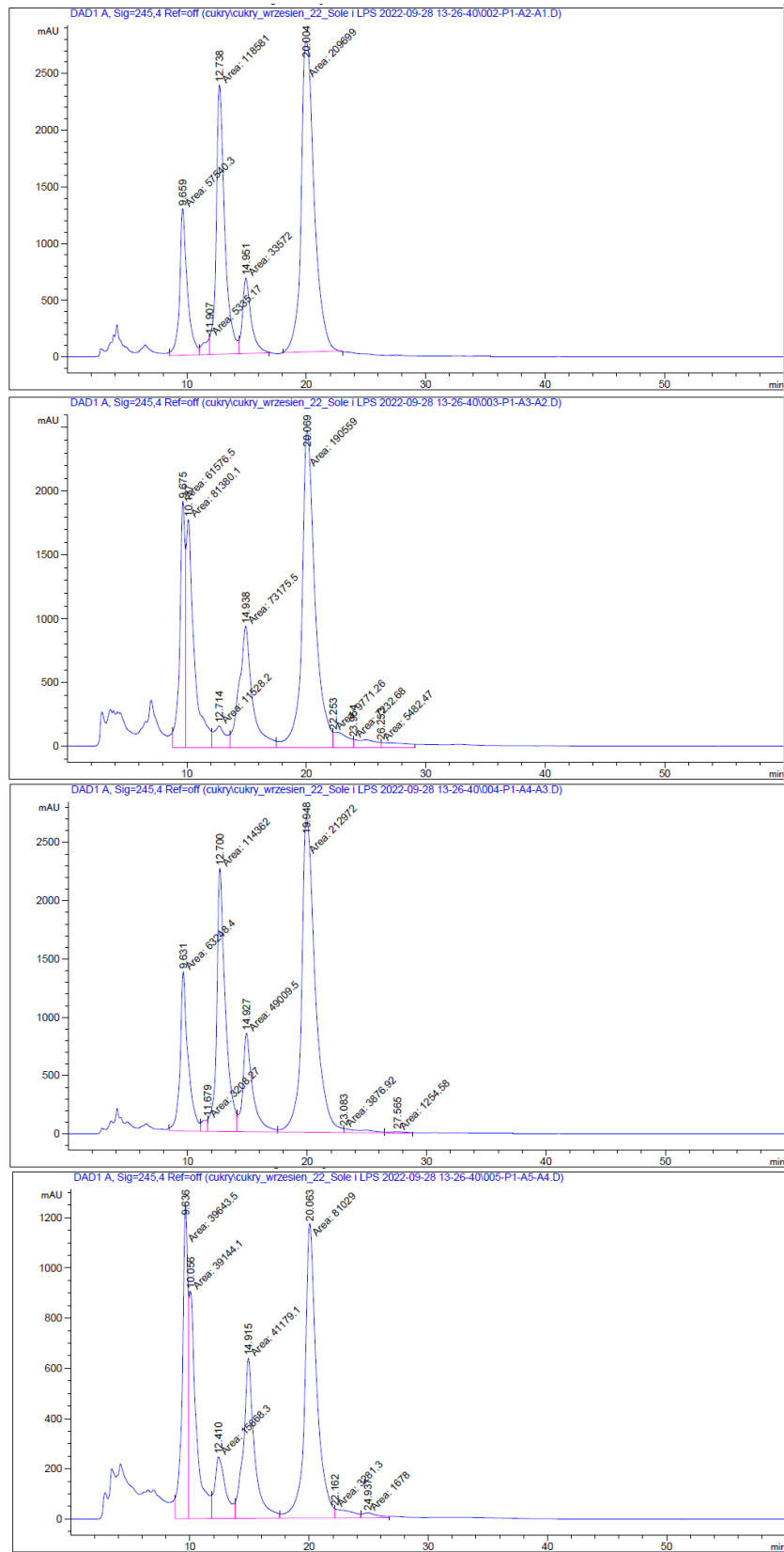


Table B5. Starting from above, A1, A2, A3 and A4 results from second attempt HPLC analysis (names are also reported in the upper part of the spectra, in blue); peaks' retention time is reported with value of integral (area).

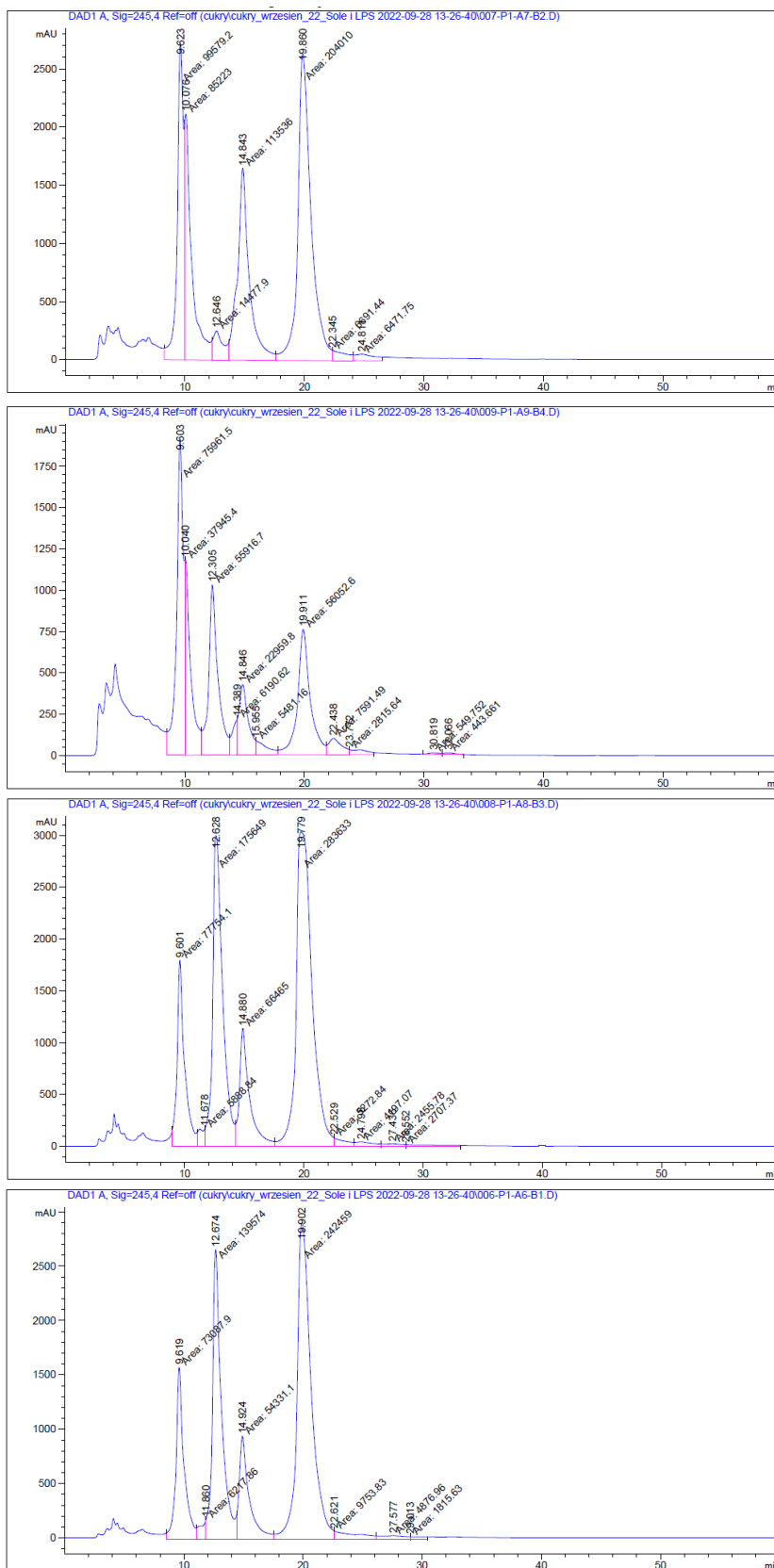


Table B6. Starting from above, B1, B2, B3 and B4 results from second attempt of HPLC analysis (names are also reported in the upper part of the spectra, in blue); peaks' retention time is together with value of integral (area).

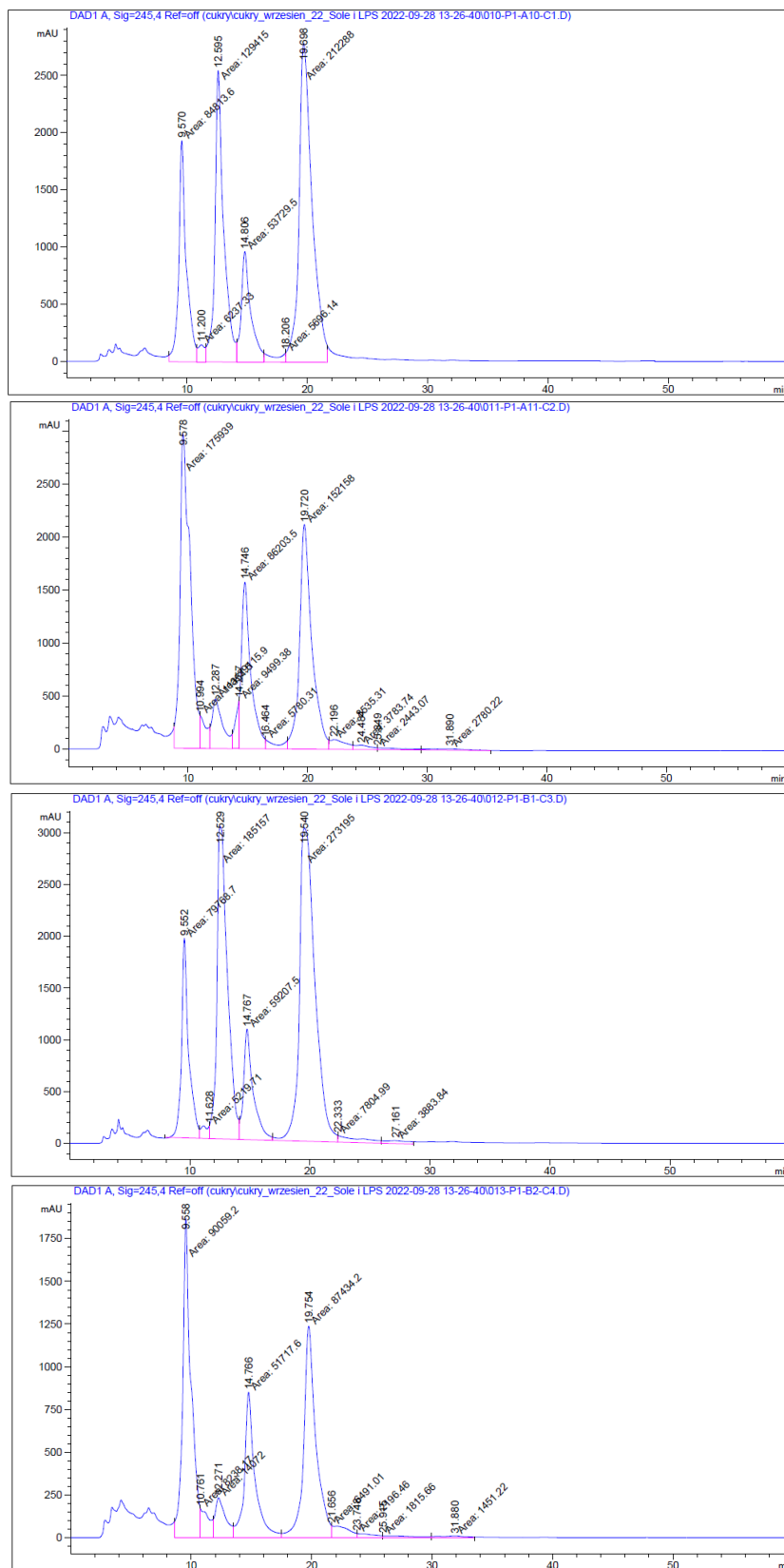


Table B7. Starting from above, C1, C2, C3 and C4 results from second attempt of HPLC analysis (names are also reported in the upper part of the spectra, in blue); peaks' retention time with value of integral (area).

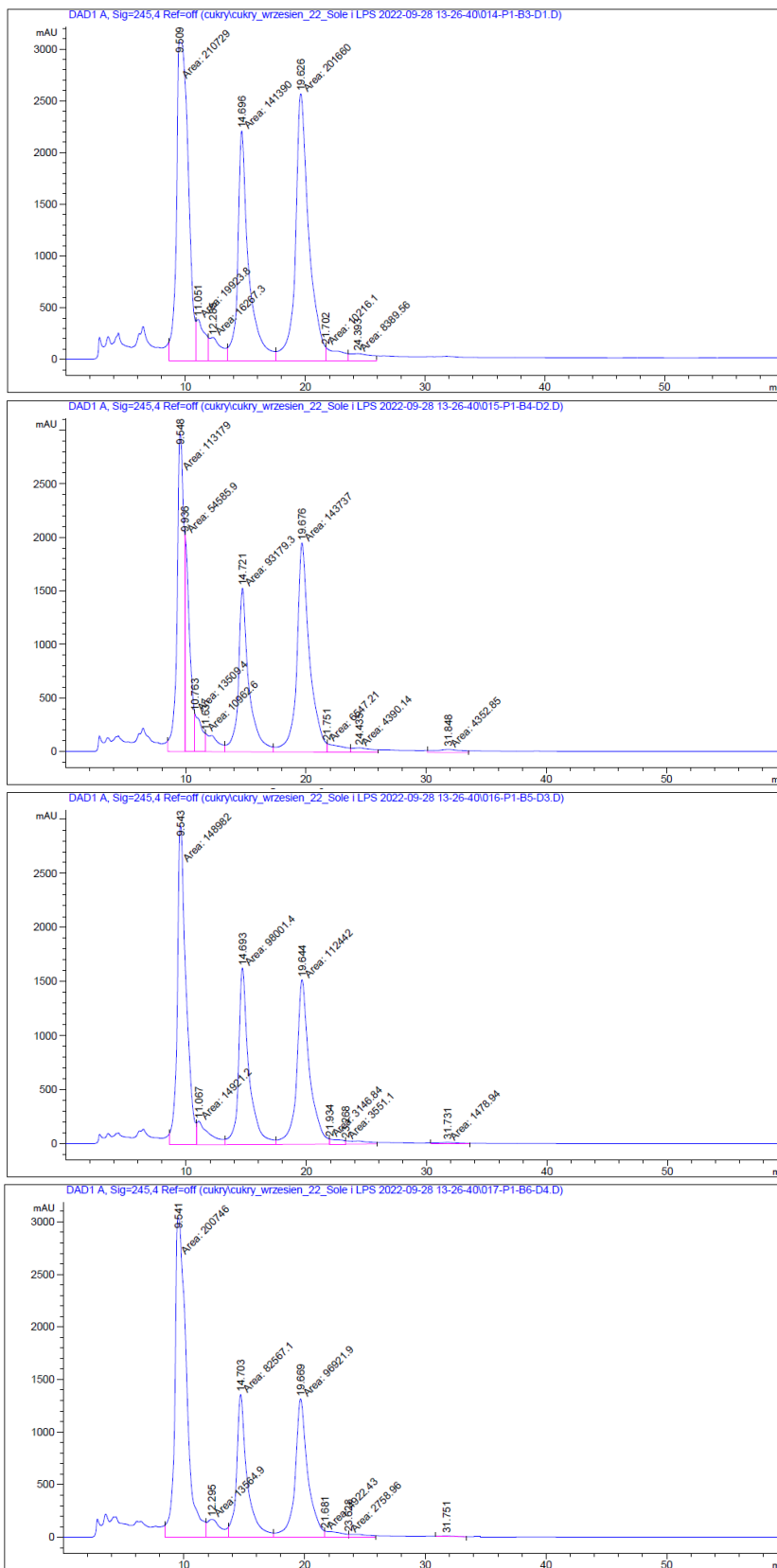


Table B8. Starting from above, D1, D2, D3 and D4 results from second attempt of HPLC analysis (names are also reported in the upper part of the spectra, in blue); retention time is reported with integral value (area).

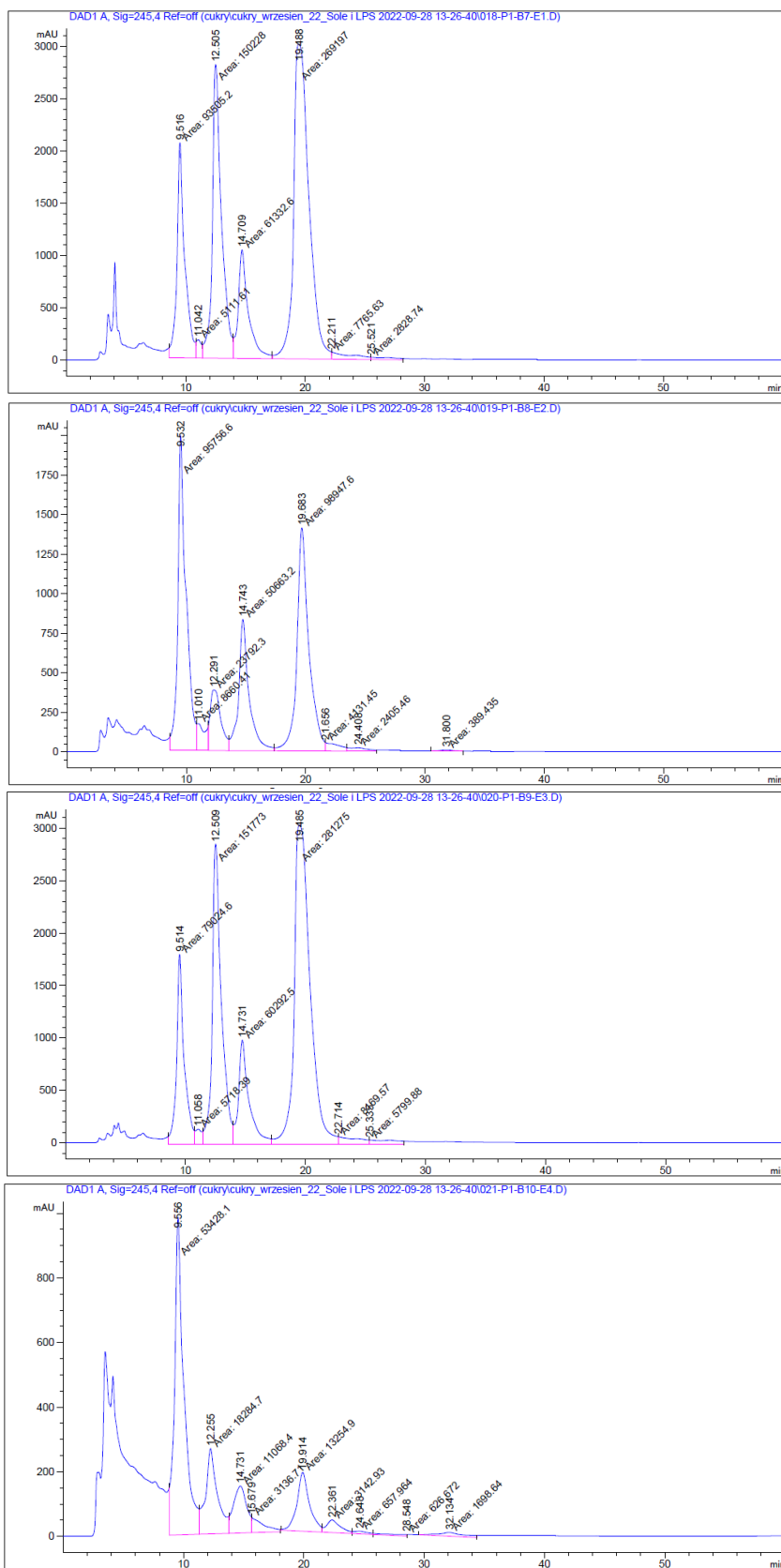


Table B9. Starting from above, E1, E2, E3 and E4 results from second attempt of HPLC analysis (names are also reported in the upper part of the spectra, in blue); peaks' retention time is reported with value of integral (area).

APPENDIX C

C.1. Absorption and fluorescence spectra

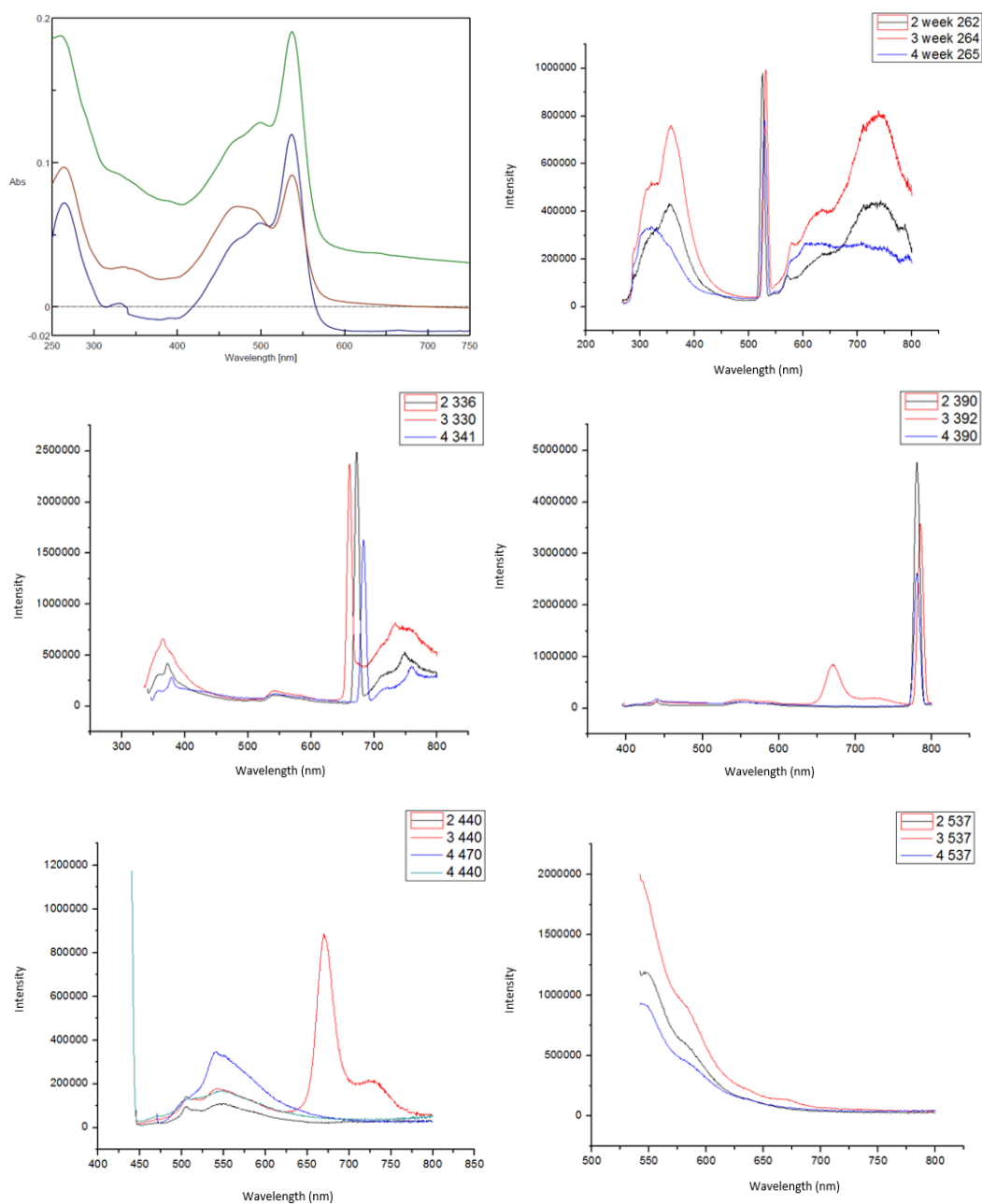


Table C1. Starting from the right above, comparison between the absorption spectrum done (in green the second measurement, in blue the third one and in red the fourth one). As followed, there are the comparisons among the fluorescence spectra from the same three samples (at the week number 2, 3 and 4) and at different wavelengths of excitation in different colours (260, 264 and 265 nm; 330, 336 and 341; 390 and 392; 440 and 470 nm and 537 nm).

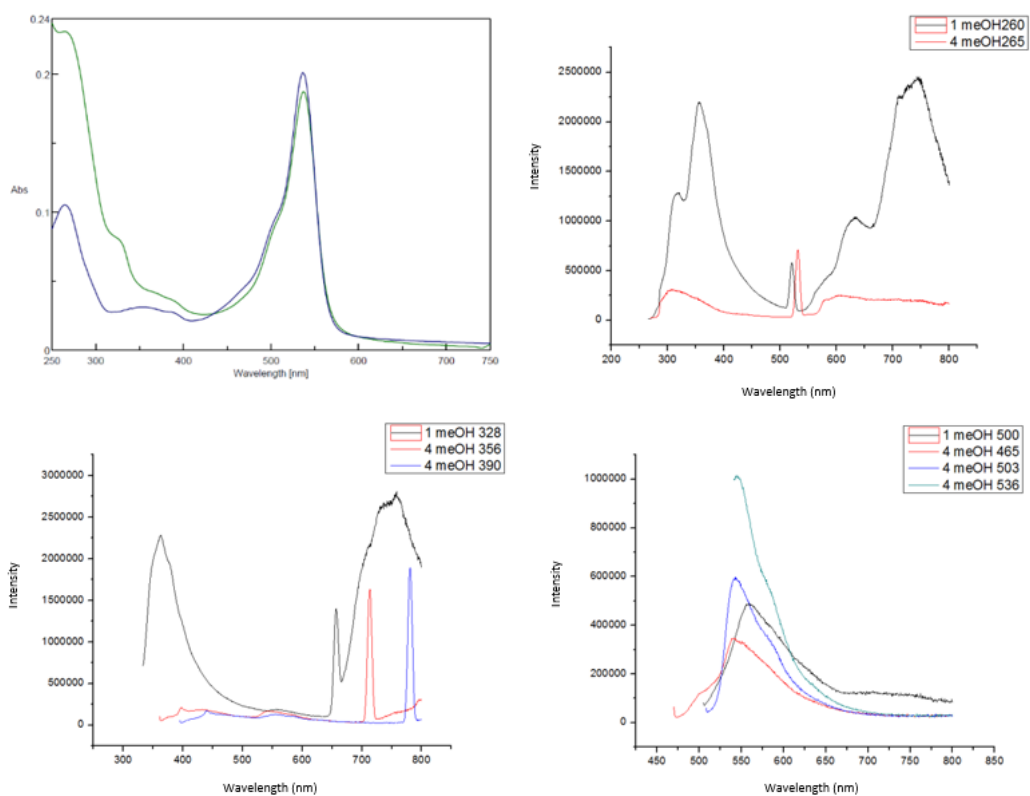


Table C2. Starting from the right above, comparison between the absorption spectrum done as first attempt (in green) and the one as second attempt (in blue); the differences are due to the different concentrations, but next analysis should verify that statement. There are the comparisons among the fluorescence spectra from the same two samples and at different wavelengths of excitation in different colours (260 and 265 nm; 328, 356 and 390 nm; 500, 465, 503 and 536 nm).

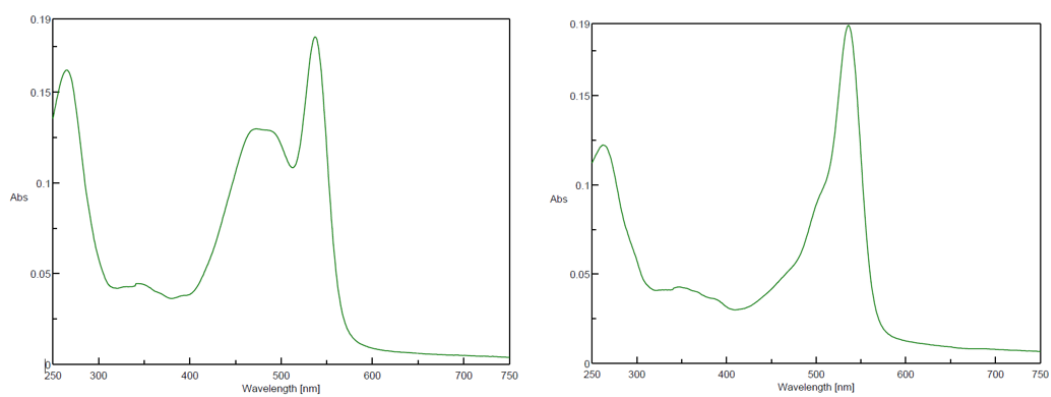


Table C3. On the left, there is the ethanol spectrum, with peaks at 265, 344, 470 and 537 nm; on the right, there is the methanol spectrum with peaks at 264, 355, 470, 500 and 537 nm. The spectra obtained at the fifth measurement are very similar to the ones from the fourth measurement.

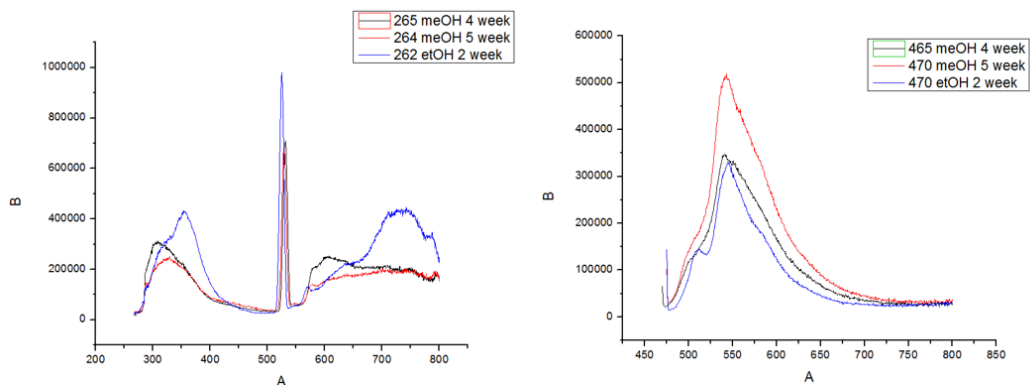


Table C4. On the left, the comparison between methanol spectra at 265 and 264 nm from the fourth and fifth measurements and ethanol spectra at 262 nm from the second measurement; on the right, the comparison between methanol spectra at 465 and 470 nm from the fourth and fifth measurements and ethanol spectra at 470 nm from the second measurement.

C.2. Prodigiosin extraction and purification by TLC

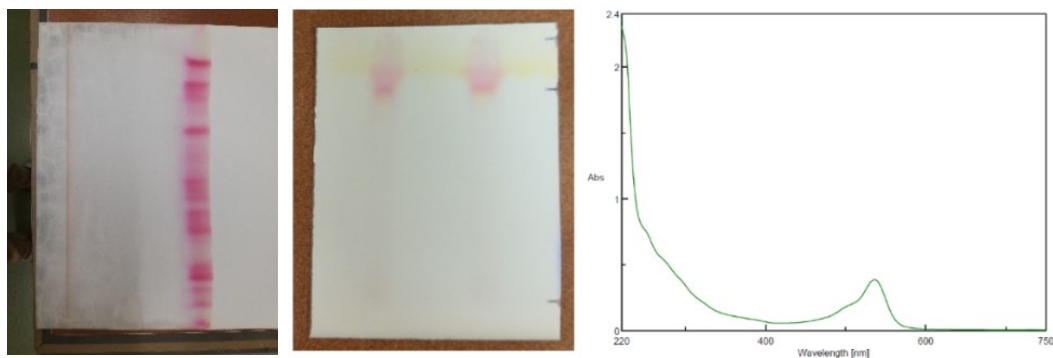


Table C5. On the left, the second TLC results using glasses, that have been previously baked; in the middle, TLC results using papers, where it is visible the presence of the prodigiosin (R_f value of 0.84); on the right, the spectrum obtained from the analysis of the samples after the TLC purification: impurities are still present, but the peaks around 250-300 nm are lower, indicating the improvement in the purification method.



Table C6. TLC papers with different ration of the solution (reported above); down below, in each photo there is the respective number. Increase of methanol decreases the R_f value; in most of the cases, the separation didn't work well.

BIBLIOGRAPHY

- Abreo, E., Altier, N. Pangenome of *Serratia marcescens* strains from nosocomial and environmental origins reveals different populations and the links between them. *Sci Rep* 9, 46 (2019). <https://doi.org/10.1038/s41598-018-37118-0>
- Aleksandra Odrobina. Czy prodigiozyna powoduje Gram zmienność i zmianę kształtu bakterii z gatunku *Serratia marcescens*? Praca licencjacka na kierunku Biotechnologia (2021).
- Beveridge TJ. Mechanism of gram variability in select bacteria. *J Bacteriol.* 1990 Mar;172(3):1609-20. doi: 10.1128/jb.172.3.1609-1620.1990. PMID: 1689718; PMCID: PMC208639.
- Beveridge, T. J.; Davies, J. A. Cellular responses of *Bacillus subtilis* and *Escherichia coli* to the Gram stain. *Journal of Bacteriology* (November 1983). 156 (2): 846–58. doi:10.1128/JB.156.2.846-858.1983. PMC 217903. PMID 6195148.
- Bonhomme D, Werts C. Purification of LPS from *Leptospira*. *Methods Mol Biol.* 2020; 2134:53-65. doi: 10.1007/978-1-0716-0459-5_6. PMID: 32632859.
- Bunting MI, Robinow CF, Bunting. H. Factors affecting the elaboration of pigment and polysaccharide by *Serratia marcescens*. *J Bacteriol.* 1949;58(1):114-115.
- Darshan N, Manonmani HK. Prodigiosin and its potential applications. *J Food Sci Technol.* 2015 Sep;52(9):5393-407. doi: 10.1007/s13197-015-1740-4. Epub 2015 Jan 24. PMID: 26344956; PMCID: PMC4554646.
- Dziwulska-Hunek. A. Szymanek. M. Matwijczuk. A. et al. Impact of electromagnetic stimulation on the mechanical and photophysical properties of alfalfa leaves. *Sci Rep* 12. 16687, 2022. <https://doi.org/10.1038/s41598-022-20737-z>
- Fatimah, Fatimah & Fitri, Rizka & Illavi, Gilva & Renjana, Elga & Pratiwi, Intan & Ni'matuzahroh, Ni'matuzahroh & Sumarsih, Sri. Cell wall response of bacteria *Serratia marcescens* LII61 -lipase and protease enzymes producer -in gram staining. *Ecology, Environment and Conservation*, 2019. 25. S76-S80.
- Fender JE. Bender CM. Stella NA. Lahr RM. Kalivoda EJ. Shanks RM. *Serratia marcescens* quinoprotein glucose dehydrogenase activity mediates medium acidification and inhibition of prodigiosin production by glucose. *Appl Environ Microbiol.* 2012;78(17):6225-6235. doi:10.1128/AEM.01778-12
- Fu. Qi & Xiao. Yujuan & Duan. Xuehui & Huang. Huabin & Zhuang. Zhixia & Shen. Jinhai & Pei. Yangyue & Haojia. Xu & Gan. Meiyu. Continuous Fermentation of a Prodigiosin-Producing *Serratia marcescens* Strain Isolated from Soil. *Advances in Bioscience and Biotechnology*, 2019. 10. 98-108. 10.4236/abb.2019.104007.
- Emad A. Shalaby, Ghada I. Mahmoud & Sanaa M. M. Shanab (2016) Suggested mechanism for the effect of sweeteners on radical scavenging activity of phenolic compounds in black and green tea, *Frontiers in Life Science*, 9:4, 241-251, DOI: 10.1080/21553769.2016.1233909
- Harris AKP. Williamson NR. Slater H et al. The *Serratia* gene cluster encoding biosynthesis of the red antibiotic. prodigiosin. shows species- and strain-dependent genome context variation. *Microbiology*, 2004 150:3547–60. doi:10.1099/mic. 0.27222-0

- Haddix PL, et al. 2008. Kinetic analysis of growth rate, ATP, and pigmentation suggests an energy-spilling function for the pigment prodigiosin of *Serratia marcescens*. *J. Bacteriol.* 190:7453–7463.
- Heinemann B, Howard AJ, Palocz HJ. Influence of dissolved oxygen levels on production of L-asparaginase and prodigiosin by *Serratia marcescens*. *Appl Microbiol.* 1970;19
- Hejazi, A., & Falkiner, F. R. *Serratia marcescens*. *Journal of medical microbiology*, 1997, 46(11), 903–912. <https://doi.org/10.1099/00222615-46-11-903>
- Hubbard R. Rimington C. The biosynthesis of prodigiosin. the tripyrrylmethene pigment from *Bacillus prodigiosus* (*Serratia marcescens*). *Biochem J*, 1950. 46:220–5
- Joshi VK, Attri D, Baja A, Bhushan S. *Microb Pigments*. 2003;2:362–369.
- Kawasaki T. Sakurai F. Nagatsuka S. Hayakawa Y. Prodigiosin biosynthesis gene cluster in the roseophilin producer *Streptomyces griseoviridis*. *J Antibiot.* 2009, 62:271–276. <https://doi.org/10.1038/ja.2009.27> 13.
- Kedare, S.B., Singh, R.P. Genesis and development of DPPH method of antioxidant assay. *J Food Sci Technol* 48, 412–422, 2011. <https://doi.org/10.1007/s13197-011-0251-1>
- Khanafari A, Assadi MM, Fakhr FA (2006). Review of prodigiosin, pigmentation in *Serratia marcescens* Qods Sqr., Tajrish Sqr. Tehran, Iran Department of Forest Sciences, Faculty of Forestry, The University of British Columbia, 4th Floor Forest Sciences Centre # 4320–2424 Main Mall Vancouver. 6:1–13
- Kimyon Ö, Das T, Ibugo AI, et al. *Serratia* Secondary Metabolite Prodigiosin Inhibits *Pseudomonas aeruginosa*, Biofilm Development by Producing Reactive Oxygen Species that Damage Biological Molecules. *Front Microbiol.* 2016; 7:972. Published 2016 Jun 27. doi:10.3389/fmicb.2016.00972
- Kostka Anna. *Mikrobiologia środowiska*, 2014. ISBN 978-83-7464-714-4
- Matsuyama T., Murakami T., Fujita M., Fujita S., Yano I. Extracellular vesicle formation and biosurfactant production by *Serratia marcescens*. *J. General Microbiol.* 1986; 132:865–875.
- Melvin, Matt & Tomlinson, John & Saluta, Gilda & Kucera, Gregory & Lindquist, Neils & Manderville, Richard. Double-Strand DNA Cleavage by Copper-Prodigiosin. *Journal of The American Chemical Society*, 2000. *J AM CHEM SOC.* 122. 10.1021/ja0000798.
- Namazkar S, Ahmad WA. Spray-dried prodigiosin from *Serratia marcescens* as a colorant. *Biosci Biotechnol Res Asia*, 2013. 10:69–76. doi:10.13005/bbra/1094
- Ravindran. A.. Sunderrajan. S.. & Pennathur. G. Phylogenetic Studies on the Prodigiosin Biosynthetic Operon. *Current microbiology.* 2019.76(5). 597–606. <https://doi.org/10.1007/s00284-019-01665-0>
- Reynolds, J.; Moyes, R. B.; Breakwell, D. P. "Appendix 3". Differential staining of bacteria: Acid fast stain. *Current Protocols in Microbiology*. Vol. Appendix 3.pp. H.2009. doi:10.1002/9780471729259.mca03hs15. ISBN 9780471729259. PMID 19885935. S2CID 45685776.
- Rice SA, Koh KS, Queck SY, Labbate M, Lam KW, Kjelleberg S. Biofilm formation and sloughing in *Serratia marcescens* are controlled by quorum sensing and nutrient

- cues. *J Bacteriol.* 2005;187(10):3477-3485. doi:10.1128/JB.187.10.3477-3485.2005
- Ryazantseva I, Andreyeva I. Application of prodigiosin as a colorant for polyolefines. *Adv Biol Chem*, 2014. 04:20–25. doi:10.4236/abc.2014.41004
- Samuel LP, Balada-Llasat JM, Harrington A, Cavagnolo R. Multicenter Assessment of Gram Stain Error Rates. *J Clin Microbiol.* 2016 Jun;54(6):1442-1447. doi: 10.1128/JCM.03066-15. Epub 2016 Feb 17. Erratum in: *J Clin Microbiol.* 2016 Sep;54(9):2405. PMID: 26888900; PMCID: PMC4879281.
- Sehdev, P. S., & Donnenberg, M. S. Arcanum: The 19th-century Italian pharmacist pictured here was the first to characterize what are now known to be bacteria of the genus *Serratia*. *Clinical infectious diseases: an official publication of the Infectious Diseases Society of America*, 1999. 29(4), 770–925. <https://doi.org/10.1086/520431>
- Slater H, Crow M, Everson L, Salmond GP. Phosphate availability regulates biosynthesis of two antibiotics, prodigiosin and carbapenem, in *Serratia* via both quorum-sensing-dependent and -independent pathways. *Mol Microbiol.* 2003 Jan;47(2):303-20. doi: 10.1046/j.1365-2958.2003.03295.x. PMID: 12519208.
- Solé, M., Rius, N., & Lorén, J. G. Rapid extracellular acidification induced by glucose metabolism in non-proliferating cells of *Serratia marcescens*. *International microbiology: the official journal of the Spanish Society for Microbiology*, 3, 39–43, 2000.
- Suryawanshi RK, Patil CD, Borase HP et al. Studies on production and biological potential of prodigiosin by *Serratia marcescens*. *Appl Biochem Biotechnol*, 2014. 173:1209–21. doi:10.1007/s12010-014-0921-3
- Tejasvini S. Pore, Ashwini B. Khanolkar, Naiem H. Nadaf. Production, purification, identification of prodigiosin from *Serratia* sp. and its antimicrobial activity. *Life Science Informatics Publications* DOI - 10.26479/2016.0106.05
- V. Godvin Sharmila, S. Kavitha, Parthiba Karthikeyan Obulisamy, J. Rajesh Banu, Chapter 8 - Production of fine chemicals from food wastes, Editor(s): J. Rajesh Banu, Gopalakrishnan Kumar, M. Gunasekaran, S. Kavitha, *Food Waste to Valuable Resources*, Academic Press, 2020, Pages 163-188, ISBN 9780128183533, <https://doi.org/10.1016/B978-0-12-818353-3.00008-0>.
- Vu Trong Luong, Nguyen Sy Le Thanh, Do Thi Tuyen, Do Thi Cuc, Do Thi Thao. Prodigiosin purification from *Serratia marcescens* M10 and its antitumor activities. *Vietnam Journal of Biotechnology* Vol. 19, N. 2, 2021, DOI: <https://doi.org/10.15625/1811-4989/15722>
- Williams RP, Gott CL, Qadri SM, Scott RH. Influence of temperature of incubation and type of growth medium on pigmentation in *Serratia marcescens*. *J Bacteriol.* 1971;106(2):438-443. doi:10.1128/jb.106.2.438-443.1971
- Williams, Robert P. Biosynthesis of prodigiosin, a secondary metabolite of *Serratia marcescens*. *Applied microbiology* 25.3, 1973: 396-402.
- Williamson NR, Simonsen HT, Ahmed RA, Goldet G, Slater H, Woodley L, Leeper FJ, Salmond GP. Biosynthesis of the red antibiotic, prodigiosin, in *Serratia*: identification of a novel 2-methyl-3-n-amyl-pyrrole (MAP) assembly pathway, definition of the terminal condensing enzyme, and implications for undecylprodigiosin

biosynthesis in *Streptomyces*. *Mol Microbiol.* 2005 May;56(4):971-89. doi: 10.1111/j.1365-2958.2005.04602.x. PMID: 15853884.

Williamson NR. Fineran PC. Leeper FJ. Salmond GPC. The biosynthesis and regulation of bacterial prodiginines. *Nat Rev Microbiol*, 2006. 4:887–899. doi:10.1038/nrmicro1531

Xu, Fang, Shunxiang Xia, and Qiyin Yang. Strategy for obtaining inexpensive prodigiosin production by *Serratia marcescens*. 3rd International Conference on Chemical, Biological and Environmental Engineering. 2011